JUSTUS-LIEBIG-UNIVERSITÄT GIESSEN

Functional characterization of *Saccharomyces cerevisiae* protein Sub2 in nuclear mRNP formation

Dissertation

Submitted in partial fulfilment of requirements for

the degree of Doctor of Philosophy Natural Sciences

(Dr. rer. nat.)

Department 08 Biochemistry

Justus Liebig University Giessen

Francisca Nana Amoah

JUSTUS-LIEBIG-UNIVERSITÄT GIESSEN

Functional characterization of *Saccharomyces cerevisiae* protein Sub2 in nuclear mRNP formation

Dissertation

Submitted in partial fulfilment of requirements for

the degree of Doctor of Philosophy Natural Sciences

(Dr. rer. nat.)

Department 08 Biochemistry

Justus Liebig University Giessen

Submitted by

Francisca Nana Amoah

June 2022, Giessen

The present work was carried out at the Institute of Biochemistry (Department 08) of the Justus Liebig University Giessen, under the supervision of Prof. Dr. Katja Sträßer.

First examiner: Prof. Dr. Katja Sträßer
Department 08: Biology and Chemistry
Institute of Biochemistry
Justus Liebig University Giessen

Second examiner: Prof. Dr. Elena Evguenieva-Hackenberg
Department 08: Biology and Chemistry
Institute of Microbiology and Molecular biology
Justus Liebig University Giessen

Contents

Abstract

RNA-protein interactions play a critical role in numerous key biological processes. These interactions form ribonucleoprotein complexes (RNPs) that regulate gene expression and are involved in all steps of RNA biogenesis, including transcription, RNA processing, nuclear export, localization, stability, and translation. Owing to their importance, failure to appropriately assemble protein-RNA complexes triggers various genetic diseases and cancers. RNA-binding proteins (RBPs) represent a large class of proteins that interact with and regulate transcripts. RBPs can mediate single RNA-protein interactions or be part of multi-protein complexes. An example of such a multi-protein complex is the TREX complex, that couples transcription with nuclear mRNA export. It is composed of the pentameric THO complex (Tho2, Hpr1, Mft1, Thp1 and Tex1), the SR-like proteins Gbp2 and Hrb1, the RNA helicase Sub2 and the export adaptor Yra1. Yra1 links the TREX-packaged mRNA with the export receptor Mex67-Mtr2, which transports the mRNP to the cytoplasm. The RNA helicase Sub2, is highly conserved and functions in splicing, polyadenylation, nuclear mRNA export and removing RNA-DNA hybrids (R-loop resolution). It is recruited to active chromatin by the THO complex and interacts with RNA using amino acid residues in its RNA-binding motifs.

In this study, we assessed the role of novel RNA-binding sites of Sub2 in mRNP formation. To achieve this, we mutated amino acids of Sub2 that were identified to interact with RNA *in vivo* and characterized them functionally. Using this approach, we identified amino acid residues that are vital for Sub2 function, as these mutations affected the viability of our cells. Of the viable *sub2* mutants, we characterized three into detail. We identified *sub2-T62D*, which had mild growth, but strong export defects, implicating it as an essential residue for mRNA export. It also demonstrated slightly reduced binding to RNA and could not resolve R-loops *in vivo*. We also identified *sub2-K70D* which was not essential for growth, as it had no growth defects, but had mRNA export defects, and reduced RNA-binding and helicase activities. Additionally, we identified the essential *sub2-K202E-Y203E* that resulted in growth and mRNA export defects, and reduced RNA-binding and helicase activities. This mutant also mislocalized Sub2. Analysis revealed the essential amino acid in this mutant to be K202. By further characterizing this mutant, we could show that, the ability of Sub2 to support growth depends on its nuclear localization.

Altogether, mutating the putative RNA-binding sites of Sub2 affects growth, mRNA export, dsRNA helicase activity, R-loop resolution and impairs interaction with other mRNP components. Moreover, not all residues of Sub2 mediate similar function. Using this mutagenic approach, we identified residues that are not essential for growth, residues vital for mRNA export and residues that are crucial for binding to RNA and protein localization.

Zusammenfassung

RNA-Protein-Wechselwirkungen spielen eine entscheidende Rolle bei zahlreichen biologischen Schlüsselprozessen. Diese Wechselwirkungen bilden Ribonukleoprotein-Komplexe (RNPs), die die Genexpression regulieren und an allen Schritten der RNA-Biogenese beteiligt sind, einschließlich Transkription, RNA-Verarbeitung, Kernexport, Lokalisierung, Stabilität und Übersetzung. Aufgrund ihrer Bedeutung ist ein unzureichender Zusammenbau von Protein-RNA-Komplexen der Auslöser für verschiedene genetische Krankheiten und Krebserkrankungen. RNA-bindende Proteine (RBPs) stellen eine große Klasse von Proteinen dar, die mit Transkripten interagieren und diese regulieren. RBPs können einzelne RNA-Protein-Wechselwirkungen vermitteln oder Teil von Multi-Protein-Komplexen sein. Ein Beispiel für einen solchen Multiproteinkomplex ist der TREX-Komplex, der die Transkription mit dem mRNA-Kernexport verbindet. Er besteht aus dem pentameren THO-Komplex (Tho2, Hpr1, Mft1, Thp1 und Tex1), den SR-ähnlichen Proteinen Gbp2 und Hrb1, der RNA-Helikase Sub2 und dem Exportadapter Yra1. Yra1 verbindet die TREX-verpackte mRNA mit dem Exportrezeptor Mex67-Mtr2, der das mRNP in das Zytoplasma transportiert. Die RNA-Helikase Sub2 ist hoch konserviert und hat Funktionen beim Spleißen, der Polyadenylierung, dem mRNA-Kernexport und der Entfernung von RNA-DNA-Hybriden (Auflösung der R-loops). Sie wird durch den THO-Komplex zu aktivem Chromatin rekrutiert und interagiert mit RNA über Aminosäurereste in ihren RNA-Bindungsmotiven.

In dieser Studie haben wir die Rolle neuartiger RNA-Bindungsstellen von Sub2 bei der mRNP-Bildung untersucht. Zu diesem Zweck mutierten wir Aminosäuren von Sub2, von denen wir wussten, dass sie *in vivo* mit RNA interagieren, und charakterisierten sie funktionell. Mit diesem Ansatz identifizierten wir Aminosäurereste, die für die Funktion von Sub2 entscheidend sind, da diese Mutationen die Lebensfähigkeit unserer Zellen beeinträchtigten. Von den lebensfähigen Sub2-Mutanten haben wir drei detailliert charakterisiert. Wir identifizierten *sub2-T62D*, dass ein leichtes Wachstum, aber starke Exportdefekte aufwies, was darauf hindeutet, dass es sich um einen essenziellen Rest für den mRNA-Export handelt. Außerdem zeigte es eine leicht reduzierte Bindung an RNA und konnte in vivo keine R-loops auflösen. Wir identifizierten auch *sub2-K70D*, das für das Wachstum nicht essentiell war, da es keine Wachstumsdefekte, aber mRNA-Exportdefekte und reduzierte RNA-Bindungs- und Helikase-Aktivitäten aufwies. Darüber hinaus identifizierten wir die essenzielle *sub2-K202E-Y203E*, die zu Wachstums- und mRNA-Exportdefekten sowie zu verringerten RNA-Bindungs- und Helikase-Aktivitäten führte. Bei dieser Mutante war Sub2 außerdem fehllokalisiert. Die Analyse ergab, dass die essenzielle Aminosäure in dieser Mutante K202 ist. Durch die weitere Charakterisierung dieser Mutante konnten wir zeigen, dass die Fähigkeit von Sub2, das Wachstum zu unterstützen, von seiner nukleären Lokalisierung abhängt.

Insgesamt beeinträchtigt die Mutation der mutmaßlichen RNA-Bindungsstellen von Sub2 das Wachstum, den mRNA-Export, die dsRNA-Helicase-Aktivität und die Auflösung der R-loops und beeinträchtigt die Interaktion mit anderen mRNP-Komponenten. Darüber hinaus vermitteln nicht alle Reste von Sub2 eine ähnliche Funktion. Mithilfe dieses mutagenen Ansatzes identifizierten wir Reste, die für das Wachstum nicht wesentlich sind, Reste, die für den mRNA-Export wichtig sind, und Reste, die für die Bindung an RNA und die Proteinlokalisierung entscheidend sind.

1 Introduction

Gene expression is an essential process that translates the information stored in DNA into proteins. From transcription to translation, gene expression is mediated by a dynamic network of RNA-protein interactions that package the nascent transcript into a messenger ribonucleoprotein (mRNP) and mediate mRNA-processing, export, translation, and decay. The RNA binding proteins (RBPs) of mRNPs regulate the co- and post-transcriptional events of gene expression (Lorković 2012; Re et al. 2014), such as transcription, RNA processing, nuclear export and translation. The central role of RBPs in these fundamental processes underlines their importance in gene expression, and failure to appropriately assemble RNA-protein complexes is detrimental and could lead to toxicity and death. The interaction of RBPs with RNA varies from single-protein-RNA interactions to multi-complex interactions (Corley et al. 2020). Their roles in gene expression have become progressively evident and many studies exist to characterize them. RBPs represent more than 10% of the total yeast proteome, and the availability of functional genomic tools (Mohammadi et al. 2015) in *Saccharomyces cerevisiae*, makes it a good model organism to study RBPs (Beckmann et al. 2015).

1.1 Messenger Ribonucleoprotein (mRNP)

RNA polymerase II (RNAPII) synthesizes a class of precursor mRNAs that are processed before they are translated into proteins. Co-transcriptionally, an m^7G cap structure is added to the 5' end (Topisirovic et al. 2011), introns are spliced out by the spliceosome (Rymond, Brian C., Michael Rosbash. 1993), a polyadenosine (poly(A)) tail is added to the 3' end of the transcript (Proudfoot 2011) and the mature mRNA is packaged into an mRNP. The packaged mRNA is then exported through the nuclear pore complex (NPC) by the export receptor Mex67-Mtr2 to the cytoplasm, where it is translated into proteins (Iglesias and Stutz 2008) by ribosomes (Figure 1). The RBPs that associate with the growing mRNA package it into an mRNP and ensure that the mRNA is properly processed which increases the stability and efficient export of the mRNA. RBPs also form parts of multi-protein complexes that recruit other proteins onto the growing mRNA through protein-protein interactions (Müller-McNicoll and Neugebauer 2013). For instance, RNAPII serves as a recruiting platform for several factors that process the mRNA co-transcriptionally (Proudfoot 2000; Meinel et al. 2013). Its largest subunit, Rpb1, has an essential characteristic carboxyl-terminal domain (CTD) consisting of highly conserved tandem peptide repeats of $Y_1S_2P_3T_4S_5P_6S_7$ (Nonet and Young 1989; Young 1991). During transcription, the heptapeptide repeats become modified and transition the polymerase between initiating and elongating states (Corden 1990). The exon junction complex (EJC), which is deposited onto splice sites, also serves as a platform to

recruit factors involved in mRNA export and nonsense-mediated mRNA decay (Zhou et al. 2000; Kim et al. 2001; Le Hir et al. 2001). However, in *S. cerevisiae*, where about 4% of all genes contain introns, only one of its core proteins eIF4AIII is conserved (Bannerman et al. 2018). The constant addition and removal of RBPs from the mRNA during transcription yields an mRNP whose composition varies as the mRNA progresses through its life cycle. This dynamic assembly and disassembly of mRNPs regulate nuclear mRNA export, translation, localization, and turnover, and drives efficient gene expression (Heinrich et al. 2017).

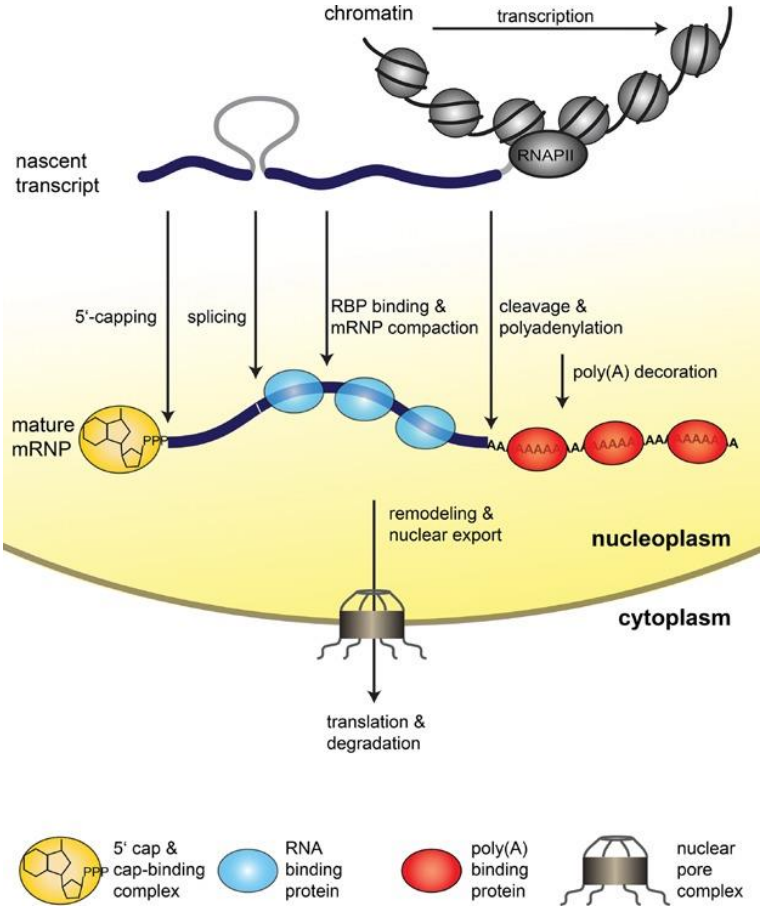

Figure 1: Gene expression, a dynamic network of mRNP assembly and disassembly
RNAPII transcripts are co-transcriptionally bound by single and multi-protein complexes that process the pre-mRNA to a matured mRNA, that can be efficiently exported into the cytoplasm. The pre-mRNA is capped (yellow circle), spliced (blue circles), polyadenylated (red circles) and transported through the NPC into the cytoplasm for translation and later degraded. The mRNA is packaged by proteins into an mRNP which influences further processing of the mRNA as well as its stability. (Meinel and Sträßer 2015).

1.2 Nuclear mRNPs

The co- and post-transcriptional events of transcription elongation, mRNA processing, and mRNP assembly are all interconnected. This ensures that only properly synthesized and processed mRNA are exported from the nucleus to the cytoplasm. For example, in *S. cerevisiae*, a defect in splicing or absence of a polyadenylation signal results in a nuclear

mRNA export defect (Long et al. 1995; Huang and Carmichael 1996), and there is also a linkage between proper 3′ end formation and mRNA export (Eckner et al. 1991; Hammell et al. 2002; Libri et al. 2002; Elbarbary and Maquat 2016). The composition of nuclear mRNPs include, but is not limited to the cap-binding complex (CBC) components Cbp80 and Cbp20 (Izaurralde et al. 1994; Izaurralde et al. 1995), which bind the 5′ cap of the mRNA, the exon junction complex (EJC), which is deposited on ligated exons in higher eukaryotes (Kataoka et al. 2000), and the poly (A)-binding protein Nab2 (Anderson et al. 1993). The transcription export (TREX) complex composed of the THO complex (Tho2, Hpr1, Mft1, Thp1 and Tex1), the SR-like proteins Gbp2 and Hrb1, the RNA helicase Sub2 and the export adaptor Yra1, also constitutes a part of nuclear mRNPs. The TREX complex recruits Mex67-Mtr2 to export the properly packaged mRNA (Zenklusen et al. 2001; Meinel et al. 2013). Hence, the recruitment of all these factors to the mRNA acts as a mark for processed mRNA and serves as an inherent control mechanism, that ensures that only correctly processed and packaged mRNAs are exported.

1.2.1 5′ end processing

The 5′ guanine-N7 methyl (m^7G) cap is the first co-transcriptional modification that occurs on the mRNA when the nascent transcript is about 30 nucleotides long. The 5′ cap is relevant for mRNA stability, efficient splicing, mRNA export, and translation (Ramanathan et al. 2016). The m^7G cap is added to the pre-mRNA in three sequential enzymatic steps: hydrolysis of the 5′γ-phosphate of the nascent pre-mRNA, transfer of a guanine monophosphate nucleoside to the 5′ diphosphate mRNA end and the methylation of the guanine N7 position (Shatkin and Manley 2000; Moteki and Price 2002). For the pre-mRNA to be efficiently capped, the transcribing RNAPII is paused, and the capping enzymes are recruited. Once capping is completed, RNAPII is reactivated to continue transcription. The pause in transcription serves as a checkpoint to ensure that only capped transcripts are elongated (Saguez et al. 2005).

1.2.2 Splicing

Another processing event that the pre-mRNA undergoes is splicing. Splicing removes introns that intersperse exons (Padgett et al. 1986) and ligates exons to produce a transcript that can be translated into proteins (Figure 2). It occurs in several steps that are catalyzed by small nuclear ribonucleoproteins (snRNPs) and associated proteins (Lerner et al. 1980). The snRNAs that constitute the spliceosome are named U1, U2, U4, U5, and U6, so-called because they are uridine rich. The spliceosome does not associate with the pre-mRNA in a pre-assembled active form, but it assembles *de novo* on the pre-mRNA substrate at the exon-intron junction (Gesteland et al. 2006).

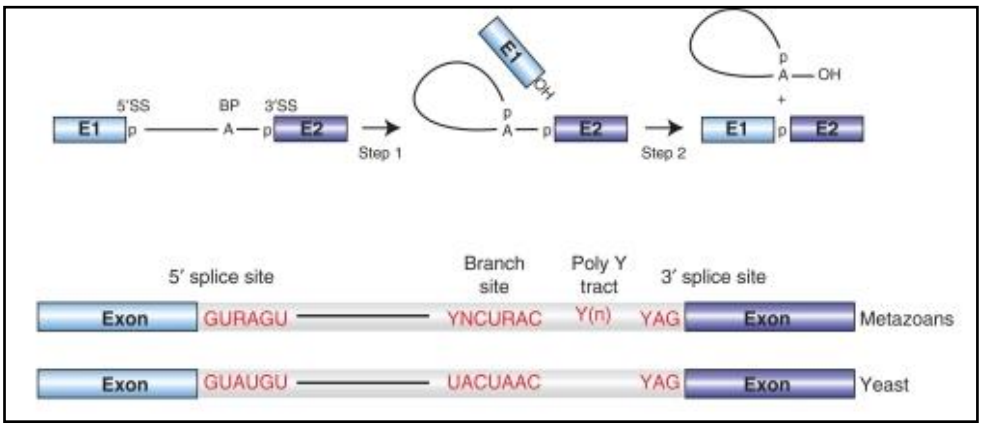

Figure 2: Schematic representation of the two-step mechanism of pre-mRNA splicing
In the first step of splicing, the branch point adenosine is used to remove the upstream intronic sequences. The second step uses the 5′ splice site to remove the downstream intron sequences and ligate the exons forming a mature messenger RNA. Boxes represent the exons, solid lines the intron. The branch point (BP) adenosine is indicated by the letter A and the phosphate groups (p) at the 5′ and 3′ splice sites, which are conserved in the splicing products, are also depicted. Also indicated are the conserved sequences found at the 5′ and 3′ splice sites, and the branch point of pre-mRNA introns in metazoans and *S. cerevisiae*. Y = pyrimidine and R = purine. The polypyrimidine tract is indicated by (Yn). (Will and Lührmann 2011).

The first step of spliceosome formation is the recognition of the 5′ splice site by U1 snRNP in an ATP-independent manner and the branchpoint adenosine by the branchpoint binding protein (BBP) (Wolf et al. 2009). Two other proteins, U2 auxiliary factors 35 and 65 (U2AF35 and U2AF65), bind to the 3′ splice site and the polypyrimidine tract, respectively, to form the commitment complex, complex E (Kent and MacMillan 2002), which is the earliest splicing-specific complex that forms on the pre-mRNA (Figure 3). The U2 snRNP then associates at the branchpoint sequence of the intron in an ATP-dependent manner. This converts complex E into complex A (Das et al. 2000) . Following this, a pre-formed tri-snRNP, U5•U4/U6 (Behrens and Lührmann 1991), is added in an ATP-dependent manner forming the pre-catalytic complex B (Staley and Guthrie 1998). Several intra- and intermolecular rearrangements take place. The U6 snRNA displaces the U1 snRNP, associates with the 5' splice site and disrupts the base pairing between the U4 and U6 snRNAs. The interactions between the U2 and U6 snRNAs contribute to the formation of the catalytic center giving rise to the active spliceosome, the B^{act} complex (Wu and Manley 1991). The DEAD-box RNA helicase Prp2 catalytically activates the B^{act} complex to generate the B* complex, which catalyzes the first step of splicing, the first trans-esterification reaction (Kim and Lin 1996). The B* complex becomes reorganized to form complex C, which catalyzes the second trans-esterification reaction. Following the first transesterification reaction, the U6 snRNP removes the branchpoint from the catalytic center and repositions the 5′ splice site close to the 3′ splice site for step 2 (Will and Lührmann 2011). The number of rearrangements required to achieve

this is not clear, but it is known that the U5 snRNA interacts with sequences in the 5′ and 3′ exons, immediately adjacent to the splice sites. These interactions are thought to be stabilized by the U5 snRNP proteins. Thus, the U5 snRNP appears to play an important role in aligning the ends of the exons correctly for their joining in the second step of splicing, exon ligation (Newman and Norman 1992). Completion of the second trans-esterification reaction leads to the formation of the post-spliceosomal complex that contains the products of splicing: a spliced mRNA and an excised intron lariat. Following spliceosome disassembly, the snRNPs are recycled for subsequent rounds of splicing, and the lariat is debranched and degraded (Grainger and Beggs 2013).

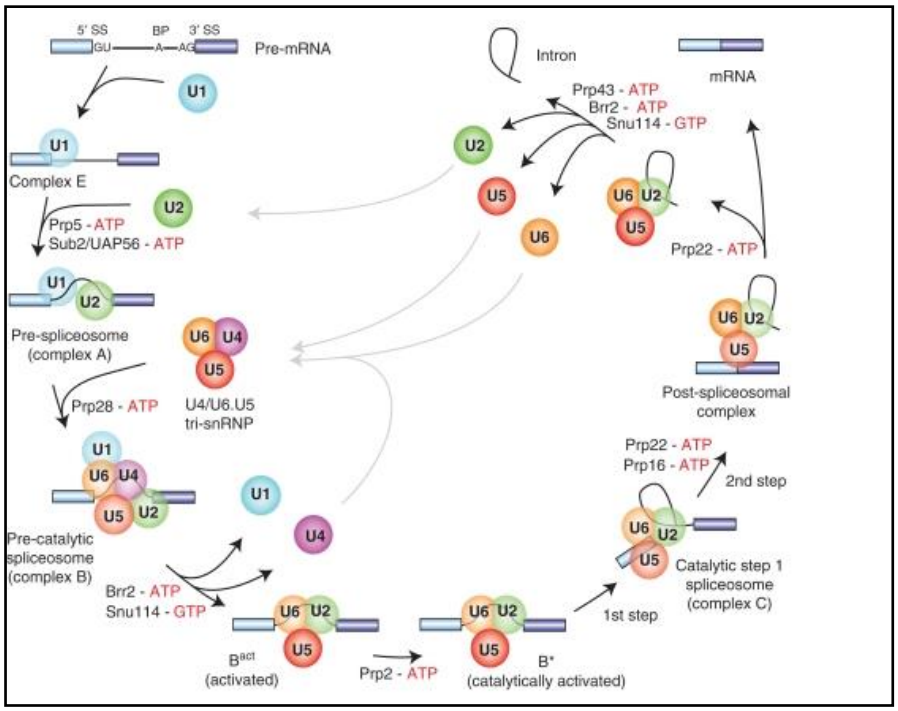

Figure 3: Canonical cross-intron assembly and disassembly pathway of the U2-dependent spliceosome.
For simplicity, the ordered interactions of the snRNPs (indicated by circles), but not those of non-snRNP proteins, are shown. The various spliceosomal complexes are named according to the metazoan nomenclature. Exon and intron sequences are indicated by boxes and lines, respectively. The stages at which the evolutionarily conserved DExH/D-box RNA ATPases/helicases Prp5, Sub2/UAP56, Prp28, Brr2, Prp2, Prp16, Prp22 and Prp43, or the GTPase Snu114, act to facilitate conformational changes are indicated (Will and Lührmann 2011).

1.2.3 3′ end processing

The pre-mRNA 3’ processing complex is conserved from yeast to mammals and most mammalian 3’ processing factors have homologs in yeast. However, the polyadenylation signals of canonical cis-elements are not conserved and show some variation (Chan et al. 2011). The process encompasses 3′ end cleavage and polyadenylation. Recognition of a polyadenylation signal in the 3′ untranslated region (UTR) leads to cleavage and addition of a

poly(A) tail. 3′ end processing of mRNA is a highly coordinated process involving a number of regulatory trans-acting protein factors and cis-acting RNA sequence elements. (Danckwardt et al. 2008). Poly(A) tail addition occurs in a two-step reaction involving endonucleolytic cleavage followed by polymerization of a poly(A) tail. The specificity and efficiency of 3′ end processing is determined by the binding of multiprotein complexes to specific elements at the 3′ end of the pre-mRNA: a canonical polyadenylation signal (PAS) AAUAAA/AUUAAA (Proudfoot and Brownlee 1976), and a G/U-rich downstream sequence element (DSE) (Gil and Proudfoot 1987). The polyadenylation signal is upstream of the cleavage site and is recognized by the multimeric cleavage and polyadenylation specificity factor (CPSF, Figure 4) consisting of the subunits CPSF160, CPSF100, CPSF73, CPSF30 and Fip1 (Bienroth et al. 1991). This RNA-protein interaction defines the cleavage site 10-30 nt downstream, preferentially immediately 3′ of a CA dinucleotide. The DSE, which is located up to 30nt downstream of the cleavage site, is bound by the 64 kDa subunit of the heterotrimeric cleavage-stimulating factor (CstF, Figure 4) (MacDonald et al. 1994) and promotes the efficiency of 3′ end processing. Following assembly of the multiprotein complexes at the respective RNA recognition motifs, the primary transcript is endonucleolytically cleaved at the cleavage site by CPSF73. Adenine residues are then added to the 3′ end by a poly A polymerase to form a poly(A) tail, which is bound by the poly(A)-binding protein nuclear 1 (PABPN1) (Bienroth et al. 1993; Wahle 1991). The interaction of the polyadenylation-polymerase (PAP) with PABPN1 and CPSF is critical to establish the processive action of the polymerase for the synthesis of approximately 250 adenine residues (Bienroth et al. 1993; Kerwitz et al. 2003). In *S. cerevisiae*, the yeast proteins Nab2 and Pab1 regulate poly(A) tail length (Minvielle-Sebastia et al. 1997; Mangus et al. 2003; Viphakone et al. 2008). and act in other stages of mRNA biogenesis. Loss of Nab2 affects cell viability and leads to mRNA export defects (Anderson et al. 1993; Hector et al. 2002), while Pab1 plays a role in translation initiation by recruiting the 40S ribosomal subunit to the mRNA (Sachs and Davis 1989; Tarun and Sachs 1995). Following polyadenylation, the interaction of PABPN1 with the poly(A) tail is characterized by a rapid on-off rate, and PABN1 is exchanged by cytoplasmic poly (A) binding protein (PABPC) during nuclear export. PABPC interacts with the translation initiation factor elF4G as part of the initiation complex thus generating a translation-competent mRNP (Hollerer et al. 2014; Wigington et al. 2014).

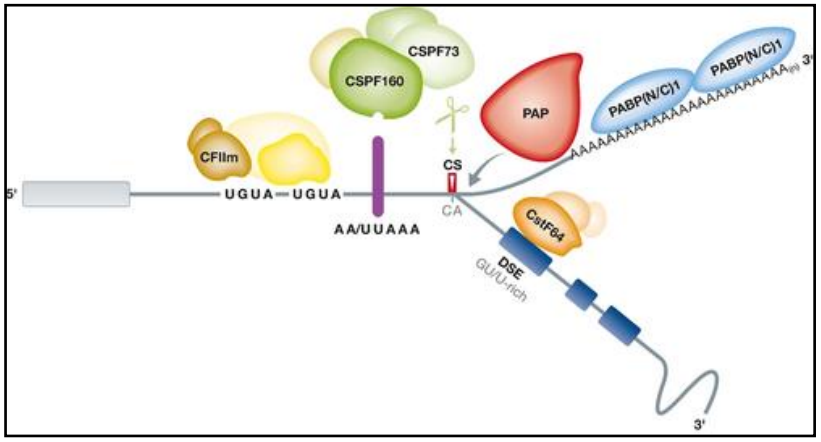

Figure 4: The trans-acting proteins and cis-acting RNA elements that mediate mRNA 3′end processing.
Endonucleolytic cleavage of pre-mRNAs and their subsequent polyadenylation requires the multi subunit complexes CPSF, CstF, cleavage factor I (CFIm), cleavage factor II (CFIIm) and the single-subunit polyadenylation-polymerase (PAP). At the polyadenylation signal (PAS), CPSF and CstF bind to the central hexamer sequence (AA/UUAAA) and to the GU/U-rich DSE, respectively, as the first step in mRNA 3′end processing. The other protein complexes assemble at specific RNA sequence elements both up- and down-stream of the PAS, including several UGUA-repeats, thereby ensuring efficient cleavage and polyadenylation of an mRNA. The pre-mRNA is cleaved at the cleavage site by the endonuclease CSPF73 before the nuclear poly(A) polymerase adds ~200 As to the 3′ end. This poly(A) tail stabilizes the processed mRNA for nuclear export upon binding of the nuclear poly(A) binding protein (PABPN1) which is subsequently exchanged for its cytoplasmic counterpart PABPC which promotes translation and RNA stability (Hollerer et al. 2014).

1.2.4 Nuclear mRNA export

The formation of an mRNA that can be efficiently exported to the cytoplasm (i.e., export-competent mRNP) begins at transcription and is necessary to maintain the efficiency and fidelity of gene expression. Eukaryotes have evolved an adept system to coordinate nuclear export of mRNAs with the different processes of gene expression. The THO complex for instance, is a nuclear protein complex that is involved in the biogenesis of mRNP particles and functions at the interface between transcription and mRNA export. It is conserved from yeast to humans and the *S. cerevisiae* complex is composed of Tho2, Hpr1, Mft1, Thp2 (Chávez et al. 2000) and Tex1 (Strässer et al. 2002; Peña et al. 2012). It associates with RNAPII through the CTD of its biggest subunit Rpb1. The THO complex associates with the DECD RNA helicase Sub2 (UAP56; metazoan) and the mRNA export adaptor Yra1 (ALY/REF; metazoans) to form the transcription export (TREX) complex, an evolutionarily conserved multiprotein complex that functionally couples different steps of mRNA biogenesis, including transcription, processing, and nuclear mRNA export (Figure 5) (Strässer et al. 2002; Katahira 2012). THO mutants show reduced mRNP biogenesis efficiency: transcription impairment, hyper-recombination, accumulation of stalled mRNP intermediates and nuclear mRNA export defects, indicating that this complex is a physical and functional unit (Strässer

et al. 2002; Libri et al. 2002; Rougemaille et al. 2007; Saguez et al. 2008). The export of mRNA can be divided into distinct stages: processing and packaging of transcripts into mRNP complexes, docking of the mRNP to the NPC, targeted translocation of the mRNP through the nuclear pore complex (NPC) and directional release of the mRNP into the cytoplasm for translation (Köhler and Hurt 2007; Carmody and Wente 2009). Unlike the karyopherin-mediated directional transport of cargos across the nucleo cytoplasmic barrier that is powered by a gradient of the GTP-bound state of the GTPase Ran (Madrid and Weis 2006), nuclear mRNA export occurs via a distinct mechanism, which is independent of karyopherins. It utilizes the heterodimer Mex67-Mtr2 in *S. cerevisiae* (NXF1-NXT1/TAP-p15; metazoan) which is recruited via the TREX component Yra1 in *S. cerevisiae* (ALY/REF; metazoan) (Strässer and Hurt 2000; Zenklusen et al. 2001) and does not rely on the RanGTP gradient (Herold et al. 2000; Segref et al. 1997).

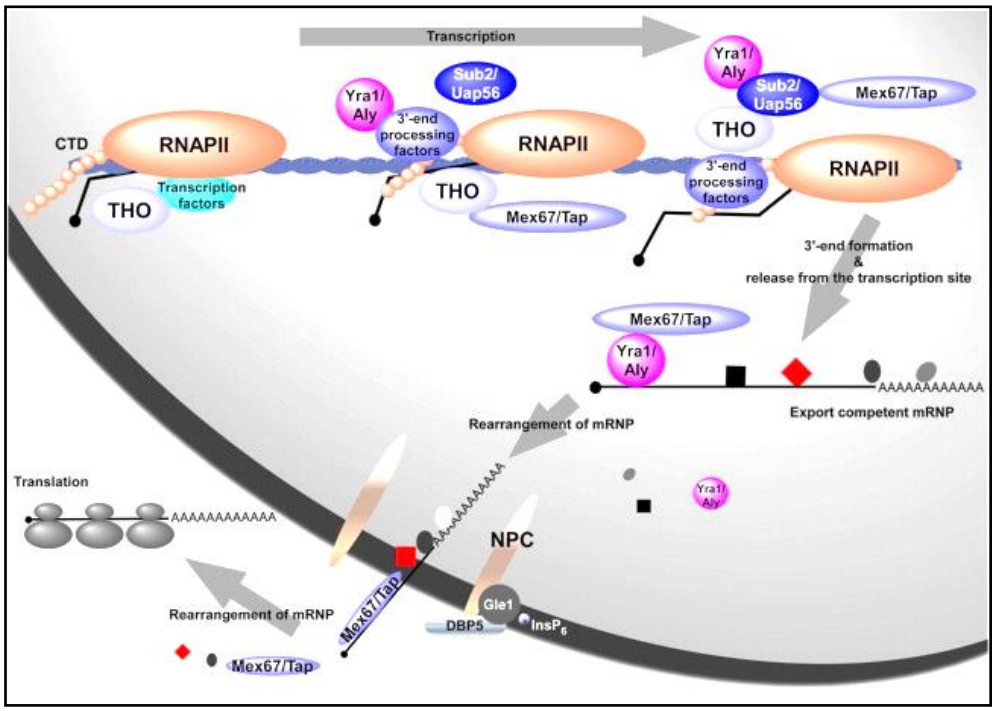

Figure 5: Nuclear export of mRNAs.
Pre-mRNA processing and nuclear export factors are loaded onto the pre-mRNA co-transcriptionally. The CTD of RNAPII serves as a recruiting platform for 3′ end processing/transcription termination factors. The THO complex associates and travels along the transcript with RNAPII. Sub2/Uap56 and the Yra1/Aly associate with the THO complex on the gene body, forming an active TREX complex. In *S. cerevisiae*, the heterodimeric mRNA export receptor Mex67-Mtr2 is recruited to the transcribed locus through its interaction with the adaptor Yra1, resulting in the formation of export-competent mRNP. The mRNP is released from the gene locus, translocated through the nuclear pore complex (NPC) with the help of Gle1, Dbp5, and the small molecule inositol hexakisphosphate ($InsP_6$) and the mRNA translated in the cytoplasm. Gray and black ovals, black square, and red diamond indicate the various RBPs that associate with or dissociate from mRNPs during mRNA processing (Köhler and Hurt 2007; Rodríguez-Navarro and Hurt 2011; Tutucci and Stutz 2011).

1.2.5 Translocation through the NPC

The export-competent mRNP is specifically targeted to the NPC by Mex67-Mtr2 to facilitate mRNA export. For some transcripts, this physically links the transcription and mRNA export (Akhtar and Gasser 2007) in a gene-gating model (Blobel 1985). At the NPC, Mex67-Mtr2 interacts with the phenylalanine-glycine (FG) repeats of nucleoporins (Nups) that span the nuclear envelope (Denning et al. 2003; Alber et al. 2007) and serve as a bridge between the mRNP and the NPC. The final step of mRNP translocation through the NPC involves directional release into the cytoplasm. The FG-Nups are symmetrical and lack directionality (Nachury and Weis 1999; Reed and Hurt 2002; Zeitler and Weis 2004), therefore an alternative mechanism exists to provide directionality. In *S. cerevisiae*, the conserved mRNA export factors, Dbp5 and Gle1, and soluble inositol hexakisphosphate ($InsP_6$) provide this directionality (Alcázar-Román et al. 2006; Weirich et al. 2006; Bolger et al. 2008; Wente and Rout 2010). Dbp5 is an RNA-dependent DEAD-box ATPase that binds to Nup159 on the NPC's cytoplasmic side (Snay-Hodge et al. 1998; Tseng et al. 1998; Schmitt et al. 1999; Weirich et al. 2004), while Gle1 binds specifically to $InsP_6$ and docks to another nucleoporin Nup42 (Murphy and Wente 1996; Strahm et al. 1999; Kendirgi et al. 2005; Alcázar-Román et al. 2006). Association of the mRNP with $InsP_6$-bound Gle1 and Dbp5 at the cytoplasmic face of the NPC stimulates the ATPase activity of Dbp5 (Tran et al. 2007), which induces a conformational change that triggers the removal of a subset of proteins from the mRNP, including Mex67-Mtr2 and the poly(A)-binding protein Nab2 (Tran and Wente 2006; Lund and Guthrie 2005). The spatially controlled remodeling of mRNP composition by the removal of certain proteins (Tran et al. 2007) confers directionality. As the mRNP enters the cytoplasm, specific cytoplasmic mRNA-binding proteins are incorporated, and nuclear factors are exchanged for their cytoplasmic counterparts. For example, the cap binding complex (CBC) is replaced with eIF4E, ribosomes bind, and translation begins before the entire mRNP is completely released from the NPC (Daneholt 2001). Aside their role in mRNA export, Dbp5, Gle1 and $InsP_6$ have roles in translation. Gle1 has a distinct role in translation initiation (Bolger et al. 2008; Wente and Rout 2010) and the assembly of the translation termination complex on the mRNA might require Gle1-$InsP_6$-dependent stimulation of Dbp5 (Gross et al. 2007). The involvement of Gle1 in mRNA export, translation initiation, and translation termination shows the inherent connections between the steps of gene expression and how some factors are adapted to perform varying roles. Given the essentiality of mRNA export in gene expression, it is not surprising that defects in this pathway lead to human neurogenerative diseases and several forms of cancer (Nousiainen et al. 2008; Kaneb et al. 2015; Culjkovic-Kraljacic and Borden 2013). For example, mutations in Gle1, that affect its role in mRNA

export, leads to a congenital syndrome that causes severe spinal cord atrophy and joint deformities (Jao et al. 2012; Folkmann et al. 2013).

1.3 The RNA helicase Sub2

Sub2 is an ATP-dependent RNA helicase with homologs in other eukaryotes and shares over 60% similarity with these homologs (HomoloGene - NCBI 2022). It belongs to the DEAD-box helicase superfamily 2 (SF2) but has a DECD motif instead of the characteristic Asp-Glu-Ala-Asp (DEAD) motif. The SF2 family of RNA helicases have a catalytic helicase core that folds like the *Escherichia coli* RecA ATPase (Story et al. 2001; Singleton et al. 2007). The 2 RecA-like domains constitute the helicase core (Figure 6) and form a cleft that harbors an ATP-binding site (Cordin et al. 2006; Linder and Jankowsky 2011) and can move freely with respect to each other in the absence of RNA and ATP (Jarmoskaite and Russell 2011). However, the cleft must be closed to efficiently bind and hydrolyze ATP (Hilbert et al. 2009). The RecA1-like domain (helicase domain 1) contains the ATP binding motifs Q, I and II, the ATP hydrolysis motif III and the RNA-binding motifs Ia and Ib. The RecA2-like domain (helicase domain 2) contains the RNA-binding motifs IV, V, and VI, which may coordinate ATPase and unwinding activities. The ATPase activity of the SF2 helicase superfamily is stimulated by binding to RNA although it does not necessarily require a specific RNA substrate (Rocak and Linder 2004).

The DEAD-box family of RNA helicases are associated with nearly all aspects of RNA metabolism, including transcription (Yan et al. 2003; Gillian and Svaren 2004), splicing (Rymond, Brian C., Michael Rosbash. 1993), ribosome biogenesis (Venema and Tollervey 1995; Kressler et al. 1998; Ripmaster et al. 1992), mRNA export (Schmitt et al. 1999; Strässer and Hurt 2001; Linder and Stutz 2001), translation (Pause and Sonenberg 1993) and RNA decay (Jacobs Anderson and Parker 1996; Margossian and Butow 1996). Many of these proteins are essential for cell viability and usually function as part of multicomplex assemblies. Considering that they are involved in a variety of mRNA biogenesis processes, no substrate specificity is expected since they will encounter a wide range of substrates. Contacts to RNA are made predominantly to the phosphate-sugar backbone by the conserved sequence motifs (Linder and Jankowsky 2011), with additional bases required for helicase activity (Saikrishnan et al. 2009; Gu and Rice 2010). They are also non-processive, unwinding short duplexes with a step size of around 5-6 bp (Rogers et al. 1999). Due to their non-processivity, they lack directionality (Pyle 2008), which makes them easily accessible to duplex RNA to initiate local strand separation (Yang and Jankowsky 2006; Yang et al. 2007), a mechanism well suited for mRNP remodeling in the cell.

Similar to other DEAD-box proteins, Sub2 contains a catalytic helicase core with eight conserved domains (Figure 6) and uses ATP to bind and remodel nucleic acids or nucleic

acid-protein complexes (Abdel-Monem et al. 1976; Singleton et al. 2007; Lohman et al. 2008; Pyle 2008).

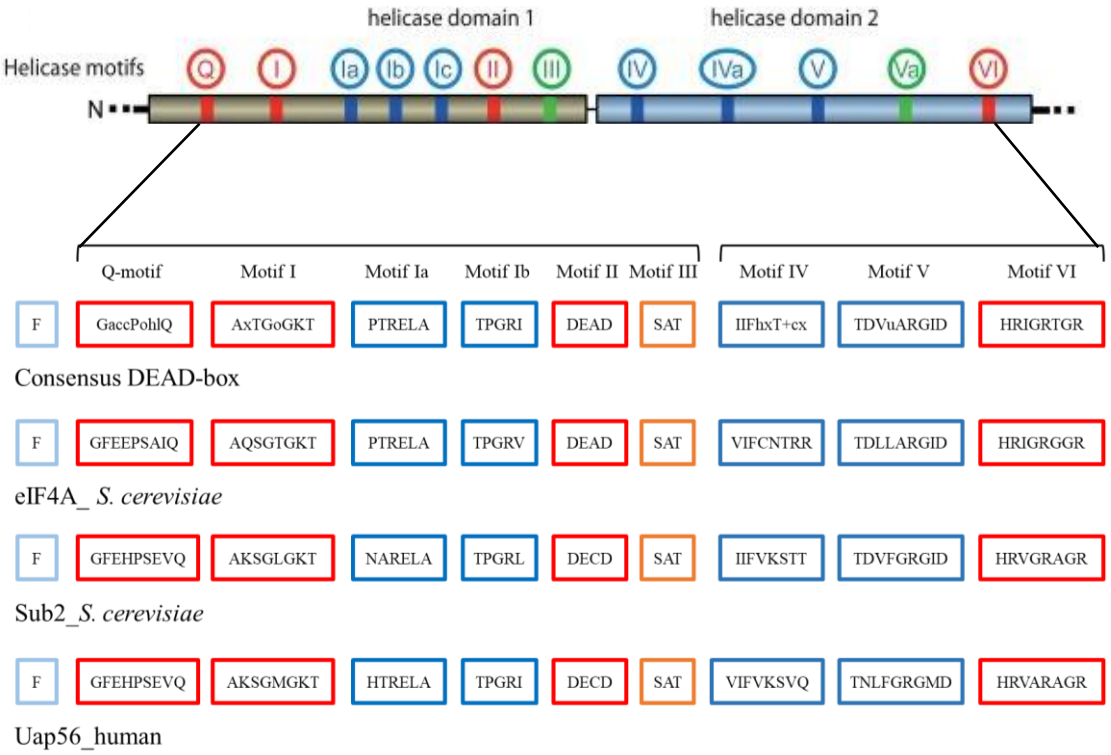

Figure 6:Conserved motifs of the DEAD-box RNA helicase family.
Sequences of the conserved motifs from S. cerevisiae eIF4A and Sub2, and Uap56 (human). The motifs Q, I, II and VI are involved in ATP binding and hydrolysis. Motifs Ia, Ib, Ic, IV, IVa and V mediate RNA binding while motifs III and Va coordinates NTP hydrolysis to RNA binding. Adapted from Cordin et al. (2006); Saguez et al. (2013).

Sub2 is involved in diverse stages of mRNA maturation. Studies have shown the role of Sub2 in splicing, polyadenylation and nuclear mRNA export. It is also important for genome stability (Fan et al. 2001; Jimeno et al. 2002) and gene expression at telomeres (Lahue et al. 2005; Yoo and Chung 2011). Sub2 together with Prp5, is involved in the formation of the pre-spliceosome (Perriman and Ares 2000; Kistler and Guthrie 2001; Perriman et al. 2003), Prp28 and Brr2 are required for activation of the spliceosome (Raghunathan and Guthrie 1998; Staley and Guthrie 1999), Prp2 and Prp16 are required for the catalytic transesterification reactions (Kim and Lin 1996; Schwer and Guthrie 1991), and Prp22 and Prp43 are required to disassemble the spliceosome (Company et al. 1991; Arenas and Abelson 1997; Tsai et al. 2005). *In vitro* spliceosome assembly requires Sub2/UAP56 (Fleckner et al. 1997; Libri et al. 2001; Kistler and Guthrie 2001). Libri et al. (2001) showed that Sub2-defective extracts were unable to splice a *RP51A* derived intron and a U3 snRNA intron *in vitro*. However, the splicing of both endogenous genes *in vivo* was not affected in Sub2-depleted cells. This contrasts the absolute requirement of Sub2 for splicing *in vitro*. Unlike most splicing factors that show a preference to specific intron consensus features, Sub2 shows no intron bias (Moore et al.

2006) and is recruited by the heterodimer Msl5/BBP and Mud2/U2AF65 to the branch site of introns. Recruitment of Sub2 to the branch site releases Msl5-Mud2 and allows the U2 snRNP to bind the branch site (Zhang and Green 2001; Wang et al. 2008). The removal of Mud2 by Sub2 facilitates association of U2 snRNP with the spliceosome, and the depletion of Mud2 can bypass the requirement of Sub2 for this step (Kistler and Guthrie 2001). Sub2 plays a role in at least two steps of spliceosome formation that precede and follow the U2 snRNP addition. Depletion of Sub2 results in the accumulation of the CC2 commitment complex (Complex E) suggesting a slow rate of pre-spliceosome formation (Libri et al. 2001; Zhang and Green 2001), but not CC1. Moore et al. (2006), showed that the recruitment of the U2 snRNP protein Lea1 and the U5 snRNP protein Brr2, to intron containing genes (ICGs) was reduced using a splicing defective mutant of Sub2. Thus, the findings from these studies strongly suggest a role of Sub2 in pre-spliceosome formation.

The role of Sub2 in efficient polyadenylation has been shown in studies where mutants of Sub2 exhibit polyadenylation defects. Inefficient polyadenylation triggers a surveillance mechanism that accelerates mRNA degradation by the nuclear exosome degradation machinery (Houseley et al. 2006). PAR-CLIP and ChIP analysis reveal that the occupancy of Sub2 and other TREX components increases from the transcription start site (TSS) and declines near the poly (A) sites as the occupancy of 3′ processing factors increase at the 3′ end of genes (Baejen et al. 2014; Johnson et al. 2011). *In vivo* nuclear run-ons in Sub2 and THO mutants show a premature transcription termination in proximity to the poly(A) site and demonstrate an exosome-dependent mRNA surveillance that recognizes a defect in transcription and prevents polyadenylation from occurring (Saguez et al. 2008). *In vitro* extracts from temperature-sensitive mutants of Sub2 mutants also show severe defects in 3′ end processing, as well as reduced 3′ end fragments of the heat shock protein transcript, *HSP104*, while the 5′ end remains unaffected *in vivo* (Libri et al. 2002; Rougemaille et al. 2007). The molecular basis for this defect is not a lack of Sub2, but rather reduced levels of the Poly(A) polymerase factor Fip1 which is removed from the transcript due to a defective Sub2 (Saguez et al. 2008). These studies suggest that Sub2 together with the THO complex influences the stability of mRNA while coordinating 3′ end processing with mRNP export.

The formation of an export-competent mRNP requires the co-transcriptional recruitment of the mRNA export factors Yra1 and Sub2 (Strässer and Hurt 2000, 2001; Zenklusen et al. 2001). Meta gene occupancy profiles from ChIP and PAR-CLIP have confirmed the occupancy of Sub2 on the gene body (Baejen et al. 2014; Johnson et al. 2011; Meinel et al. 2013). The THO complex contacts Sub2, which forms a semi-open conformation and primes Sub2 for mRNP engagement (Ren et al. 2017). Sub2 recruits Yra1 to the mRNP, which then recruits Mex67-Mtr2 (Strässer and Hurt 2000). Binding of Yra1 to Mex67-Mtr2 may displace Sub2 from the

mRNP (Strässer and Hurt 2001) since binding of Sub2 and Mex67-Mtr2 to Yra1 is mutually exclusive (Ren et al. 2017). Both THO and Yra1 also stimulate the ATPase activity of Sub2 (Ren et al. 2017). Taniguchi and Ohno (2008) showed that ATP-bound UAP56 (Sub2) stimulates the binding of ALY (Yra1) to mRNA, which further increases the ATPase activity of UAP56 to remodel the mRNP landscape. ALY then binds NXF1-NXT1 (Mex67-Mtr2), which gains an RNA-binding affinity in the presence of ALY, to form a ternary complex. The RNA-binding ability of NXF1 (Mex67) is essential as mutants that bind ALY, but not mRNA have an mRNA export defect (Hautbergue et al. 2008). This suggests a coordinated mode of protein recruitment that ensures mRNA export from the nucleus. If a transcript is not properly processed, it is retained in the nucleus and degraded by the nuclear surveillance machinery, the exosome.

Recombination during transcription is a common phenomenon that occurs from bacteria to humans (Ikeda and Kobayashi 1977; Thomas and Rothstein 1989; Nickoloff and Reynolds 1990). Recombination can result in the formation R-loops. An R-loop is formed when mRNA hybridizes to a template DNA strand leaving an unpaired non-template DNA strand (Gan et al. 2011). R-loops are intermediates of transcription associated recombination (TAR) and play a role in origin-independent replication in prokaryotes (Kogoma 1997), immunoglobulin class-switching recombination (Yu et al. 2003), pause site-dependent transcription termination (Skourti-Stathaki et al. 2011) and regulation of lncRNA expression (Sun et al. 2013). Although R-loops are relevant physiologically, they can contribute to genome instability as a result of DNA rearrangements when allowed to persist (Huertas and Aguilera 2003; Li and Manley 2005). The co-transcriptional packaging and processing of the mRNA into an mRNP packages the mRNA and prevents it from hybridizing with the template DNA (González-Aguilera et al. 2008; Wahba et al. 2011; Gómez-González et al. 2011; Stirling et al. 2012; Luna et al. 2005). Helicases also act to resolve R-loops by unwinding the RNA:DNA hybrid to generate a double-stranded (ds) DNA and a free mRNA (Mischo et al. 2011; Cargill et al. 2021). The importance of Sub2 in R-loop resolution has been shown in studies where mutations in Sub2 (Saguez et al. 2013) or a lack of Sub2/UAP56 results in transcription-dependent hyperrecombination leading to genome instability (García-Rubio et al. 2008; Domínguez-Sánchez et al. 2011). Aguilera and Klein 1990 showed in a THO mutant (Δ*hpr1*) strain that has a hyperrecombination phenotype, that overexpressing Sub2 rescues this phenotype (Fan et al. 2001; Jimeno et al. 2002), presumably by removing the R-loops. The ability of Sub2 to resolve R-loops lies in its affinity for RNA:DNA duplexes (Pérez-Calero et al. 2020) where binding to the RNA in the hybrid induces its helicase activity to unwind the RNA:DNA hybrid (Schuller et al. 2020).

1.4 Approaches to the study of the function of Sub2

Sub2 was initially identified as suppressor of the cold sensitive phenotype of *brr1-1* (Noble 1995). To characterize it, sequence comparison similar to proteins in other organisms (Nair et al. 1992; Zhang and Green 2001) and other helicases were performed (Gorbalenya and Koonin 1993). Based on these initial studies, the functions of Sub2 were proposed from the functions of related RNA helicases. This comparative analysis provided preliminary information that enabled the characterization of Sub2 and the processes it may be involved in. Further on, deletion mutants of Sub2 were also generated to study its role. Recent studies have generated conditional mutants. Conditional mutants were randomly generated that have growth defects and impaired protein function (Libri et al. 2001; Kistler and Guthrie 2001; Zhang and Green 2001; Jensen et al. 2001; Strässer and Hurt 2001). These studies of Sub2 provided insight into the function of Sub2 in the cell, as for the first time, specific roles were assigned to Sub2. However, they selected against mutations that had no visible growth and mRNA export defects but may have been involved in other processes involved in gene expression, had they been further characterized. Recent approaches to study Sub2 function now involve mutation of specific residues in its motifs (Saguez et al. 2013). These studies have the advantage that they define motifs that are important for specific functions in mRNA biogenesis. For example, Saguez et al. (2013). showed that, the N-terminal motif of Sub2 functions as an autonomous unit that has a role in growth and mRNA export but not RNA helicase activity using mutational analysis. Studies aimed at solving the structure of Sub2 in association with other macromolecules and how these complexes are vital to Sub2 function are currently ongoing.

To gain more insight into the molecular mechanisms of Sub2 in mRNP biogenesis, this study focused on the mRNA-binding sites of Sub2, and we generated mutants thereof.
The specific aims of the study were to:

1. Generate mutants of amino acids identified to crosslink to RNA *in vivo*.

Amino acids that have been identified to interact with mRNA (Keil 2021) were mutated based on amino acid conservation and structural predictions of how a mutation would affect protein structure and stability. *In silico* prediction tools were employed to select for appropriate mutations.

2. Determine how these mutations affect the function of Sub2 in mRNA biogenesis.

Biochemical analyses were employed to study the effects of the amino acid mutations on growth, splicing and mRNA export. Changes in mRNP composition were studied, using TAP purifications.

3. Identify the relevance of the amino acid for Sub2's helicase function.

The effect of the mutations on the helicase function of Sub2 were tested. Binding of the mutants to RNA, helicase activity and R-loop resolution were studied.

2 Materials

2.1 Chemicals and consumables

Table 1: Chemicals and Consumables

Chemicals and Consumables	Supplier
2-Propanol	Carl Roth
4-Thiouracil	Abcr GmbH
5-Fluoroorotic acid (5-FOA)	Apollo Scientific Ltd
Acetic acid	VWR Chemicals
Acrylamide (29:1) 40 %	AppliChem GmbH
Adenine hemisulfate salt	Sigma-Aldrich
Agar Bacteriology grade	Applichem GmbH
Agarose	Applichem GmbH
Ammonium persulfate (APS)	VWR Chemicals
Ampicillin	Applichem GmbH
Bacto™ Peptone	BD Biosciences
Bacto™ Yeast extract	BD Biosciences
Benzamidine HCl	MP Biomedicals
Boric acid (BH_3O_3)	Applichem GmbH
Bovine serum albumin (BSA)	Carl Roth
Bromophenol blue	Applichem
Calcium chloride ($CaCl_2$)	Fluka
Calmodulin Affinity resin	Agilent Technologies
Chloroform	Merck
Coomassie Brilliant Blue G-250	Applichem
Coomassie Brilliant Blue R-250	Applichem
Dextran sulfate	Sigma-Aldrich
D-Galactose	Applichem GmbH
D-Glucose Monohydrate	Sigma-Aldrich
Dimethyl sulfoxide (DMSO)	Grüssing GmbH
Dipotassium phosphate (K_2HPO_4)	Grüssing GmbH
Disodium phosphate (Na_2HPO_4)	Carl Roth
Dithiothreitol (DTT)	Sigma-Aldrich
dNTPs (dATP, dTTP, dCTP, dGTP)	Thermo Fisher Scientific
D-Sorbitol	Carl Roth
Dynabeads™ M-280 Tosylactivated	Invitrogen
E. coli tRNA	Roche diagnostics
ECL Solution	Applichem
Ethanol	Fisher Chemical
Ethylenediaminetetraacetic acid (EDTA)	Sigma-Aldrich
Ethyleneglycol-bis(aminoethylether)tetraacetic acid (EGTA)	Merck
FLAG® Peptide	Sigma-Aldrich
Formaldehyde	ORG Laborchemie
Formamide	Merck
Gel loading dye, purple (6x)	NEB
Gel loading dye, purple (6x) w/o SDS	NEB
Genetecin (G418)	ThermoFisher (Gibco)
Glycerol	Carl Roth
Glycine	Labochem international
HDGreen™ DNA stain	Intas
HEPES	Carl Roth
Herring Sperm DNA	ThermoFisher (Invitrogen)

Hydrochloric acid (HCl)	Carl Roth
IGEPAL CA-630	Sigma-Aldrich
IgG Sepharose 6 Fast Flow	GE Healthcare
Imidazole	Merck
Isopropyl β-D-1-thiogalactopyranoside (IPTG)	Carl Roth
Kanamycin	Merck
L-Arginine-HCl	Biomol GmbH
L-Aspartic acid	Sigma-Aldrich
Leupeptin (Hemisulfate)	Carl Roth
L-Histidine	Sigma-Aldrich
L-Isoleucine	Sigma-Aldrich
Lithium acetate (LiOAc)	Carl Roth
Lithium chloride (LiCl)	Merck
L-Leucine	Sigma-Aldrich
L-Lysine Monohydrochloride	Sigma-Aldrich
L-Methionine	Sigma-Aldrich
L-Phenylalanine	Sigma-Aldrich
L-Threonine	Sigma-Aldrich
L-Tryptophan	Sigma-Aldrich
L-Tyrosine	Sigma-Aldrich
L-Valine	Biomol GmbH
Magnesium chloride ($MgCl_2$)	Merck
Magnesium sulfate ($MgSO_4$)	Carl Roth
Methanol	Merck-Millipore
Monopotassium phosphate (KH_2PO_4)	Carl Roth
Monosodium phosphate (NaH_2PO_4)	Merck
Nicotinamide adenine dinucleotide (NAD)	Sigma Aldrich
Octylphenoxypolyethoxyethanol (IGEPAL CA-630)	Sigma-Aldrich
Pepstatin A	Applichem GmbH
Phenylmethane sulfonyl fluoride (PMSF)	Carl Roth
Phosphoric acid	Carl Roth
Polyethylene glycol (PEG) 3800/4000	Carl Roth
Polylysine	Sigma-Aldrich
Polysorbate 20 (Tween 20)	Merck
Polyvinylpyrrolidone (PVP)	Sigma-Aldrich
Ponceau S	Serva
Potassium chloride (KCl)	ORG Laborchemie
Potassium hydroxide (KOH)	Merck
Powdered milk, fat free, blotting grade	Carl Roth
Protino® Ni-NTA Agarose	Macherey-Nagel
Rothi®-Mount FluorCare DAPI	Carl Roth
Roti®-Aqua-Phenol	Carl Roth
Salmon sperm DNA (SSD)	Applichem GmbH
Sodium acetate (NaOAc)	Merck
Sodium chloride (NaCl)	Merck
Sodium citrate	Carl Roth
Sodium deoxycholate	Sigma-Aldrich
Sodium dodecyl sulfate (SDS)	Serva
Sodium hydroxide (NaOH)	Merck
Sorbitol	Carl Roth
Sulfosalicylic acid	Merck
Tetramethylethylendiamin (TEMED)	Carl Roth
Trichloroacetic acid (TCA)	Merck

Tris(hydroxymethyl)aminomethane (Tris)	Applichem GmbH
Triton X-100	Applichem GmbH
Tryptone BioChemica	Applichem GmbH
Uracil	Sigma-Aldrich
Yeast nitrogen base, w/o amino acids	Formedium

2.2 Equipment and devices

Table 2: Equipment and devices

Name	Supplier
70 Ti	Beckman Coulter
AM100, micro scale	Mettler-Toledo
Apollo®, liquid nitrogen container	Cryotherm
Avanti JXN-26 Centrifuge	Beckman Coulter
Axio observer, fluorescence microscope	Zeiss
BLX-254, UV-crosslinker	Vilber Lourmat
ChemoCam Imager ECL HR 16-3200	Intas
DeltaVision Ultra microscope	GE Healthcare
Duomax 1030, tumbling shaker	Heidolph Instruments
EPS 301, electrophoresis power supply	GE Healthcare
FastPrep-24^{TM} 5G	MP Biomedicals
Freezer/Mill® 6870D	Spex®SamplePrep
Gel iX20, Transilluminator/gel docu	Intas
Hera safe, laminar flow cabinet	Thermo Fisher Scientific
HeraFreeze HFU T Series	Thermo Scientific
HT Multitron Pro shaking incubator	Infors
HXP 120 V, light source	Kübler Codix
IKA® KS 4000 ic control, shakingincubator	IKA Labortechnik
IKAMAG® RCT, magnetic stirrer	IKA Labortechnik
Incubator with HT Labotron, shaker	Aqua Lytic / Infors
Incubators	Memmert
Innova®44 shaking incubator	Eppendorf / New Brunswick
JLA-8.1, JA-25.50, JA-10	Beckman Coulter
Lab phenomenal pH 1000L, pH meter	VWR
LED bluelight transilluminator	Nippon genetics
Megafuge 40R	Thermo Scientific, Heraeus
Milli-Q® integral water purificationsystem	Merck
Mini-Protean® Tetra Electrophoresis Cell	Bio-Rad Laboratories
ND-1000, Spectrophotometer	NanoDrop
Optima XPN-80 Ultracentrifuge	Beckman Coulter
PeqStar XS Thermocycler	Peqlab
Pipetboy acu	IBS Integra Biosciences
PM2000, scale	Mettler-Toledo
Quant Studio 3, Real Time PCR System	Applied Biosystems, ThermoFisher Scientific
RCT basic, magnetic stirrer	IKA Labortechnik
Research Pipettes 2.5, 10, 20, 100, 200,1000	Eppendorf
Rotator	NeoLab
SBH130D, block heater	Stuart®
Superdex 75 10/300 GL	GE Healthcare
SW22, shaking waterbath	Julabo

T3 Thermocycler	Biometra
Tabletop Centrifuge 5424, 5424R	Eppendorf
Tabletop Centrifuge 5430, 5430R	Eppendorf
Thermomixer 5436	Eppendorf
Trans-Blot® Turbo Transfer System	Bio-Rad Laboratories
Typhoon FLA 9500	GE Healthcare
Vakulan CVC 3000	Vacuubrand
VF2, vortex mixer	IKA Labortechnik
VX-150, autoclave	Systec
WT 12, tumbling shaker	Biometra

Table 3: Software for image analysis and quantification

Name	Developer
GelQuantNet	BiochemLab Solutions
ImageJ	National Institutes of Health
ImageQuantTL	Cytiva
Origin	OriginLab Corporation
QuantStudio Design and Analysis software	ThermoFischer Scientific

2.3 Buffers, Media, and Solutions

2.3.1 Media

All solutions and media were prepared using water filtered by the Milli-Q-synthesis System (Millipore) and autoclaved at 120°C for 20 min. Heat sensitive solutions and buffers were sterile filtered through a 0.22 µm filter.

Lysogeny broth (LB) for 1 L
10 g peptone
5 g yeast extract
5 g NaCl
adjust to pH 7.2 (NaOH)
(15 g agar for plates)

SOC for 100 mL
2 g tryptone
0.5 g yeast extract
10 mM NaCl
0.5 mM KCl
10 mM $MgCl_2$
10 mM $MgSO_4$
adjust pH to 7.0 (NaOH)

Synthetic dropout medium (SDC) for 1 L
6.75 g yeast nitrogen base (w/o aa)
0.6 g complete synthetic amino acid mix CSM
20 g glucose
10 mL of each 100x amino acid stock except the
required drop out
adjust pH to 5.5 (NaOH)
(15 g agar for plates // 1 g 5-FOA if required)

Yeast complete medium (YPD) for 1 L
10 g yeast extract
20 g peptone
20 g glucose
adjust to pH 5.5 (HCl)
(15 g agar for plates)

2.3.2 Buffers and solutions

Cloning

50x TAE buffer
2 M TRIS
1 M NaOAc
50 mM EDTA (pH 8.0)
adjust to pH 8.0 (acetic acid)

6 x Agarose loading dye
0.03 % Bromophenol blue
0.03 % Xylene cyanol
60 % Glycerin
60 mM EDTA
10 mM TRIS

5x Isothermal reaction buffer
25 % PEG-8000
500 mM TRIS (pH 7.5)
50 mM $MgCl_2$
50 mM DTT
1 mM of each dNTP
5 mM NAD^+

Gibson assembly master mix
1x Isothermal reaction buffer
4 U/µL T5 exonuclease
4 U/µL Taq DNA ligase
25 U/mL Phusion DNA polymerase

SDS-PAGE

4x Separating buffer
1.5 M TRIS (pH 8.8)
8 mM EDTA
0.6% SDS

4x Stacking buffer
0.5 M TRIS (pH 6.8)
8 mM EDTA
0.6% SDS

Separating gel (10 %)
3 mL Acrylamide (40%, 29:1)
3 mL 4x separating buffer
6 mL H2O
100 µL 10% APS
100 µL TEMED

Stacking gel (4%)
400 µL Acrylamide (40%, 29:1)
1 ml 4x Stacking buffer
2.6 ml H2O
30 µL 10% APS
10 µL TEMED

6x SDS loading dye
7 mL stacking buffer
40 % glycerol
10 % SDS
0.5 M DTT
0.03 % bromophenol blue
1 % β-mercaptoethanol

Hot-Coomassie
0.5 % Coomassie R250
25% Isopropanol
10% Acetic acid

Destaining solution
10 % acetic acid

10x Running buffer
250 mM TRIS
1.9 M Glycine
1 % SDS

Western blotting

10x TBST (TRIS buffered saline + tween)
500 mM TRIS (pH 7.5)
1.4 mM NaCl
1% Tween 20

Semi dry Western blot buffer
25 mM TRIS
192 mM Glycine
20% Methanol

Pre-treatment solution
7.5% ß-Mercaptoethanol
1.85 M NaOH

10x TBS-T (TRIS buffered saline + tween)
500 mM TRIS (pH 7.5)
1.4 mM NaCl
1% Tween 20

Yeast transformation

Solution I
1X TE
100 mM LiOAc

Solution II
1X TE
100 mM LiOAc
40% PEG 3,800 (or PEG 4,000)

10x TE
100 mM TRIS (pH 7.5)
10 mM EDTA (pH 8.0)

Tandem affinity purification (TAP)

Wash buffer
50 mM TRIS (pH 7.5)
1.5 mM $MgCl_2$
100 mM NaCl
0.15% NP 40
1 mM DTT
(1x Protease inhibitor)

100x protease inhibitor (in 50 mL EtOH)
6.85 mg pepstatin A
1.42 mg Leupeptin hemisulfate
850mg PMSF
1.65 g Benzamide HCl

RNA immunoprecipitation (RIP)

RNA IP-Buffer
25 mM TRIS (pH 7.5)
150 mM NaCl
2 mM MgCl
0.5% Triton X 100
500 µL DTT

Fluorescence *in situ* hybridization

Prehybridization buffer
50 % formamide
10 % dextran sulphate
125 µg/mL tRNA (E. coli)
500 µg/mL herring sperm DNA
4 x SSC
1 x Denhardt's solution

Sorbitol wash buffer
1.2 M Sorbitol
100 mM KPO_4 (pH 6.4)

20 x SSC (pH 7.0)
3 M NaCl
300 mM sodium citrate

50x Denhardt's solution
1 % polyvinylpyrrolidone (PVP)
1 % bovine serum albumin (BSA)
1 % ficoll-400

Immunofluorescence

Cell resuspension buffer
1% BSA
0.5% NaN_3
1x PBS

Antibody dilution buffer
1% BSA
0.5% NaN_3
1% BSA
0.15M NaCl
0.04M K_2HPO_4
1x PBS
0.15 M NaCl

Antibody wash buffer
1% BSA
0.5% NaN_3
1x PBS
0.3% Triton X-100
0.04 M K_2HPO_4
0.01 M KH_2PO_4

***In vitro* Protein purification**

Lysis Buffer
300 mM KCl
50 mM HEPES pH 7.5
10% glycerol
5 mM Imidazole
5 mM ß-Mercaptoethanol

Wash buffer
5 mM ß-Mercaptoethanol
1 M KCl
50 mM HEPES pH 7.5
15 mM imidazole
5 mM ß-Mercaptoethanol

Dialysis buffer
50 mM Bis-Tris pH 6.5
50 mM KCl
5 mM ß-Mercaptoethanol

Elution buffer
300 mM KCl
50 mM HEPES pH 7.5
10% glycerol
500 mM Imidazole
5 mM ß-Mercaptoethanol

Equilibration buffer
100 mM KCl
50 mM Bis-Tris pH 6.5
5 mM ß-Mercaptoethanol

Storage buffer
1M KCl
50 mM Bis-Tris pH 6.5
5 mM ß-Mercaptoethanol
30% Glycerol

Helicase buffer
20 mM MES (pH 6.5)
4 mM TCEP
2 mM $MgCl_2$

Binding buffer
10 mM MES (pH 6.5)
2 mM TCEP
5% Glycerol
0.5 mM $MgCl_2$
1 mM ADNDP

Annealing buffer
60 mM KCl
6 mM HEPES-pH 7.5
0.2 mM $MgCl_2$

2.4 Organisms

2.4.1 Yeast strains

Table 4: Yeast strains

Yeast strain	Genotype	Reference
RS453	MAT a, ade2-1, his3-11,15, ura3-52, leu2-3,112, trp1-1, can1-100, GAL+	(Strässer and Hurt 2000)
W303	MAT a, ura3-1, trp1-1, his3-11,15, leu2-3,112, ade2-1, can1-100, GAL+	(Thomas and Rothstein 1989)
Δmex67, pUN100-*mex67-5*	MAT a, ura3-1, trp1-1, his3-11,15, leu2-3,112, ade2-1, can1-100, GAL+, MEX67::HIS3, mex67-5::	(Hurt et al. 1999)
SUB2-yeGFP	MAT a, ade2-1, his3-11,15, ura3-52, leu2-3,112, trp1-1, can1-100, GAL+, SUB2-yeGFP::klTRP1	Sträßer Lab, 2007
Sub2-shuffle (RS453)	MAT a, ura3-1, trp1-1, his3-11,15, leu2-3,112, ade2-1, can1-100, GAL+, *SUB2*::KanMX, pYCH-*SUB2*::*URA3*	This study
Sub2-shuffle (W303)	MAT a, ura3-1, trp1-1, his3-11,15, leu2-3,112, ade2-1, can1-100, GAL+, *SUB2*::KanMX, pYCH-*SUB2*::*URA3*	This study
Sub2-shuffle, *KAP95*-Myc	MAT a, ade2-1, his3-11,15, ura3-52, leu2-3,112, trp1-1, can1-100, GAL+, *SUB2*::KanMX, pYCH-*SUB2*::*URA3*, *KAP95*-Myc::TRP1	This study
SUB2-yeGFP, *Δmtr10*	MAT a, ade2-1, his3-11,15, ura3-52, leu2-3,112, trp1-1, can1-100, GAL+, SUB2-yeGFP::klTRP1, MTR10::HIS3	This study

2.4.2 *Escherichia coli* strains

For any kind of cloning, DH5α cells were used and BL21 Star (DE3) cells were used for protein expression.

Table 5: *E. coli* strains

E. coli strain	Genotype	Reference
DH5α	F– endA1 glnV44 thi-1 recA1 relA1 gyrA96 deoR nupG purB20 φ80dlacZΔM15 Δ(lacZYA-argF) U169, hsdR17(rK–mK+), λ–	(Taylor et al. 1993)
BL21 Star (DE3) Rosetta	F– ompT gal dcm lon hsdSB(rB–mB–) λ (DE3 [lacI lacUV5-T7p07 ind1 sam7 nin5]) [malB+] K-12(λS) rne131	(Wood 1966)

2.5 Plasmids

Table 6: Plasmids

Plasmid	Description	Reference
pYCG-*SUB2*	pBlueScript based yeast centromere vector wit ORF + 500 bp of 5' and 300 bp of 3' UTR of *SUB2 URA3*	Euroscarf
pRS315	pBlueScript based yeast centromere vector, *LEU*	(Sikorski and Hieter 1989)
pRS315-TAP-ADH1	TAP-tag cloned into the XhoI and SalI sites (pRS315	Sträßer Lab, 2006
pRS315-*SUB2*	ORF + 500 bp of 5' and 300 bp of 3' UTR of *SUB2* was cloned into pRS315	Sträßer Lab, 2011
pRS315-*sub2-K53D, Y56D*	*sub2-K53D, Y56D*	This study
pRS315-*sub2-T62A*	*sub2-T62A*	This study
pRS315-*sub2-T62D*	*sub2-T62D*	This study
pRS315-*sub2-K70D*	*sub2-K70D*	This study
pRS315-*sub2-Y144E*	*sub2-Y144E*	This study
pRS315-*sub2-K202E, Y203E*	*sub2-K202E, Y203E*	This study
pRS315-*sub2-F234E, R235E*	*sub2-F234E, R235E*	This study
pRS315-*sub2-R260A, F261A*	*sub2-R260A, F261A*	This study
pRS315-*sub2-R368A*	*sub2-R368A*	This study
pRS315-*sub2-Y390A, Y393E*	*sub2-Y390A, Y393E*	This study
pRS315-*sub2-K403D*	*sub2-K403D*	This study
pRS315-*SUB2*-TAP	*SUB2*-2x protein A-TEV-CBP	This study
pRS315-*sub2-K53A, Y56A*-TAP	*sub2-K53A, Y56A*-2x protein A-TEV-CBP	This study
pRS315-*sub2-K53D, Y56D*-TAP	*sub2-K53D, Y56D*-2x protein A-TEV-CBP	This study
pRS315-*sub2-T62A*-TAP	*sub2-T62A*-2x protein A-TEV-CBP	This study
pRS315-*sub2-T62D*-TAP	*sub2-T62D*-2x protein A-TEV-CBP	This study
pRS315-*sub2-K70D*-TAP	*sub2-K70D*-2x protein A-TEV-CBP	This study
pRS315-*sub2-Y144E*-TAP	*sub2-Y144E*-2x protein A-TEV-CBP	This study
pRS315-*sub2-K202E, Y203E*-TAP	*sub2-K202E*, Y203E-2x protein A-TEV-CBP	This study
pRS315-*sub2-K403D*-TAP	*sub2-K403D*-2x protein A-TEV-CBP	This study
pRS315-*sub2-K202E*-TAP	*sub2-K202E*-2x protein A-TEV-CBP	This study
pRS315-*sub2-Y202E*-TAP	*sub2-Y203E*-2x protein A-TEV-CBP	This study
pKW430	pBluescript based yeast centromere vector with *URA3* gene, NES, 2x GFP and NLS	Gift from Karsten Weis
pNOP-GFP-NLS	GFP-NLS	This study
GFP-*sub2-K202E, Y203E*-NLS	*sub2-K202E-Y203E* cloned into pNOP-GFP-NLS	This study
sub2-K202E, Y203E-NLS-TAP	*sub2-K202E, Y203E*-NLS cloned into pRS315-TAP-ADH1	This study
pNOP-2xGFP-NES	2xGFP-NES	This study

GFP-*SUB2*-NES	NES tagged onto *SUB2* in pNOP-GFP-*SUB2*	This study
SUB2-NES-TAP	NES tagged onto *SUB2* in pRS315-*SUB2*-TAP	This study
pT7-His_6-TEV-*SUB2*	Recombinant expression of *SUB2* in *E. coli*	Sträßer Lab
pT7-His_6-TEV-*sub2-T62D*	Recombinant expression of *sub2-T62D* in *E. coli*	This study
pT7-His_6-TEV-*sub2-K70D*	Recombinant expression of *sub2-K70D* in *E. col*	This study
pT7-His_6-TEV-*sub2-K202E*, *Y203E*	Recombinant expression of *sub2-K202E*, *Y203* in *E. coli*	This study

2.6 Oligonucleotides

Table 7: Oligonucleotides used for fluorescence *in situ* hybridization

Name	Sequence	Assay
Cy3-Oligo(dT_{50})	50x T coupled with Cy3 fluorescent dye	FISH

Table 8: Oligonucleotides used for *in vitro* assays

Name	Sequence	Modification
RNA Putnam13	AGC-ACC-GUA-AAG-A	
RNA_Putnam_25_Cy5	UCU-UUA-CGG-UGC-UUA-AAA-CAA-AAC-AAA-ACA-AAA-CAA-AA	Cy5 5'
RNA_Putnam_13_Cy3	AGC-ACC-GUA-AAG-A	Cy3 3'

Table 9: Oligonucleotides used for cloning and gene tagging

Name	Sequence
pRS315 fwd	GGCCAGTGAATTGTAATACGACTCA
pRS315 rev	CCCTCACTAAAGGGAACAAAAGCTG
pRS315-TAP fwd	ATTTGAATAATGAGAAGAGAAGATGGAAAAAGAATTTCATAGC
pRS315-TAP rev	TGAGTCGTATTACAATTCACTGGCC
SUB2-TAP fwd	GGCCAGTGAATTGTAATACGACTCA
SUB2-TAP rev	TCTTCTCTTCTCATTATTCAAATAAGTGGACGGATCAATG
sub2-K53A-Y56A fwd	GCTGGCGACAAGGCAGGTTCCGCTGTTGGTATCCAT
sub2-K53A-Y56A rev	ATGGATACCAACAGCGGAACCTGCCTTGTCGCCAGC
sub2-K53D-Y56D fwd	GCAGCTGGCGACAAGGATGGTTCCGATGTTG
sub2-K53D-Y56D rev	CAACATCGGAACCATCCTTGTCGCCAGCTGC
sub2-T62A fwd	GGTATCCATTCCGCCGGTTTCAAAGAT
sub2-T62A rev	ATCTTTGAAACCGGCGGAATGGATACC
sub2-T62D fwd	GGTATCCATTCCGACGGTTTCAAAGAT
sub2-T62D rev	ATCTTTGAAACCGTCGGAATGGATACC
sub2-K70D fwd	AAGATTTCTTGCTAGACCCAGAACTATCAAG
sub2-K70D rev	CTTGATAGTTCTGGGTCTAGCAAGAAATCTT
sub2-Y144E fwd	AGAGAACTGGCCGAACAAATTCGTAAC
sub2-Y144E rev	GTTACGAATTTGTTCGGCCAGTTCTCT

sub2-K202E fwd	GTTAGTGAGAGAAGAATACATTGATTTGTCAC
sub2-K202E rev	GTGACAAATCAATGTATTCTTCTCTCACTAAC
sub2-Y203E fwd	GTTAGTGAGAGAAAAAGAGATTGATTTGTCAC
sub2-Y203E rev	GTGACAAATCAATCTCTTTTTCTCTCACTAAC
sub2-K202E-Y203E fwd	GTTAGTGAGAGAA GAAGAG ATTGATTTGTCAC
sub2-K202E-Y203E rev	GTGACAAATCAAT CTCTTC TTCTCTCACTAAC
sub2-F234E-R235E fwd	GTGCAAGAAATT GAGGAA GCTACTCCAAGA
sub2-F234E-R235E rev	TCTTGGAGTAGC TTCCTC AATTTCTTGCAC
sub2-R260A-F261D fwd	CCAATTTGTAGA GCC GAC TTACAGAATCCA
sub2-R260A-F261D rev	TGGATTCTGTAA GTC GGC TCTACAAATTGG
sub2-R368A fwd	AGATGTTTTTGGT GCA GGTATCGATATTG
sub2-R368A rev	CAATATCGATACC TGCA CCAAAAACATCT
sub2-Y390A-R393E fwd	GAAGCTGACCAA GCT TTACAT GAA GTCGGTAGAGCT
sub2-Y390A-R393E rev	AGCTCTACCGAC TTC ATGTAA AGC TTGGTCAGCTTC
sub2-K403D fwd	AGATTTGGTACT GAT GGTTTGGCTATT
sub2-K403D rev	AATAGCCAAACC ATC AGTACCAAATCT
SUB2::KanMX6 fwd	TGGTCATGGAAGATTCGCGT
SUB2::KanMX6 rev	GGCCTTCACCTCTTACGACA
pT7-His_6-TEV fwd	TTATTTGAATAATGGATCCGGCTGCTAACAAAGCCC
pT7-His_6-TEV rev	TTCTGCCCTCTAGGCCCTGAAAATACAGGTTTTCG
SUB2 fwd	TATTTTCAGGGCCTAGAGGGCAGAAGTTTGAG
SUB2 rev	TAGCAGCCGGATCCATTATTCAAATAAGTGGACGGATCAATG
pNOP-GFP-NLS fwd	TTGAATAATTAACCAAGCTAATTCCGGGC
pNOP-GFP-NLS rev	GACATCTGCAGCTTGTACAGCTCGTCCATGCCG
GFP-*sub2-K202E-Y203E*-NLS fwd	TACAAGCTGCAGATGTCACACGAAGGTGAAGAAGA
GFP-*sub2-K202E-Y203E*-NLS rev	GGAATTAGCTTGGTTAATTATTCAAATAAGTGGACGGATCAATGC
pNOP-NES-GFP fwd	TGGACGAGCTGTACAAGTAATTCCGGGCGAATTTCTTATGATTTATG
pNOP-NES-GFP rev	CTTCGTGTGACATGCATGCTGACATTACTGTTTTAGTTGATTTG
SUB2-NES-GFP fwd	CAGTAATGTCAGCATGCATGTCACACGAAGGTGAAGAAG
SUB2-NES-GFP rev	ATTCATTGAATTCGGGAGAATTATTCAAATAAGTGGACGG
sub2-K202E-Y203E-NLS-TAP fwd	CATTTTTTTAAAAACAGCAACGATGCCAAAAAAGAAGAGAAAGGTAATGTCACACGAAGGTGAAGAAG
sub2-K202E-Y203E-NLS-TAP rev	GAAATTCTTTTTCCATCTTCTCTTCTCTACCTTTCTCTTCTTTTTTGGATTATTCAAATAAGTGGACGG
SUB2-NES-TAP fwd	TAAAAACAGCAACGATGTCACACGAAGGTGAAGAAG
SUB2-NES-TAP rev	CTTCTCTTCTCGAGGTGGATCCCTGTCTTGTTGATATC
KAP95-myc fwd	CACAAAAGATACAGCAAGATGGGCTAGAGAGCAACAGAAGCGTCAATTATCCTTATCGTACGCTGCAGGTCGAC
KAP95-myc rev	AAGAAACAAAGATGGAAAAGAACCAAAATCAGCTTGTAAGTTCTATCGTAATTAATCGATGAATTCGAGCTCG
MTR10::HIS3 fwd	GGCCTTGGTTTTAACTTTGTTCGACATTCCAAGCCTCTTGTTTTTGACATGGAGGCCCAGAATACCCTC

MTR10::HIS3 rev	GCAACATTGCAACAGAAGCCATTAGATCCGGTACTGCAACTT AGTATAGCGACCAGCATTCACATAC

Table 10: Oligonucleotides used for qPCR

Name	Sequence
PMA1 3' fwd	CAGAGCTGCTGGTCCATTCTG
PMA1 3' rev	GAAGACGGCACCAGCCAAT
CCW12 3' fwd	TGAAGCTCCAAAGAACACCACC
CCW12 3' rev	AGCAGCAGCACCAGTGTAAG
YEF3 3' fwd	TCTGGTCACAACTGGGTTAGTG
YEF3 3' rev	GCAATCTTGTTACCCATAGCATCGA
PGK1-3' fwd	TGACAAGATCTCCCATGTCTCTACTG
PGK1-3' rev	TGGCAATTCCTTACCTTCCAA
ASC1 fwd 3'	TACAGCAAGGCCGCTGAACC
ASC1 rev 3'	CCGGCAAACAAAGTTTGACCGTC
ASC1 over intron fwd	GACTCTGTCACCATCATTTCTGCC
ASC1 over intron rev	CAAAGTTCCGTCTGGGGAAGC
DBP2 fwd	CTTCACCGAACAAAACAAAGGTT
DBP2 rev	TCGGGAGGAATATTTTGATTAGCT
DBP2 over intron fwd	CAAGGAATTGGCTTTTCAGCTT
DBP2 over intron rev	TGAAAAAAACAACGATCAACGAA
RPL28 fwd	TGGAAGCCAGTCTTGAACTTGG
RPL28 rev	TTGGTCTCTCTTGTCTTCTGGGA

2.7 Enzymes

Table 11: Enzymes

Enzyme	Supplier
Phusion® High-Fidelity DNA Polymerase	NEB
RNase T1	Thermo Fisher Scientific
DNase I	Thermo Fisher Scientific
Proteinase K	Sigma Aldrich
Tobacco etch virus (TEV)-protease	Home-made
Zymolyase 100T	Carl Roth
Zymolyase 20T	Carl Roth
Taq DNA Polymerase	Home-made
RNase H	Thermo Fisher Scientific
RNase III	Thermo Fisher Scientific
Superscript II reverse transcriptase	Thermo Fisher Scientific
T5 Exonuclease	NEB
Taq DNA Ligase	NEB
Restriction Enzymes	NEB

2.8 Antibodies

Table 12: Antibodies

Name	Source	Dilution	Supplier
anti-Mex67	Rabbit	1:5000	(Strässer and Hurt 2000)
anti-Nab2	Mouse	1:5000	Swanson lab (3F2)
anti-Npl3	Rabbit	1:5000	Tracy Kress lab
anti-Cbp80	Rabbit	1:20000	Dirk Görlich lab
anti-Sub2	Rabbit	1:10000	(Strässer et al. 2002)
anti-Tho1	Rabbit	1:5000	Pineda lab
anti-Yra1	Rabbit	1:5000	(Strässer et al. 2002)
anti-Pgk1	Mouse, monoclona	1:5000	Abcam
Peroxidase anti- Peroxidase (PAP)	Rabbit, monoclona	1:5000	Sigma-Aldrich
anti-Myc	Rabbit	1:5000	Millipore
ChromPure rabbit IgG	Rabbit		Jackson IR LAboratories
anti-rabbit-HRP	Goat, monoclonal	1:3000	Biorad; #170-6515
anti-mouse-HRP	Goat, monoclonal	1:3000	Biorad; #170-6516
dsDNA	Mouse	1:1000	Abcam
S9.6 R-loop	Mouse	1:1000	Millipore
anti-GFP	Mouse	1:1000	Sigma-Aldrich
anti-rabbit-Alexa488	Goat	1:200	Invitrogen
anti-mouse-Alexa488	Goat	1:200	Invitrogen

3 Methods

3.1 Standard methods

Standard cloning techniques such as growth of bacteria, DNA isolation and DNA analysis on agarose gels were done according to (Sambrook and Russell 2001) or the manufacture's manuals. NucleoSpin® Plasmid (NoLid)-kit and NucleoSnap Plasmid Midi-kit (Macherey-Nagel) were used for small- and medium-scale plasmid preparation from *E. coli* respectively. PCR amplified DNA products were visualized with Intas HDGreen™ on agarose gels following electrophoresis. Gel extracted DNA and PCR products were purified using NucleoSpin® Gel and PCR Clean-up-kit (Macherey-Nagel). Cloned plasmids were sequenced by Microsynth AG.

3.2 Cloning

3.2.1 Polymerase chain reaction (PCR)

All PCR amplifications were done using Phusion High-Fidelity DNA (cloning and genomic integration) or Taq DNA polymerase (colony PCR). An example of a PCR reaction using Phusion High-Fidelity DNA polymerase is shown in Table 13. A total of 400 µL PCR product was used for genomic integration in yeast cells.

Table 13: Standard PCR reaction

Component	Amount [µL]	Final concentration	Stock concentration
dNTPs	4	200 µM	2.5 mM
Buffer	10	1x	5x
Primer fwd.	0.25	500 nM	100 µM
Primer rev.	0.25	500 nM	100 µM
Template (plasmid DNA)	0.5	≤ 10 ng	Variable
Water	34.5		
Phusion DNA Polymerase	0.5	1 U	2 U/µL
	50 µL		

Temperature	Time	
98°C	30 sec	
98°C	10 sec	32x
54°C	30 sec	
72°C	30 sec/kb	
72°C	5-10 min	
4°C	∞	

3.2.2 Gibson Assembly

Gibson assembly was used for cloning and mutagenesis (adapted to (Gibson et al. 2009)). Vector backbones and inserts were amplified using oligonucleotides that generate PCR fragments with an overlapping region of about 20-25 bp to each other. Resulting PCR products were digested with DpnI to degrade template plasmid DNA used for PCR and then assembled by Gibson. The Gibson assembly reaction was composed of 50 ng of vector and a 3:1 ratio of insert to vector mixed with 15 µL of Gibson assembly master mix and filled up to 20 µL with water. The mixture was incubated for 60 min at 50°C. For transformation in *E. coli*, 5 µL of the mixture was used.

3.2.3 Transformation of *E. coli*

Competent cells were prepared according to the manufacturer's manual of the Mix & Go *E. coli* Transformation Kit (Zymo Research Corp.) and stored at -80°C until needed. 50 µL iced thawed competent cells were transformed with 5 µL Gibson assembly mix or 0.5 µL plasmid DNA. Thawing on ice maintains the permeability of the cell membrane and maintains the efficiency of the cell to uptake DNA. Cells were incubated with exogenous DNA on ice for 10 min and then heat shocked at 42°C for 45 sec. The heat shock creates a pressure difference between the external and internal of the cell, which leads to pore formation and enhances the uptake of the exogenous DNA. Immediately after heat shock, the cells were placed on ice for 1 min to constrict the pores that were induced during the heat shock. This allows the cells to retain the plasmid and increases the efficiency of the transformation. Cells were recovered in 300 µL SOC medium and incubated for 60 min at 37°C on a shaker at 200 rpm. 100 µL of cell suspension was spread out on selective LB-plate and incubated overnight at 37°C.

3.2.4 Colony PCR for *E. coli*

To screen for positive plasmids, single colonies were picked and suspended in 20 µL water. 5 µL of this suspension was used for PCR as shown in Table 14 and the size verified on a 1 % agarose gel in 1x TAE. The remaining cell suspension of three positive clones were inoculated in 3 mL LB culture with appropriate antibiotic and grown overnight at 37°C.

Table 14: *E. coli* colony PCR

Component	Amount [µL]	Final concentration	Stock concentration
dNTPs	1.6	200 µM	2.5 mM
Buffer	2	1x	10x
Primer fwd.	0.1	500 nM	100 µM
Primer rev.	0.1	500 nM	100 µM
Template (cell suspension)	5		
Water	10.8		
Taq DNA Polymerase	0.4		
	20		

Temperature	Time	
95°C	5 min	
95°C	30 sec	32x
48°C	45 sec	
68°C	1 min/kb	
68°C	5-10 min	
4°C	∞	

3.2.5 Ethanol (EtOH) precipitation of DNA

To precipitate DNA, 2.5 volumes of 100 % EtOH and 1/10 volume of 3 M NaOAc (pH 5.2) was added to the sample and mixed by inverting the tube. The samples were then incubated at -20°C for 20 min and centrifuged after at 4°C, 12,000 g for 20 min. The pellet was washed once with 70 % EtOH, and dried. The pellet was redissolved in 15µL water or 1x TE.

3.2.6 Transformation in *S. cerevisiae*

To transform exogenous DNA into *S. cerevisiae*, an overnight pre-culture was diluted in 50 mL of appropriate media to OD_{600} 0.2 and grown with shaking at 200 rpm at 30°C. At mid-log phase (OD_{600} 0.6-0.8), cells were harvested by centrifuging at 2,800 g for 3 min and washed with 10 mL water. The cells were then resuspended in 500 µL solution I, transferred to a 2 mL tube and centrifuged as before. Cell pellet was resuspended in 250 µL of solution I. For each transformation, 50 µL of cell suspension were mixed with 5 µl single-stranded carrier DNA (2 mg/mL), 300 µL solution II and 500 ng plasmid DNA or EtOH-precipitated-PCR reaction for genomic integration. A negative control without DNA was also included. This negative control served as an internal control to check for the growth of positive transformants and not growth of contaminated cells. The transformation mix was incubated for 30 min on a rotating wheel at RT, heat shocked for 10 min at 42°C and immediately incubated on ice for 3 min. Cells were then washed with 1mL water by pelleting at 1,200 g for 3 min at RT in a tabletop centrifuge. For genomic integration, cells were recovered in 1mL of YPD for a minimum of 2 h at 30°C with shaking. Recovered cells were pelleted fand resuspended in 150 µL water and spread on selective media plates. Plasmid transformations were directly spread on selective media plates without recovery. Plates were incubated for 2 - 4 days at 30°C until colonies were observed.

3.2.7 Yeast colony PCR

To screen for positive genomic integration of protein tags or genomic deletions, a small amount of yeast colonies was picked and suspended in 15 µL zymolyase 20T solution (2.5 mg/mL) in $NaHPO_4$ to digest the cell wall. The mixture was incubated for 20 min at RT, then at 37°C for 5 min and then at 95°C for 5 min. The cell suspension was diluted with 60 µL water and 5µL used as for PCR. The PCR was performed as shown in Table 14 and ran on a 1% agarose gel in 1x TAE.

3.3 Plasmid shuffling

To study essential genes that cannot be removed from the genome, plasmid shuffling can be conveniently employed to study essential gene function. The essential gene is first cloned into a plasmid with a *URA3* selection marker, or the gene tagged with a *URA3* selection marker on the gene locus. The plasmid-borne gene is then transformed into host cells. The wild-type gene or its mutant is then cloned into another plasmid with a different selectable marker. In this case, the *LEU2* selectable marker was used. Plasmids carrying the wild-type or mutated gene are transformed into the wild-type-*URA3* cells, resulting in a strain carrying two copies of the gene of interest, the genomic wild-type, and the mutant gene. These cells are then grown in medium containing 5-Fluoroorotic acid (5-FOA) that selects *ura3* cells. Only 5-FOA resistant cells survive, carrying the mutated essential gene, whose function can now be assessed.

3.4 SDS-PAGE for protein size analysis

Sodium dodecyl sulfate polyacrylamide gel electrophoresis (SDS-PAGE) was done according to (LAEMMLI 1970). The gels were cast according to (Sambrook and Russell 2001), using a Mini-Protean II system (Biorad). Proteins were separated using gel electrophoresis and the proteins were either transferred to a membrane for subsequent Western blot or stained with modified Fairbanks-Coomassie staining method (Fairbanks et al. 1971; Wong et al. 2000). SDS gels were stained with Coomassie solution, heated shortly in a microwave until warm and incubated for 15 min on a rocker. Gels were destained in 10% acetic acid. Destaining was accelerated by heating multiple times and incubating on a rocker. This was repeated until the gel background was completely destained.

3.5 Dot spots

Freshly grown yeast cells were picked with a small loop and suspended in 1 mL of water. The OD_{600} of the suspension was measured and diluted to OD_{600} 0.20 for all strains. A 10-fold serial dilution was made from this dilution and 5 µL of the dilution spotted on respective media plate, air dried and incubated at 16°C, 25°C, 30°C and 37°C until colonies were observed.

3.6 Growth curve in liquid media

An overnight pre-culture was diluted to an OD_{600} of 0.2 and grown for ~2 h for cells to exit the lag phase before the measurement of the growth curve started. The OD_{600} of cells were measured every hour and cells were diluted to avoid them reaching an OD_{600} of 1.0. For growth curve at 37°C, cells were transferred to a shaking water bath after the lag phase and measurement done at this temperature.

3.7 Tandem Affinity Purification (TAP)

Tandem affinity purification (TAP) was performed according to (Puig et al. 2001; Rigaut et al. 1999). The TAP fusion tag consists of two protein A tags, a TEV cleavage site, and a calmodulin binding peptide (CBP). TAP was used to purify the fused protein with its interacting proteins from *in vivo*. TAP-tagged proteins were purified from 2 L culture grown to OD_{600} 3.0 - 3.5. Cells were harvested at 4000g for 4 min at RT and pellet resuspended in 2mL TAP-buffer. The suspension was dropped into liquid nitrogen and flash frozen. These deep-frozen cell drops were cryomilled in a freezer mill 6870D (SPEX SamplePrep) and milled pellet stored at -80°C until needed. The pellet was thawed in 10 mL TAP-buffer + 1x protease inhibitor and 1 mM DTT. The thawed lysate was precleared by centrifuging at 4°C and at 3,500 g for 12 min. The precleared lysate was centrifuged at 165,000 g for 1 h at 4°C and the upper fatty phase removed by aspiration. The supernatant was transferred to a 50 mL tube, 600 µL IgG-Sepharose 6 fast flow affinity resin added and incubated at 4°C for 1.5 h on a turning wheel. Before use, the affinity resin was washed three times with 10 mL buffer TAP-buffer. Following binding, the resins were centrifuged at 700 g for 3 min at 4°C The supernatant was removed by vacuum pump and resins washed once with 10 mL TAP-buffer containing 0.5 mM DTT and transferred to a Mobicol (Mobitec). A 10 mL syringe was plugged atop the Mobicol to wash the resin with 10 mL TAP-buffer (0.5 mM DTT) by gravity flow. To release the bound protein complexes from the resins, 150 µL TAP-buffer containing 0.5 mM DTT + 5 µL TEV-protease was added to the resins in the Mobicol and incubated at 16°C for 1 h on a rotating wheel. Cleaved proteins were eluted into a fresh 2 mL tube. A second step purification was done to increase the purity. Per sample, 600 µL calmodulin resin was washed 3x in TAP-buffer containing 1 mM DTT and 2 mM $CaCl_2$. Before use, the calmodulin resin was incubated in TAP-buffer containing 1 mM DTT and 4 mM $CaCl_2$ to increase the protein yield. The washed calmodulin resin was added to the TEV-eluate and incubated for 1 h at 4°C on a turning wheel. The resin was washed with 10 mL TAP-buffer (1 mM DTT+2 mM $CaCl_2$) and proteins eluted by adding elution buffer and incubating at 37°C for 15 min with shaking at 500 rpm. The calmodulin eluate was precipitated with TCA to a final concentration of 10 % for 20 min on ice, followed by centrifugation at 13,500 g for 20 min at 4°C. The supernatant was removed as much as possible from the pellet and the protein pellet resuspended in 60 µL 1x SDS-sample loading buffer. The pH of the sample was neutralized with approximately 10 µL 1 M Tris base (until SDS-buffer changed from yellow to blue again).

3.8 Quantitative Western blot

Quantitative Western blot was done according to (Kushnirov 2000). 10 mL of cells grown to mid-log phase (OD_{600} 0.8) were harvested at 4°C, 2,800 g for 3 min. The supernatant was discarded, and cells washed in 10 mL of water. The pellet was resuspended in 150 µL

pretreatment solution and incubated on ice for 15 min. The pellet was precipitated with TCA to a final concentration of 10 % for 10 min on ice, followed by centrifugation at 4°C, 13,500 g for 10 min. The protein pellet was resuspended in 1x SDS-sample loading buffer and pH neutralized with approximately 2 µL 1 M Tris base. For quantification, equal volume of samples was ran on an SDS-PAGE, semi-dry blotted (Towbin et al. 1979) and proteins detected with the corresponding primary antibody and a horse radish peroxidase-coupled secondaryantibody. Protein signals were developed after probing samples on a membrane with CheLuminate-HRP ECLsolution (Applichem) and the chemiluminescence signals detected with a ChemoCam Imager (Intas) and quantified with GelQuantNET.

3.9 Fluorescence *in situ* hybridization (FISH) with oligo d(T)

In situ hybridization against poly(A)$^+$ RNA was done according to (Amberg et al. 1992). Cells were grown to mid-log phase (OD_{600} 0.6-0.8) and 10 mL harvested. For heat shock FISH, cells at OD_{600} 0.6-0.8 were shifted to 37°C with prewarmed media and transferred to a water bath for 50 min. 10 mL of cells at 30°C and 37°C were immediately fixed with 4% formaldehyde at RT. Heat shocked samples were fixed at 37°C for 15 min before transferring to RT. The cells were washed in 100 mM KPO_4 (pH 6.4) after fixation, and spheroplasted with 100T zymolyase dissolved in 100 mM KPO_4 (pH 6.4) and 1.2 M Sorbitol for 30 min. Spheroplasted cells were washed in sorbitol wash buffer, resuspended in sorbitol wash buffer, and pipetted onto a poly-lysine-coated slide. The cells were allowed to sit on the slide for 5 min and then sucked off with a vacuum pump and then the slide was washed once with sorbitol wash buffer. The cells were prehybridized at 37°C in prehybridization buffer for 1 h in a humid chamber. 0.75 µl of 1 pmol/µl oligo d(T)$_{50}$-Cy3 probe with was added to the prehybridization buffer on the slide and incubated at 37°C O/N in a humid chamber. The slides were washed in 0.05% SSC at RT for 30 min, allowed to dry, mounted with ROTI® Mount Fluor Care DAPI, and covered with a coverslip. DNA and poly(A)$^+$ RNA was visualized using the Delta Vision Ultra microscope and images analyzed with ImageJ.

3.10 Immunofluorescence

Cells for immunofluorescence were treated like samples for FISH until spheroplasting. Spheroplasted cells were resuspended in buffer containing 1x PBS, 1% BSA and 0.5% NaN_3 and pipetted onto a poly-lysine-coated slide. The cells were allowed to sit on the slide for 5 min and then sucked off with a vacuum pump and then the slide was washed once with buffer containing 1x PBS, 1% BSA and 0.5% NaN_3. Proteins were probed with primary antibodies dissolved in antibody dilution buffer and incubated at RT for 2 h in a hybridization chamber. Cells were washed in antibody wash buffer 3x. Alexa-Fluor coupled secondary antibodies were added to the slide and incubated at RT in the dark for 1 hr. Cells were then washed 3x in antibody wash buffer. The slides were allowed to dry, mounted with ROTI®

Mount Fluor Care DAPI, and covered with a coverslip. DNA and proteins were visualized using the Delta Vision Ultra microscope and images analyzed with ImageJ.

3.11 RNA extraction

For total RNA extraction, harvested cell pellet was resuspended in 1 mL Trizol reagent and mixed by vertexing, incubated at RT for 5 min, 200 µL chloroform added, vortexed and incubated an additional 5 min at RT. The sample was centrifuged at RT, 18,000 g for 20 min to separate the proteins and nucleic acids into an aqueous and organic phase. The upper aqueous phase containing the RNA was transferred to a fresh tube and precipitated by adding equal volume of isopropanol. The mixture was incubated at -20°C for 20 min and then pelleted at 13,500 g for 20 min. The pellet was washed with 70 % EtOH, dried and dissolved in DEPC-treated RNase-free water. When needed, DNA was digested by DNase I in presence of RNase inhibitor for 30 min at 37°C.

3.12 RNA Immunoprecipitation (RIP)

TAP-tagged *S. cerevisiae* strains were grown in 400 mL YDP to an OD_{600} 0.8, harvested and stored at -80°C. Pellets were thawed on ice, resuspended in 1 mL RNA IP-buffer containing protease inhibitor and lysed using the FastPrep-24 5G device (3x 20 sec at 6 m/sec). The lysate was cleared by centrifugation for 5 min at 1,500 g and at 4°C, 13,000 g for 10 min. 900 µl of the cleared lysate was incubated with 660 units DNase I for 30 min on ice. 40 µl of prewashed IgG-coupled Dynabeads M-280 were added and incubated at 4°C for 3 h on a turning wheel. The immunoprecipitated beads were washed 8 times with RNA-IP-buffer with 5 sec of vertexing and 2 min on turning wheel in between. For RNA extraction 1 mL Trizol reagent was added to the beads and vortexed strongly for 20 sec. RNA was extracted according to the procedure in section 3.9. The RNA of the input and IP samples were reversed transcribed using super script II reverse transcriptase according to the manufacturer's protocol and subsequently analyzed by quantitative PCR on an Applied Biosystems StepOnePlus cycler using Applied Biosystems Power SYBR Green PCR Master Mix. As a control the RIP was also performed with an untagged strain. PCR efficiencies (E) were determined withstandard curves. Protein enrichment over the untagged strain was calculated according to the formula

$$\frac{E^{(ct\_IP - ct\_input)nc}}{E^{(ct\_IP - ct\_input)}}$$

Mean values were calculated of at least three biological replicates. For protein purification, acetone precipitation of the organic inter- and lower phase was performed. Samples were centrifuged at 4°C, 13,000 g for 2 h, washed 2x in acetone at 4°C, 13,000 g for 1 h. Pellet was air dried, resuspended in 1x SDS, boiled at 95°C for 10 min and centrifuged at RT,

13,000 g. samples were vigorously vortexed and loaded onto an SDS gel.

3.13 RNA splicing efficiency

To assess splicing efficiency, total RNA was extracted from cells according to the procedure in section 3.9. cDNA was transcribed using super script II according to the manufacturer's protocol. The resulting cDNA was analyzed by qPCR. Analysis of intron retention was done by using one primer pair flanking an intron and the other primer targeting the 3' end of the transcript. Afterwards the ratio of the CT values of the two primer pairs was calculated to determine the efficiency of splicing.

3.14 Protein expression and purification

E. coli BL21(DE3) Rosetta cells transformed with His_6-tagged Sub2 plasmids were grown to mid-log phase at 37°C in LB + Kanamycin, induced with 1mM IPTG grown at 25°C overnight, and lysed in lysis buffer. After sonicating and clearing the lysate by centrifugation, it was passed over a Ni affinity column (Qiagen) and washed in high salt wash buffer. Bound protein was eluted in lysis buffer with 500 mM imidazole using a gradient and was dialyzed overnight in the presence of TEV protease in dialysis buffer. The cleaved protein was passed a second time over the Nickel column to remove impurities, then loaded onto a Source Q column equilibrated in buffer A. The proteins were eluted in elution buffer and stored in buffer with 30% glycerol at -80°C.

3.15 Annealing of Substrates

Prior to the use of the double stranded substrates for either binding or unwinding, two single stranded substrates were annealed to each other, according to Putnam and Jankowsky (2012). The two strands were mixed in equimolar amounts in 1x annealing buffer and heated to 95°C in a thermocycler. They were then cooled down to 4°C stepwise. The substrates were aliquoted and stored in the dark at -80°C. In Figure 7 are the annealed substrates used in the experimental procedures. Putnam substrates were taken from Putnam and Jankowsky (2013). ssRNA Putnam-13-Cy3 was green labelled, while dsRNA Putnam13 and Putnam-25-Cy5 was red.

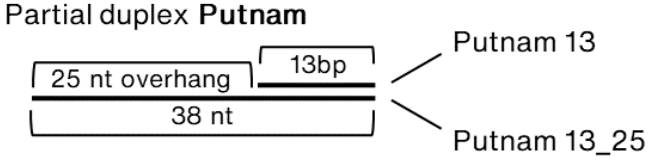

Figure 7: dsRNA used for *in vitro* assays.
Putnam RNA sequence composed of a 13bp and a 25nt overhang.

3.16 Electrophoretic Mobility Shift Assay (EMSA)

The substrate binding activity of Sub2 was studied using Electrophoretic Mobility Shift Assay (EMSA) and was modified according to Saguez et al. (2013). The substrates used were either Cy3 labelled or Cy5 labelled. Prior to use, the Cy5 labelled RNA was preincubated with an unlabelled complementary strand to yield a double stranded RNA of 13bp and a 25 nt overhang. Sub2 (1 µM) was preincubated in binding buffer with 0.5 mM $MgCl_2$ and 1 mM ADPNP for 15 min. Following this, the Cy3 labelled ssRNA and Cy5 labelled dsRNA substrates (100 nM) were added and incubated in the dark for 30 min. The samples were then loaded onto a pre-cooled 10% TBE-gel and run in 1x TBE buffer at 100 mA, 100 V in a cold room for 1.5 h. The gel was washed with distilled water for 5 min and scanned with the Typhoon FLA 9500 and image analyzed with ImageQuantTL.

3.17 Helicase assay

The reaction solution to study the unwinding activity of Sub2 and the mutants contained 20 mM MES pH 6.5 and 4 mM TCEP. One strand of the dsRNA used was Cy5 labelled while the other was labelled with a BHQ2 quencher. When in proximity, BHQ2 quenches the fluorescence signal of Cy5, and an unwound RNA emits a signal which can be subsequently measured. The helicase assay assessed the unwinding of RNA, DNA, or hybrid substrates by Sub2 wild-type and mutant proteins. Compared to a gel-based approach, this setup is advantageous and thus allows real monitoring of substrate unwinding. This method was modified according to Ordabayev et al. (2018). The helicase assay was conducted at room temperature using the plate reader Tecan Infinite F200 pro. 100 µL reaction mixture of helicase buffer, 4 µM of Sub2 proteins, 4 mM ATP and 2 mM $MgCl_2$ were prepared in a flat-bottomed black 96-well plates. Another mix of 100 µL of helicase buffer containing 20 nM of substrate was also prepared. To start the assay, the pre-mixed RNA was added to the reaction and the measurement of fluorescence began immediately. The fluorophore was excited at a wavelength of 620 nm and the emitted fluorescence signal measured at a wavelength of 670 nm. The obtained measurement points were fitted with a single exponential function using Origin: $y = y_0 + A_1 e^{-\frac{x}{t_1}}$.

3.18 R-loop assay

The levels of R-loop in cells were detected in genomic DNA extracts that had been treated with RNases followed by detection with antibodies against DNA-RNA hybrids. Genomic DNA extraction and RNase treatments were done according to the protocol below.

3.18.1 Genomic DNA extraction

10 mL of cells grown to mid-log phase (OD_{600} 0.8) were pelleted at 2,800 g for 3 min at 4°C. The supernatant was discarded, and cells washed in 10 mL of water. The pellet was

resuspended in 200 µL water, 500 µL 1x TNSTE, and 300 µL phenol chloroform. Glass beads were added and sample vortexed for 3 min to lyse the cells. The cells were centrifuged at 12,000 × g for 10 min. water and vortexed for 10 sec. The aqueous phase was transferred to a new tube and nucleic acids extracted using equal volume of chloroform, vortex for 10 sec and spun at 12,000 × g for 5 min. The aqueous phase was transferred to a new tube and nucleic acid precipitated with 1/10th 3 M sodium acetate (pH 5.2) and 2.5x ice-cold 100% ethanol. Samples were then centrifuged at 12,000 × g for 30 min at 4 °C, and precipitate washed with 80% ethanol. The supernatant was discarded, and pellet dried in a speed vacuum. The pellet was resuspended in RNase free water and DNA concentration measured.

3.18.2 RNase digest

10 µg of DNA was digested with 1000 U RNase T1 and 0.5 U RNase III to degrade ssRNA and dsRNA. A control sample was additionally degraded with 10 U RNase H to degrade ssRNA in the DNA-RNA hybrid. RNA was digested at 37°C for 2 h 30 min. The reaction components were as shown in Table 15.

Table 15: RNase digest of genomic DNA

Component	Amount	
Genomic DNA		
10x RNase III buffer	1x	
Ambion RNase III	5 U	10 U RNaseH (5 U/ µl)
RNase T1 (1000 U/ C)	500 U	
H2O		
Total	100 µl	

3.18.3 Sample blotting and R-loop detection

Serial dilutions of RNase treated nucleic acids were made in 1x SSC. These samples with a range of concentrations (200, 100, 50, 25, 12.5 ng) ensure that there will be signals within the linear range 40 µL of each sample was spotted onto 2 membranes: one for the S9.6 antibody and the other for dsDNA antibody using a dot blot apparatus. Samples were allowed to saturate into the membrane and vacuum applied to suck the sample. Following this, the membrane was crosslinked with a UV light crosslinker using the “Auto Crosslink” setting (1,200 µJ × 100) at 254 nm. The membranes were incubated in blocking solution (5% milk in PBS with 0.05% Tween-20 (PBST)) for 1 h at room temperature on a shaker. The membranes are then incubated overnight in primary antibody (1:1000 dilution anti-dsDNA and S9.6-R-loop antibodies) in 5% milk in PBST at 4°C with shaking. Primary antibodies were removed and washed 3x with PBST 10 min with shaking at room temperature and incubated with horseradish peroxidase (HRP) conjugated secondary antibody (anti-mouse, 1:3,000 dilution) in 5% milk in PBST with shaking at room temperature for 1 h. CheLuminate-HRP ECLsolution

(Applichem). Chemiluminescence signals were detected using a ChemoCam Imager (Intas) and quantified with GelQuantNET.

4 Results

4.1 Identification of residues that crosslink to RNA

To provide insight into the molecular mechanisms of Sub2 in mRNP biogenesis, its role has been mostly analyzed using deletion mutants, conditional mutants and mutation of its conserved motifs and domains. In this study, we focused on the mRNA-binding sites of Sub2 and generated mutants thereof. Amino acids of Sub2 in contact with RNA *in vivo* were identified by UV cross-linking followed by mass spectrometric (MS) analysis (Keil 2021). Several amino acids were identified to crosslink to RNA *in vivo*. Sequence alignment with 100 eukaryotic Sub2 orthologs revealed that most of these amino acid residues are conserved (Figure 8).

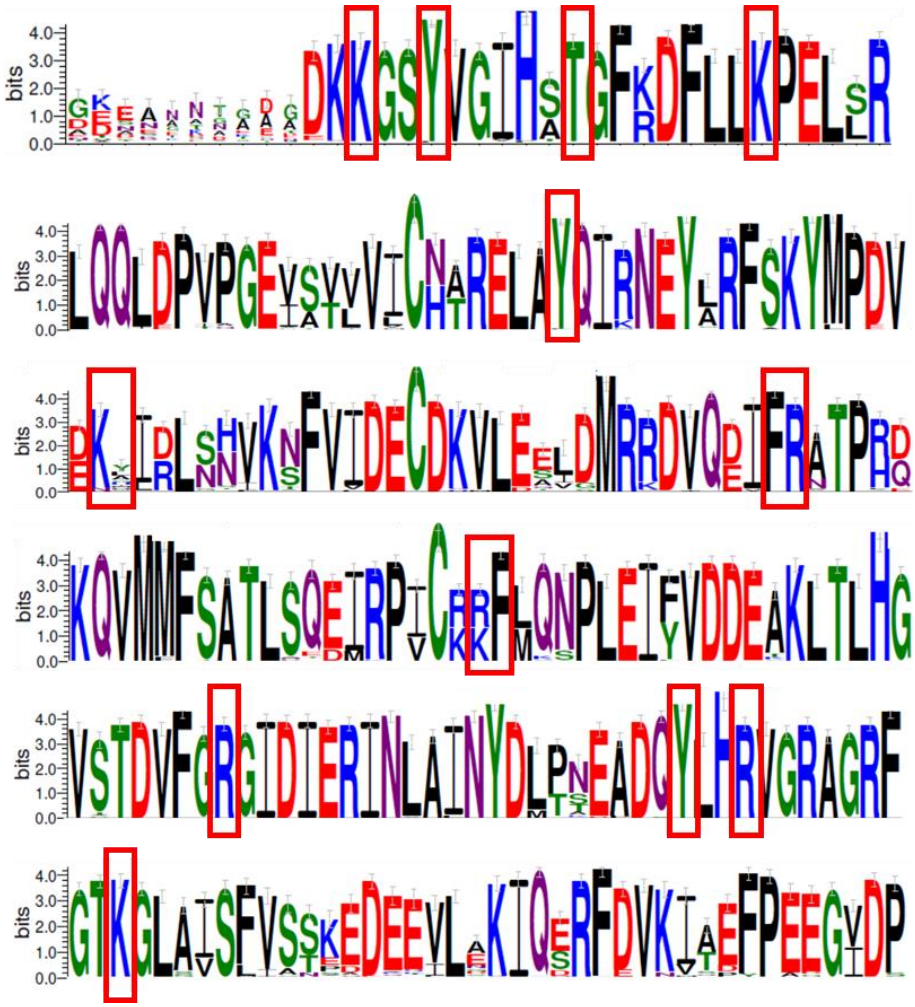

Figure 8: Sequence logo of multiple Sub2 sequences in different *Saccharomyces cerevisiae* strains, highlighting residues crosslinked to RNA.
WebLogo showing conservation of Sub2 as retrieved from 100 nonredundant protein sequences. The y-axis indicates relative frequency of each amino acid. Red box indicates amino acids that were identified to crosslink to RNA *in vivo*.

Based on the amino acid conservation, we selected for residues that are most conserved and using the *in-silico* prediction software PoPMuSiC, we predicted the thermodynamic stability of these Sub2 mutants. Mutations that were not predicted to have deleterious effects were selected for this study. The final mutations that we generated and worked with are shown in Table 16, indicating the position, the cross-linked amino acid and the mutation.

Table 16: Mutation of amino acids

Position	Amino acid	Mutation
53	Lysine (K)	Alanine (A), Aspartate (D)
56	Tyrosine (Y)	Alanine (A), Aspartate (D)
62	Threonine (T)	Alanine (A), Aspartate (D)
70	Lysine (K)	Aspartate (D)
144	Tyrosine (Y)	Glutamate (E)
202	Lysine (K)	Glutamate (E)
203	Tyrosine (Y)	Glutamate (E)
234	Phenylalanine (F)	Glutamate (E)
235	Arginine (R)	Glutamate (E)
260	Arginine (R)	Alanine (A)
261	Phenylalanine (F)	Aspartate (A)
368	Arginine (R)	Alanine (A)
390	Tyrosine (Y)	Alanine (A)
393	Arginine (R)	Glutamate (E)
403	Lysine (K)	Aspartate (D)

4.2 Mutation of some amino acids affect cell viability

Sub2 is a highly conserved RNA helicase with roles in splicing, polyadenylation, and mRNA export. Null mutants are nonviable in some genetic backgrounds (Giaever et al. 2002), while conditional mutants show decreased growth (Saguez et al. 2008), abnormal nucleolar morphology (Neumüller et al. 2013) and increased formation of wedge-shaped sectors, accompanied by a different color or appearance (Stirling et al. 2011). To assess the ability of the putative RNA-binding mutants to rescue the loss of wild-type *SUB2*, the mutants were tested for their ability to support growth. In the RS453 strain background, used in this study, *SUB2* is essential and is required for cell viability. Most of the mutants were viable, as shown in Figure 9, except for mutations of phenylalanine (F) and arginine (R) residues (F234E, R235E; R260A, F261A; R368A; Y390A, R393E), which were all nonviable.

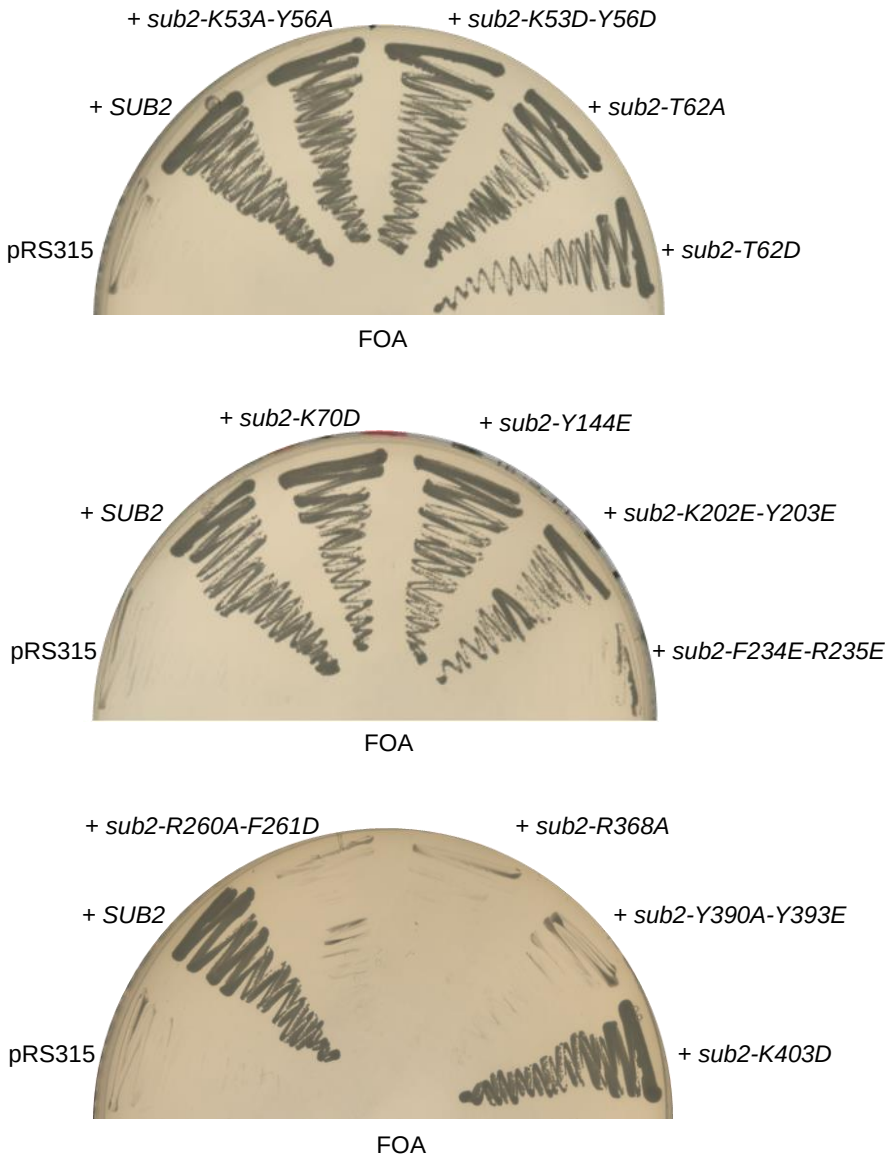

Figure 9: Complementation of *SUB2* deletion by *sub2* mRNA-binding mutants.
A plasmid shuffle strategy was employed to introduce the mutants. A knockout strain of *SUB2* carrying *SUB2* on a *URA3* plasmid transformed with wild-type or mutated *SUB2* on a LEU2 plasmid and plated on media containing 5-FOA. Growth on 5-FOA plates indicates a complementation of the *SUB2* deletion by the mutated gene. Lack of growth on 5-FOA indicates that the mutation results in a nonfunctional protein. Strains were streaked on 5-FOA-containing media and incubated for 3 days at 30°C.

Since protein stability affects protein function (Tanford 1968), we checked the expression of Sub2 in the mutants (Figure 10A). Whole cell extracts were immunoblotted using the PAP antibody to detect Sub2-TAP. Pgk1 served as a loading control. In viable mutants, Sub2 was expressed and there was not an observable change in protein levels (Figure 10A-B). However, nonviable mutants did not express Sub2-TAP (Figure 10C).

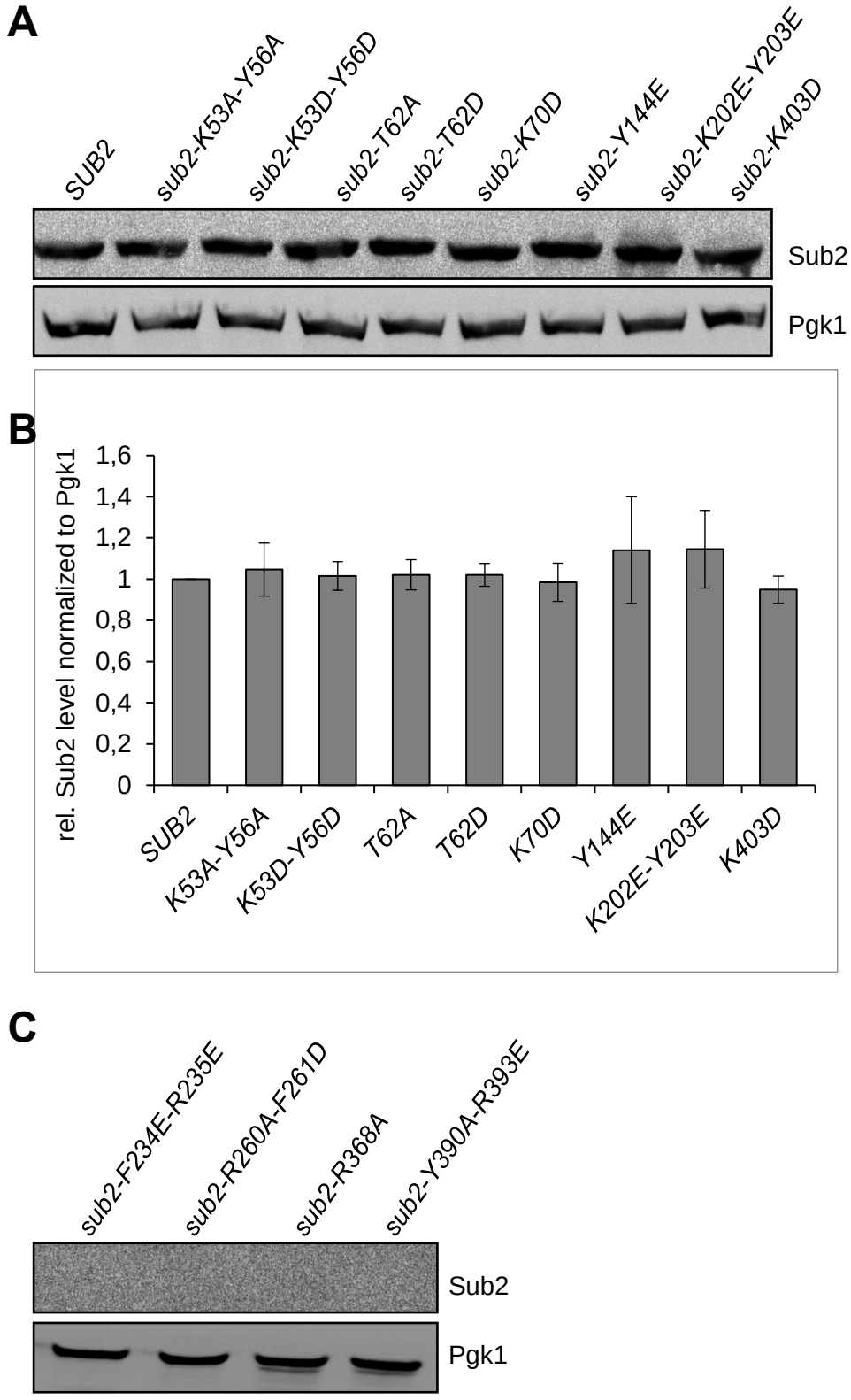

Figure 10: *In vivo* expression of Sub2 in RNA-binding mutants.
Western blotting analysis of whole cell lysates. Cells expressing Sub2-TAP were harvested at log phase and membranes probed with PAP and αPgk1 for Sub2 and loading control, respectively. **(A)** Viable mutants. **(B)** Quantification of viable *sub2* mutants. Bars represent the mean ± SD of three independent biological replicates. **(C)** Nonviable mutants that could not complement loss of *SUB2*.

4.3 Growth is affected in *sub2* RNA binding mutants

To assess the effects of the mutations on cellular fitness, growth assays were performed (Figure 11). Cells were also grown in liquid media and their OD_{600} measured every hour and their doubling rate calculated (Figure 12). The mutants *sub2-K53A-Y56A*, *sub2-K53D-Y56D*, *sub2-T62A*, *sub2-K70D*, *sub2-Y144E* and *sub2-K403D* grew like wild-type and did not show any growth defects at any of the temperatures tested (Figure 11). The mutant *sub2-T62D* showed a growth defect at 16°C, and mild defects at 25°C, 30°C and 37°C. The double mutant *sub2-K202E-Y203E* showed the strongest defect at all temperatures. The doubling rate of cells were calculated from the OD_{600} of cells growing in liquid culture at 30°C (Figure 12A, B) and 37°C (Figure 12C, D). Consistent with the dot spots assay, the mutants *sub2-K53A-Y56A*, *sub2-T62A* and *sub2-K70D* grew like wild-type. In contrast, the mutants *sub2-K53D-Y56D*, *sub2-Y144E* and *sub2-K403D* grew slow. The mutants *sub2-T62D* grew slower with *sub2-K202E-Y203E* growing the slowest.

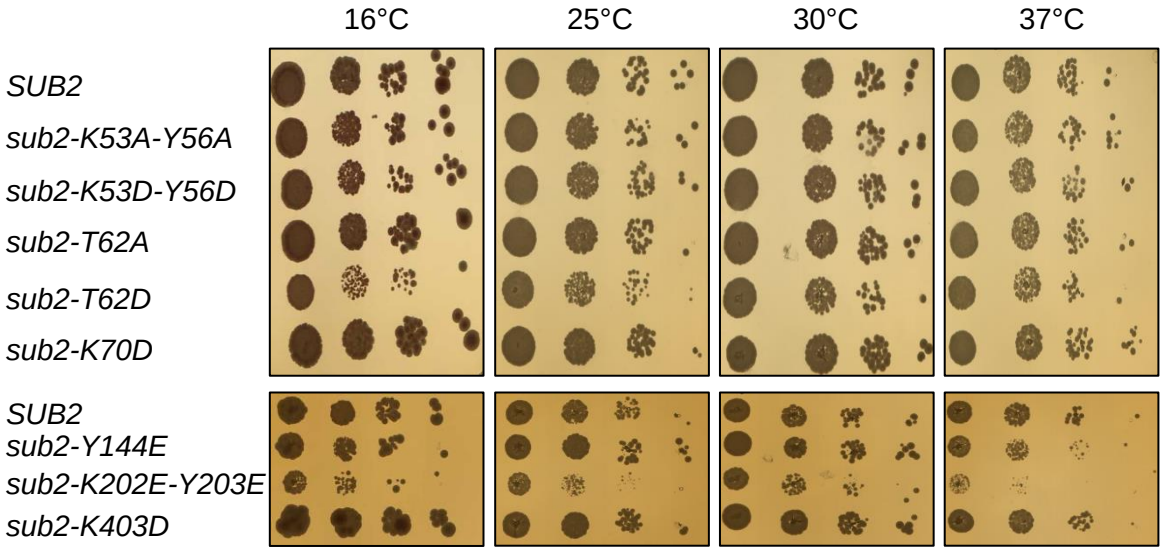

Figure 11: Growth of *sub2* mRNA-binding mutants.
Tenfold serial dilution of cells transformed with sub2 mutants were spotted on YPD and incubated at the indicated temperatures until growth was observed.

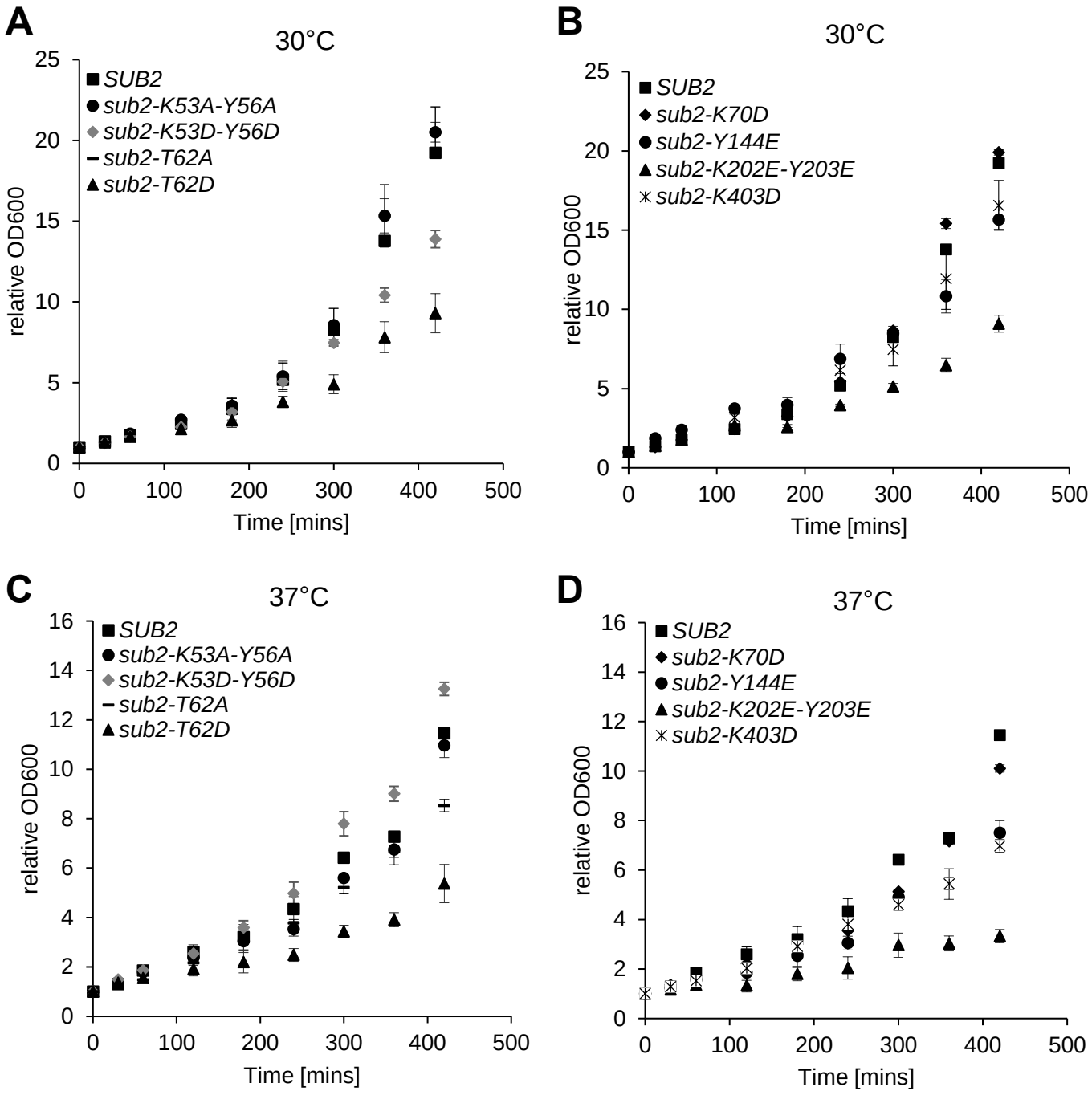

Figure 12: Growth curves of *sub2* mRNA-binding mutants.
Cells were grown in liquid culture at 30°C and 37°C and cell density (OD_{600}) measured at various timepoints. Data were presented as mean ± SD of triplicates. Average growth and standard deviations were calculated from biological triplicates.

4.4 Growth defects are independent of nuclear mRNA export defects

The essential protein Sub2 is required for mRNA export and its inactivation or overexpression results in nuclear poly(A)$^+$ RNA accumulation (Strässer and Hurt 2001). Having observed that some mutations resulted in growth defects, we examined the ability of these mutants to efficiently export mRNA. We investigated RNA localization by fluorescence *in situ* hybridization

(FISH) using oligo(dT_{50}) probes coupled to Cy3. The RNA-FISH revealed that the mutations, *sub2-T62A*, *sub2-Y144E* and *sub2-K403D* exported mRNA like wild-type cells at 30°C and 37°C (Figure 13). Whereas a mutation of threonine 62 to alanine (*sub2-T62A*) had no export defect, the same amino acid mutated to aspartate (i.e., *sub2-T62D*) resulted in a strong mRNA export defect at both temperatures. The mutant *sub2-K53A-Y56A* had a slight export defect which was intensified when the lysine and tryptophan residues were mutated to aspartate (*sub2-K53D-Y56D*). The mutants *sub2-K70D* and *sub2-K202E-Y203E* had no mRNA export defect at 30°C, but showed export defects at 37°C. Importantly, the export defect observed was not due to reduced protein levels of Sub2 at 37°C, as Western blot analysis confirmed that all proteins were expressed at wild-type levels (Figure 14). The growth and export defects coincided in the mutants *sub2-K53D-Y56D*, *sub2-T62D* and *sub2-K202E-Y203E*.

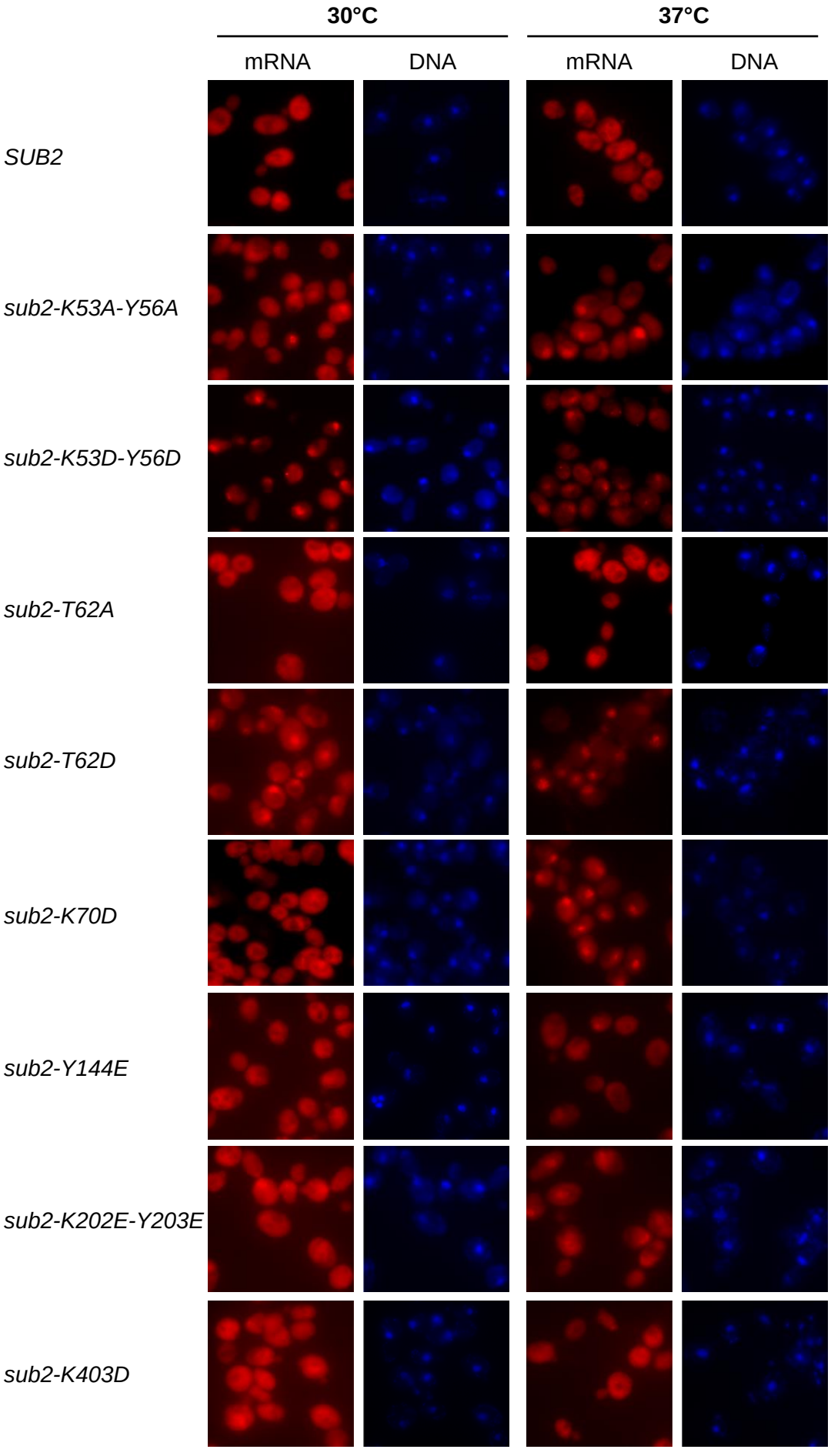
30°C
37°C
mRNA
DNA
mRNA
DNA
SUB2
sub2-K53A-Y56A
sub2-K53D-Y56D
sub2-T62A
sub2-T62D
sub2-K70D
sub2-Y144E
sub2-K202E-Y203E
sub2-K403D

Figure 13: Some *sub2* mutations lead to nuclear accumulation of poly(A)$^+$ RNA.
Localization of poly(A)$^+$ RNA was assessed by *in situ* hybridization in RS453 at 30°C or at 37°C for 50 min before fixation and processing. A Cy3-labelled oligo(dT_{50}) probe was used to label poly(A)$^+$ RNA, and DNA was stained with 4,6-diamidino-2-phenylindole (DAPI).

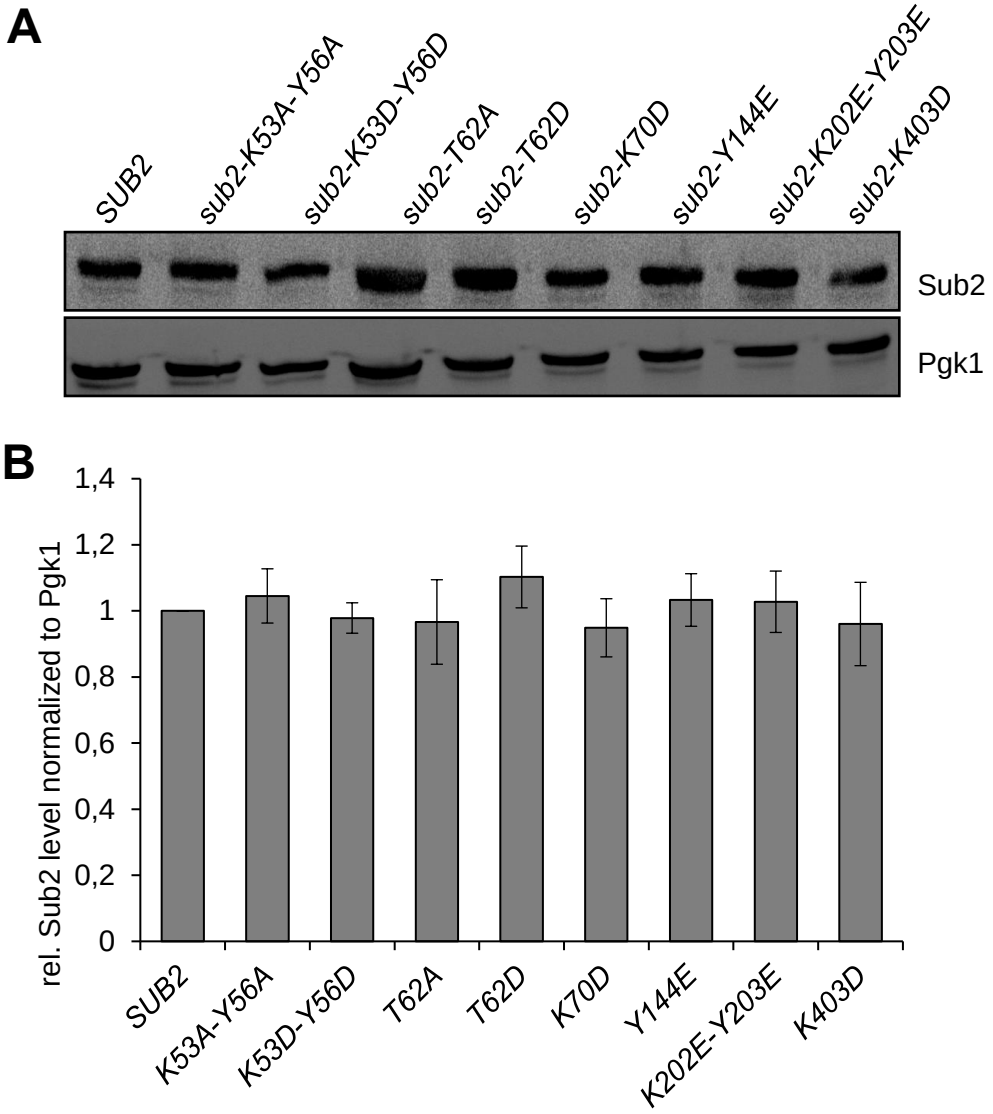

Figure 14:Western blotting analysis of Sub2 proteins at 37°C.
Western blotting analysis of whole cell lysates. Cells expressing Sub2-TAP were harvested at log phase and immunoblotted with PAP and αPgk1 for Sub2 and loading control, respectively. **(A)** Viable mutants. **(B)** Quantification of viable *sub2* mutants. Bars represent the mean ± SD of three independent biological replicates.

4.5 The mutation *sub2-K202E-Y203E* affects Sub2 localization

Next, we probed the localization of the mutants using immunofluorescence (Figure 15). Like wild-type Sub2, most mutants localized to the nucleus. Interestingly, the mutant sub2-K202E-Y203E mislocalized to the cytoplasm. A similar result was observed by live imaging of a GFP-tagged sub2-K202E-Y203E (Figure 25). Following the mislocalization of Sub2 in *sub2-K202E-*

Y203E, we asked if this phenotype was limited to Sub2 or affected other mRNP components. Figure 16 shows that Nab2, Npl3 and Yra1, were not mislocalized in this mutant. However, Cbp80 and Tho1 mislocalized to the cytoplasm, indicating that the mislocalization was specific to some proteins and not a general occurrence.

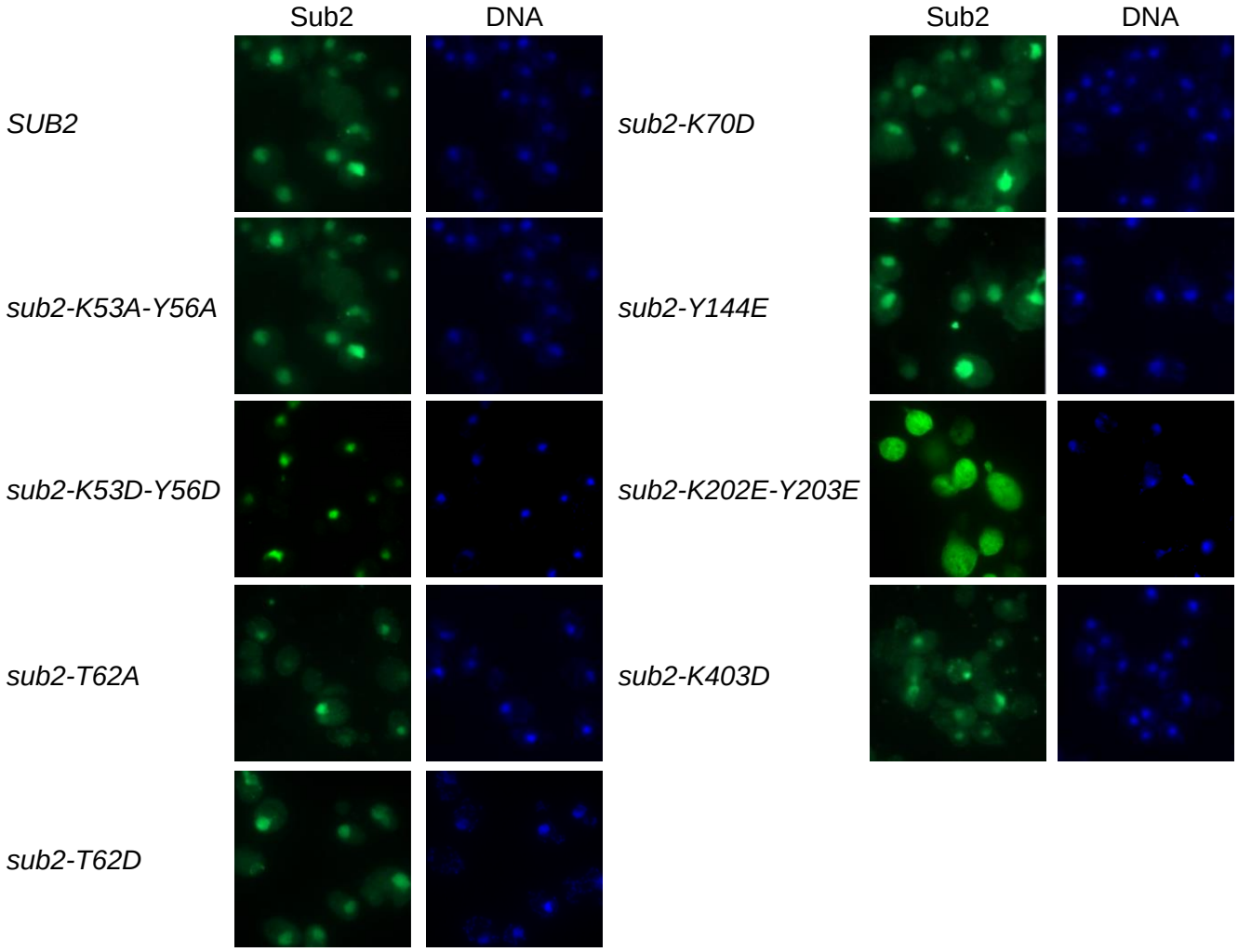

Figure 15: Immunofluorescence of Sub2 in wild-type cells and mRNA-binding mutants. *sub2-K202E-Y203E* mislocalizes Sub2 to the cytoplasm unlike the rest of the *sub2* mutants. Cells at log phase were harvested, fixed, permeabilized and incubated with Sub2 antibody. Proteins were visualized using a Sub2 antibody, and an Alexa Fluor 488-coupled secondary antibody. DNA was visualized with DAPI.

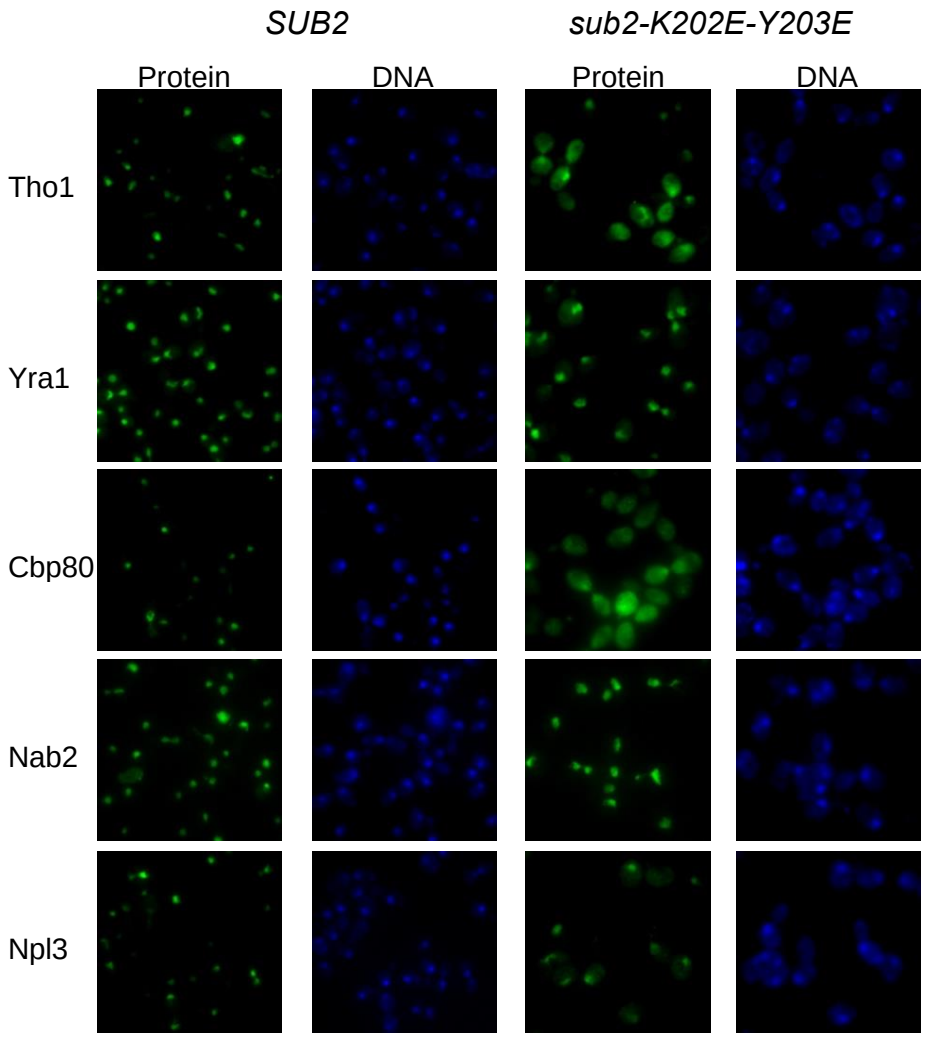

Figure 16: Immunofluorescence of other mRNP components in *SUB2* wild-type and *sub2-K202E-Y203E* cells.
Imaging of protein localization in *sub2-K202E-Y203E* cells show a mislocalization of Cbp80 and Tho1, but not of Yra1, Nab2 and Npl3. Cells at log phase were harvested, fixed, permeabilized and incubated with each primary antibody. Proteins were visualized with an Alexa Fluor 488-coupled secondary antibody. DNA was visualized with DAPI.

4.6 The mutation *sub2-K202E* causes the phenotypes associated with *sub2-K202E-Y203E*

We had observed growth and mRNA export defects, as well as a mislocalization of Sub2, Cbp80 and Tho1 in the double mutant *sub2-K202E-Y203E*. Therefore, we generated the single mutants *sub2-K202E* and *sub2-Y203E* to identify which mutation caused the phenotypes. We performed growth assays (Figure 17A), fluorescence *in situ* hybridization (Figure 17B) and immunofluorescence (Figure 18). We observed that *sub2-K202E* had a growth defect at all the temperatures tested. Analysis of mRNA export using FISH also revealed that *sub2-K202E* had an mRNA export defect at 37°C but not at 30°C. In contrast, *sub2-Y203E* did not show any growth or mRNA export defects. Like the double mutant *sub2-K202E-Y203E*, the proteins Sub2, Cbp80 and Tho1 were cytoplasmic in *sub2-K202E*, but were nuclear in *sub2-Y203E*.

Thus, the growth, mRNA export and localization assays revealed that *sub2-K202E* caused the phenotypes associated with the double mutant *sub2-K202E-Y203E*.

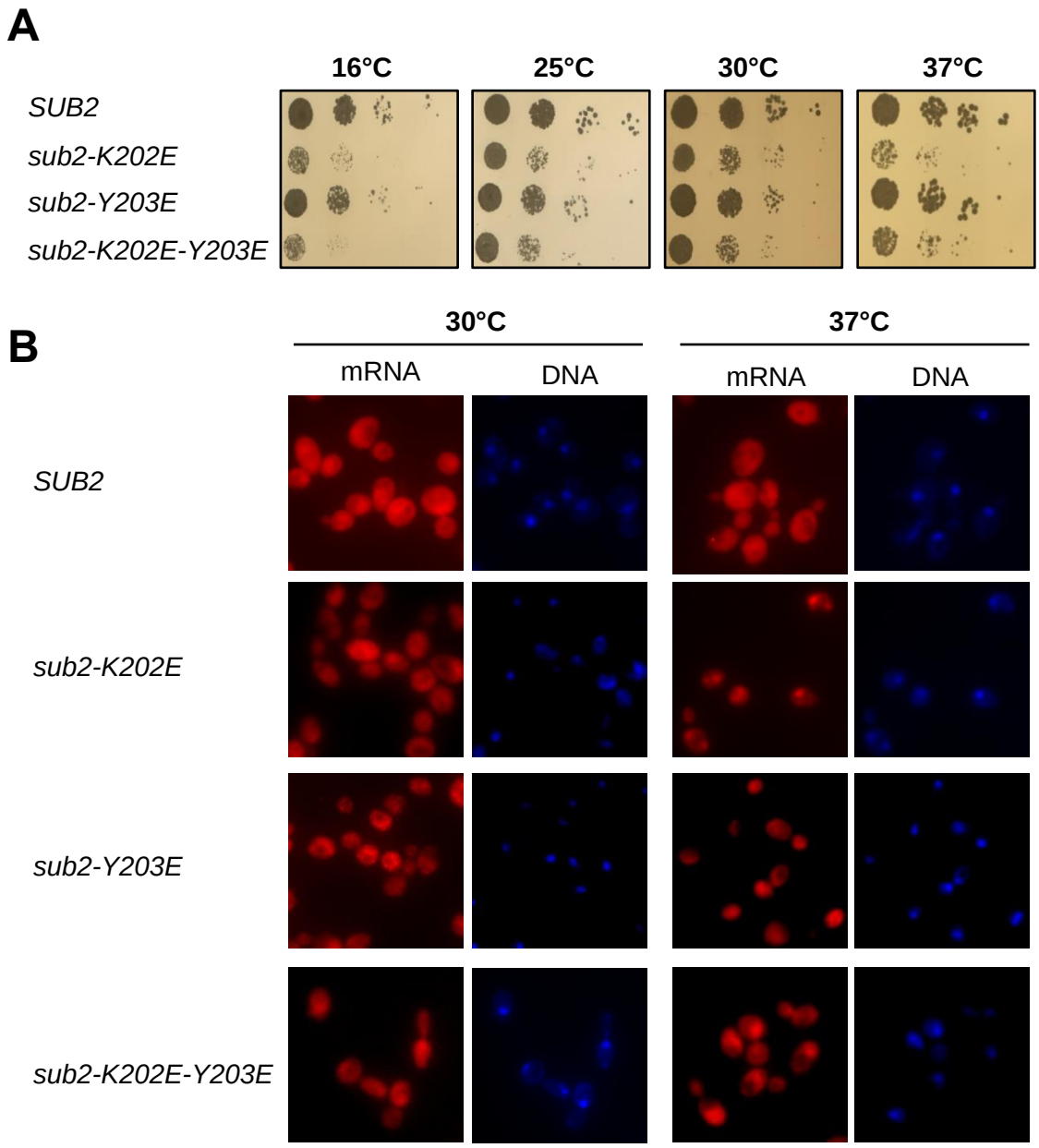

Figure 17: *sub2-K202E* causes the growth and mRNA export defects in *sub2 K202E-Y203E*.
(A) Serial dilution of single and double mutants of *sub2-K202E* and *sub2-Y203E*. **(B)** mRNA export of *sub2* mutants. Poly(A)$^+$ RNA visualized with Cy3-labelled oligo(dT_{50}) and DNA was visualized with DAPI.

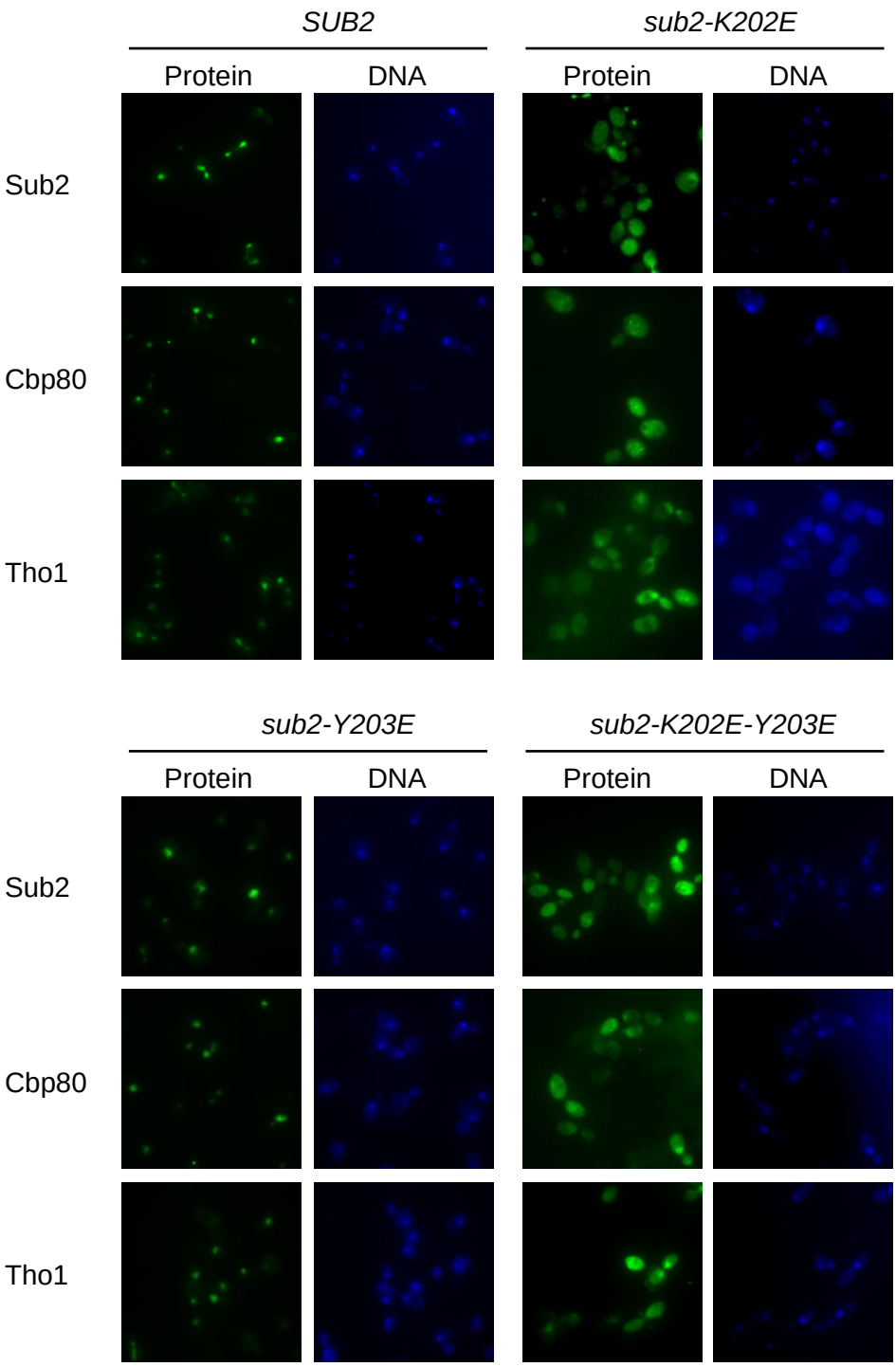

Figure 18: Immunofluorescence of *sub2-K202E, sub2-Y203E*
Localization of Sub2, Cbp80 and Tho1 in the single mutants *sub2-K202E* and *sub2-Y203E*. Proteins were visualized with an Alexa Fluor 488-coupled secondary antibody, directed against each primary antibody.

4.7 The mutations have no observable *in vivo* mRNA splicing defect

In the next series of experiments, we focused on the mutants *sub2-T62D*, *sub2-K70D* and *sub2-K202E-Y203E*. They were selected for further analysis because they had interesting phenotypes with respect to growth and mRNA export. To determine if splicing is affected in the

sub2 mutants, the splicing efficiency of three intron-containing genes, *DBP2*, *ASC1* and *RPL28* were analyzed. From the splicing assay, no differences were observed between *SUB2* and the mutants *sub2-T62D*, *sub2-K70D* and *sub2-K202E-Y203E* (Figure 19).

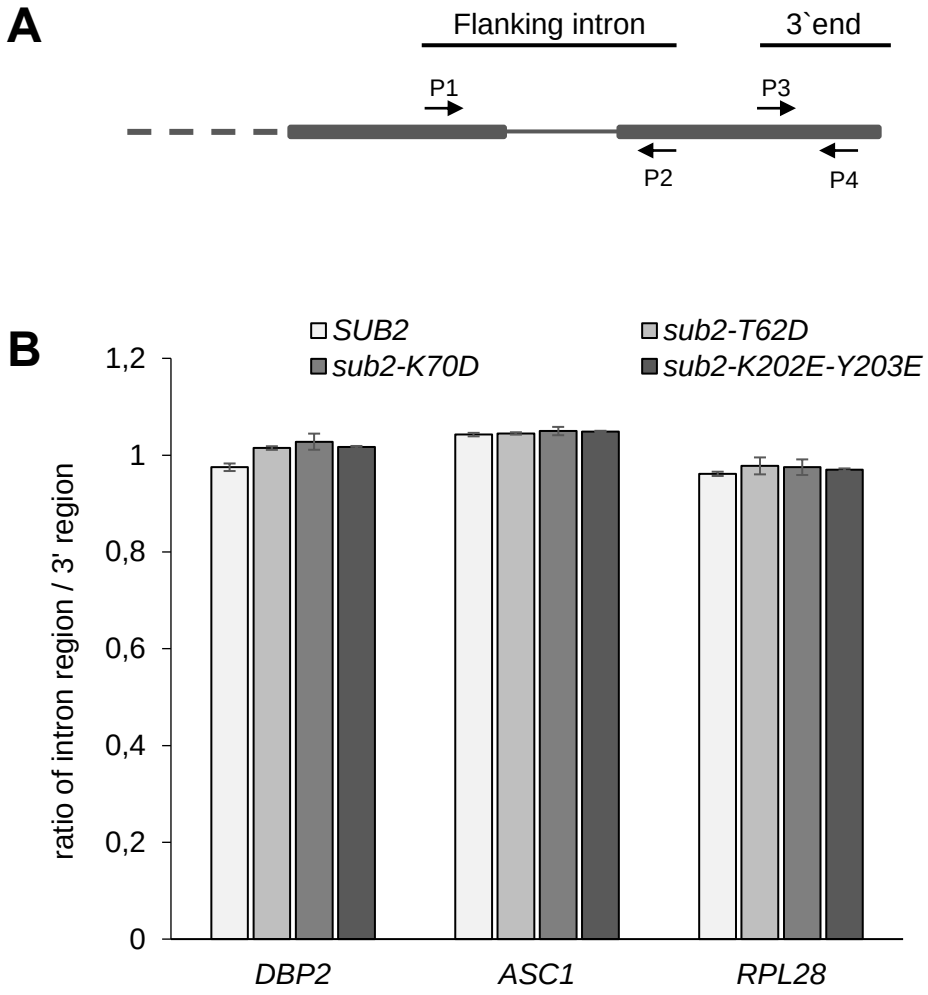

Figure 19: A splicing defect is not observed in *sub2* mutants.
Splicing efficiency was determined using primers that flank an intron-flanking and the 3' region of the intron-containing genes *DBP2*, *ASC1* and *RPL28*. mRNA was extracted, reverse transcribed and quantified by qPCR. **(A)**. Scheme of primer pairs (P1-P2 and P3-P4) used for the qPCR. **(B)** Ratio of intron region to 3' region of *SUB2* wild-type and mutants.

4.8 RNA binding of *sub2-K202E-Y203E* is impaired

Next, we tested the ability of the mutants to modulate helicase functions, i.e., RNA binding and RNA duplex unwinding. For RNA binding we performed an EMSA. Purified Sub2 proteins were pre-incubated with single and double stranded RNA in the presence of a non-hydrolyzable ATP analogue, ADPNP to keep Sub2 in a closed conformation with the RNA and prevent the Sub2-RNA complex from disassembling. Wild-type Sub2, sub2-T62D, sub2-K70D and sub2-K202E-Y203E bound ssRNA with similar efficiency (Figure 20A), indicating that binding to ssRNA was not impaired in the mutants. However, the mutants bound dsRNA with different affinities. The mutant sub2-T62D bound dsRNA like wild-type. It produced two distinct shifts

on the gel, - a lower band, resulting from a simple complex involving a 1:1 ratio of Sub2-dsRNA, and - an upper band (i.e., super shift), resulting from a Sub2-dsRNA complex, involving multiple molecules of Sub2 aggregating on the dsRNA. In contrast sub2-K70D and sub2-K202E-Y203E showed reduced binding to dsRNA. About half of the dsRNA remained unbound with the other half split into a super shift and a lower shift. Whereas the effect was not significant in *sub2-K70D*, the defect in dsRNA binding was very significant in *sub2-K202E-Y203E* (Figure 20B, p***≤0.001), indicating that these mutants have reduced ability to bind to dsRNA and form aggregates.

We also tested the RNA binding of the proteins to specific mRNAs *in vivo* using RNA immunoprecipitation (RIP). TAP-tagged Sub2 was immunoprecipitated and co-purified RNA reversed transcribed and quantified by qPCR. We determined the binding of the Sub2 wild-type and mutants to *YEF3*, *DBP2*, *RPL28* and *ASC1* (Figure 20C). Generally, there was reduced binding to all transcripts except *RPL28*, which did not reveal a significant difference in binding between the wild-type and mutant proteins (Figure 20C). Of the mRNA transcripts that were quantified, sub2-T62D, sub2-K70D and sub2-K202E-Y203E showed reduced binding to *YEF3*, *DBP2* and *ASC1*. sub2-T62D showed reduced binding to the intron-containing genes *DBP2* and *ASC1*, but not the intronless gene *YEF3*. However, sub2-K70D and sub2-K202E-Y203E showed significantly reduced binding to all the transcripts analyzed (P=*≤ 0.05, ** ≤ 0.01).

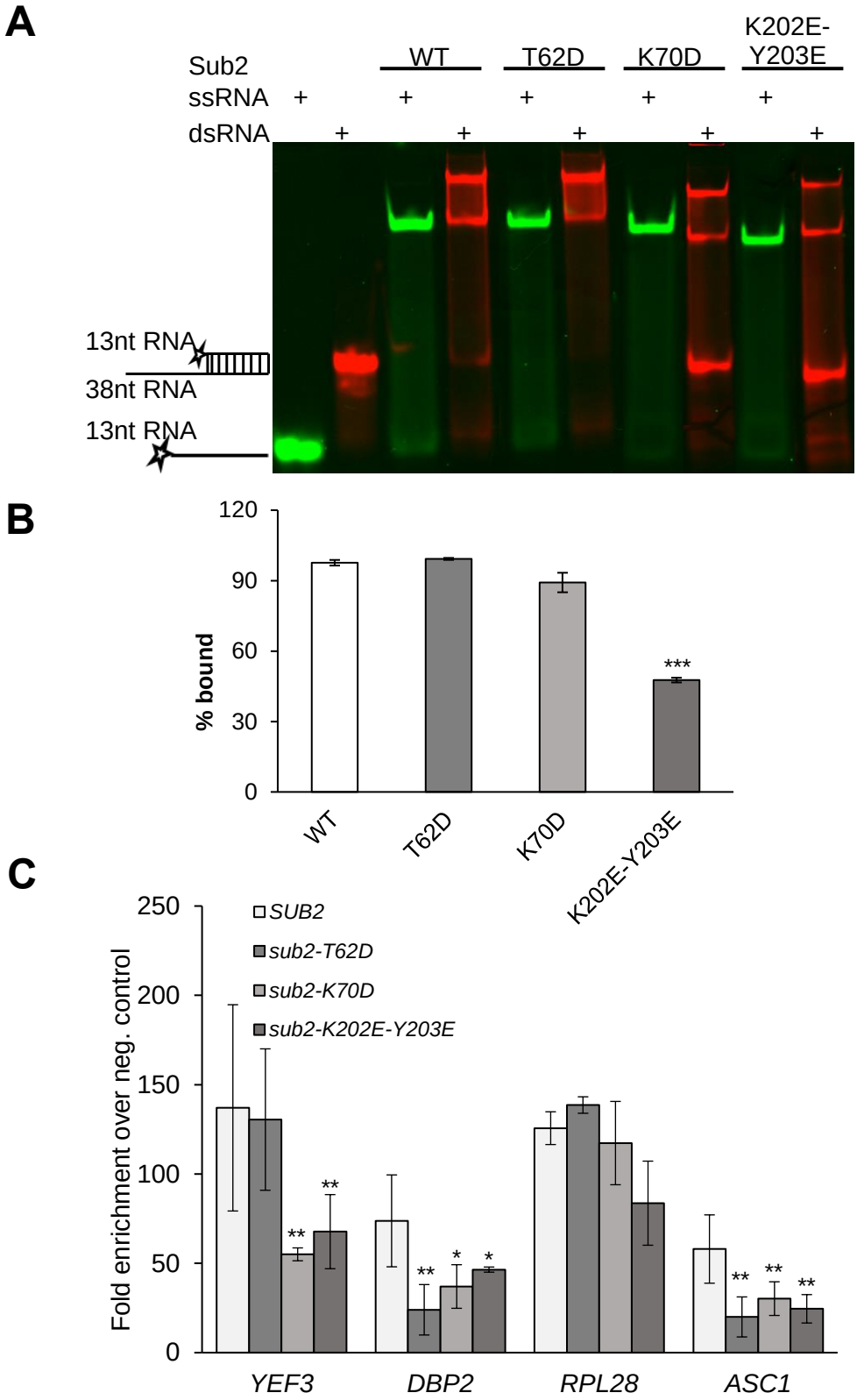

Figure 20: RNA binding in *sub2-K202E-Y203E* is impaired.
(A) EMSA of Sub2 proteins. *In vitro* RNA binding gel shift assay using fluorophore-labelled ss and dsRNA. **(B)** RNA binding measured with the Typhoon imager and quantified. **(C)** Co-purified mRNA from protein immunoprecipitations analyzed by RT-qPCR. Fold enrichment was calculated over a non-tagged Sub2 control. P-values of student's t-test: *≤ 0.05, ** ≤ 0.01, *** ≤ 0.001 (Miosga Matthias, 2022).

4.9 The RNA binding mutation also affects RNA helicase activity *in vitro*

ATP-dependent unwinding of RNA duplexes is a classical function of RNA helicases. However, not all helicases can unwind *in vitro*, and some *in vivo* functions do not depend on duplex unwinding. We assessed the ability of the purified proteins to unwind a dsRNA composed of 13 nt and 38 nt strands (Figure 21A). The helicase activity of sub2-T62D was comparable to Sub2 wild-type, while the helicase activities of sub2-K70D and sub2-K202E-Y203E were reduced to 80%, and 60% respectively. This reduction was significant in sub2-K202E-Y203E ($p^* \leq 0.05$), but not sub2-K70D.

In vivo, RNA helicases play a role in R-loop removal. R-loops arise when the mRNA transcript invades a dsDNA, displacing one DNA strand to generate an RNA-DNA hybrid and a free ssDNA. Their abundance is tightly regulated to ensure normal cell function. To detect the level of R-loops in wild-type and mutant cells, nucleic acids were extracted, RNase digested, and extracts probed with the S9.6 antibody for R-loops and a dsDNA antibody to control for total amounts (Figure 21B). The R-loop and dsDNA signals were quantified using the GelQuantNET software. The R-loop levels were normalized to dsDNA of the *SUB2* wild-type (Figure 21C). We observed that the mutants *sub2-T62D*, *sub2-K70D*, and *sub2-K202E-Y203E* had increased R-loop levels. The R-loop levels in the mutants were significantly increased compared to the wild-type *SUB2* ($p=^* \leq 0.05$, $^{**} \leq 0.01$).

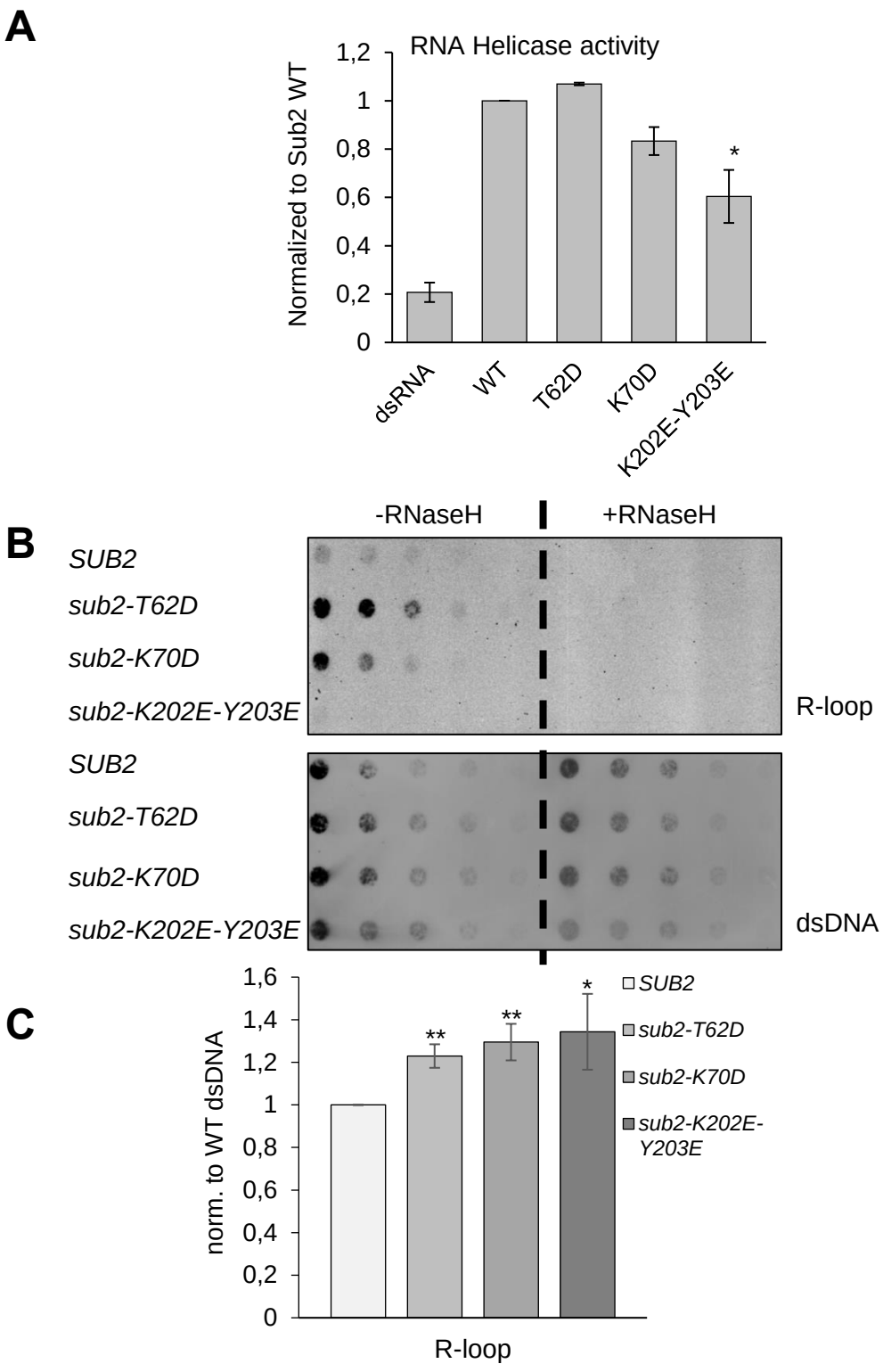

Figure 21: *sub2* mutants have increased R-loop levels.
(A) Quantification of RNA helicase activity using a Cy5 and a BHQ quencher coupled dsRNA and wild-type or mutant Sub2 protein. **(B)** R-loop detection in wild-type and mutant cells. Nucleic acid samples were treated with RNase T1 and RNase II or RNase H and 40 µL spotted onto nylon membranes in a dilution series. Membranes were then probed with S9.6 antibody or dsDNA antibody. **(C)** Quantification of S9.6 signal was divided by dsDNA signal intensity, then normalized to wild-type Sub2. Mean ± SD were calculated based on three biologically independent experiments. P-values of student's t-test: *≤ 0.05, ** ≤ 0.01 (The i*n vitro* assay was performed by Miosga Matthias, 2022).

4.10 The interaction of *sub2* mutants with other nuclear mRNP components is altered

Sub2 is a component of the TREX complex that couples transcription with mRNA export and is required for nuclear mRNA export. To determine if the observed mRNA export defects in *sub2-T62D*, *sub2-K70D,* and *sub2-K202E-Y203E* cells are partly due to a change in mRNP composition, we analyzed Sub2's interactions with other mRNP components. Sub2-TAP was purified, and co-purified proteins were detected by Western blotting (Figure 22A). The changes in interaction were quantified by measuring the signal intensities and normalized to Sub2 wild-type levels (Figure 22B). The interaction of sub2-T62D, sub2-K70D and sub2-K202E-Y203E with Cbp80, Mex67, Tho1 and Yra1 were significantly reduced (Figure 22A). sub2-T62D, however, had an increased interaction with Nab2 which was significant ($p^* \leq 0.05$). Noticeably, sub2-K70D had the strongest reduction of Cbp80, Mex67 and Nab2 protein levels. The amount of co-purifying Tho1 was significantly reduced in all three mutants.

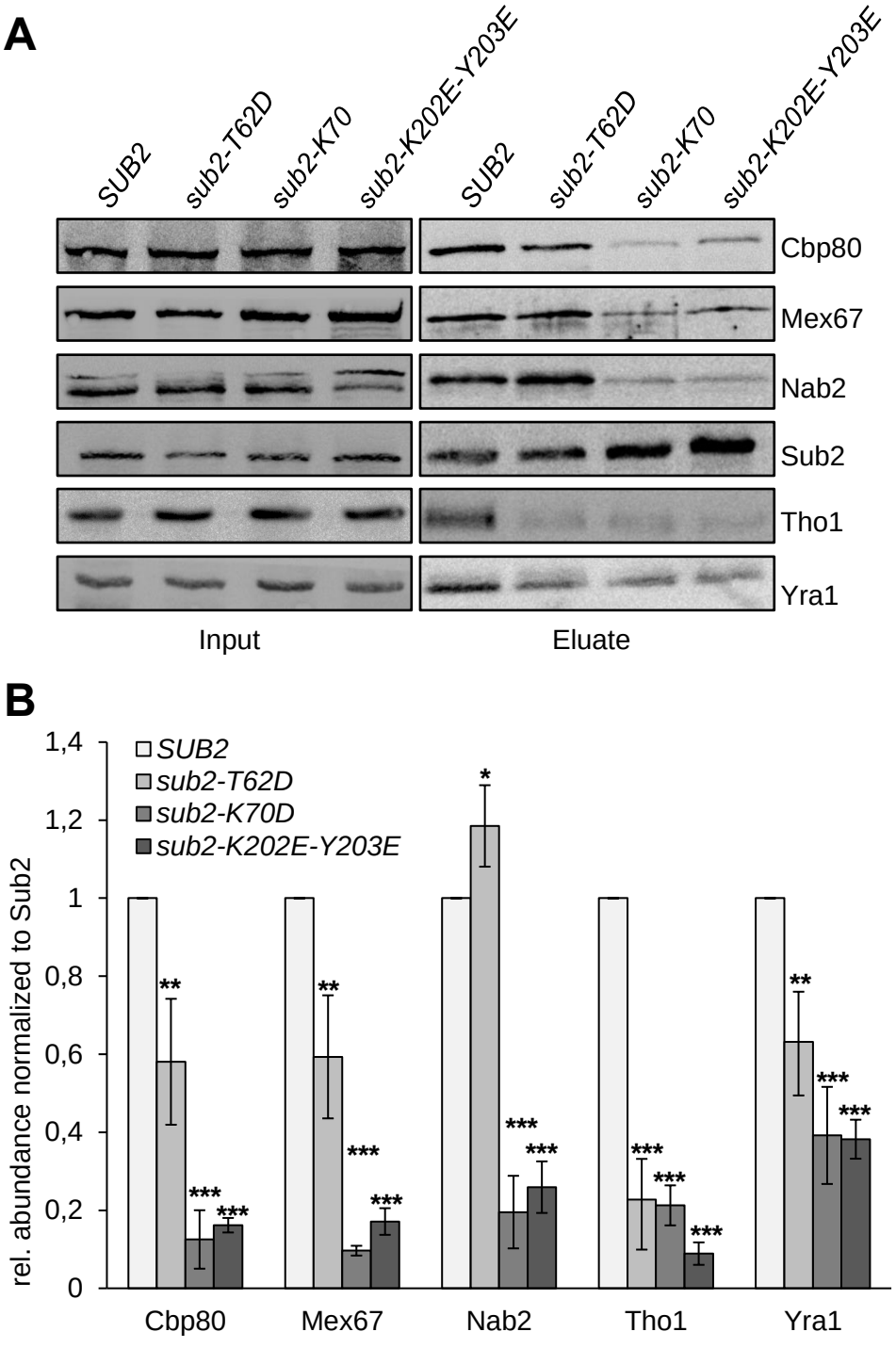

Figure 22: ***sub2* mutants exhibit reduced binding to other RBPs**.
(A) TAP-tagged wild-type and mutant Sub2 were purified by a two-step affinity purification and co-purifying proteins detected by Western blot. **(B)** Bars represent the quantification of three independent biological replicates. Protein levels were normalized to Sub2, and wild-type levels set to 1. P-values of student's t-test: *≤ 0.05, ** ≤ 0.01, *** ≤ 0.001.

4.11 Rescuing the nuclear localization of *sub2-K202E-Y203E* restores its growth

To uncover the mechanism underlying the mislocalization of Sub2, CBC and Tho1 to the cytoplasm in *sub2-K202E-Y203E* cells, we attached the HIV Rev nuclear localization signal (NLS) to *sub2-K202E-Y203E* to redirect the mutant protein to the nucleus. This fusion rescued the mislocalization of all three proteins (Figure 23A) and surprisingly, also rescued the growth defect associated with the mutant (Figure 23B-C). However, attaching an NLS to *sub2-K202E-Y203E* did not rescue the mRNA export defect of *sub2-K202E-Y203E*, as cells had mild export defects (Figure 24A) and increased R-loops (Figure 24A-B) (P-value: **≤0.01, *** ≤ 0.001). Thus, attaching an NLS to *sub2-K202E-Y203E* was not sufficient to rescue the mRNA mediated events of mRNA export and R-loops. Next, we attached a nuclear export signal (NES) from the protein kinase inhibitor to *SUB2* to replicate the phenotype associated with *sub2-K202E-Y203E*. As expected, *SUB2*-NES mislocalized Sub2. However. Cbp80 and Tho1 remained nuclear (Figure 23A). This fusion protein also had strong growth (Figure 23B-C) and export defects (Figure 24A). The export defect at 37°C was visible already 10 min after heat shock (data not shown). The level of R-loops was also increased in SUB2-NES, although it was not significant in comparison to the wild-type *SUB2* (Figure 24A-B).

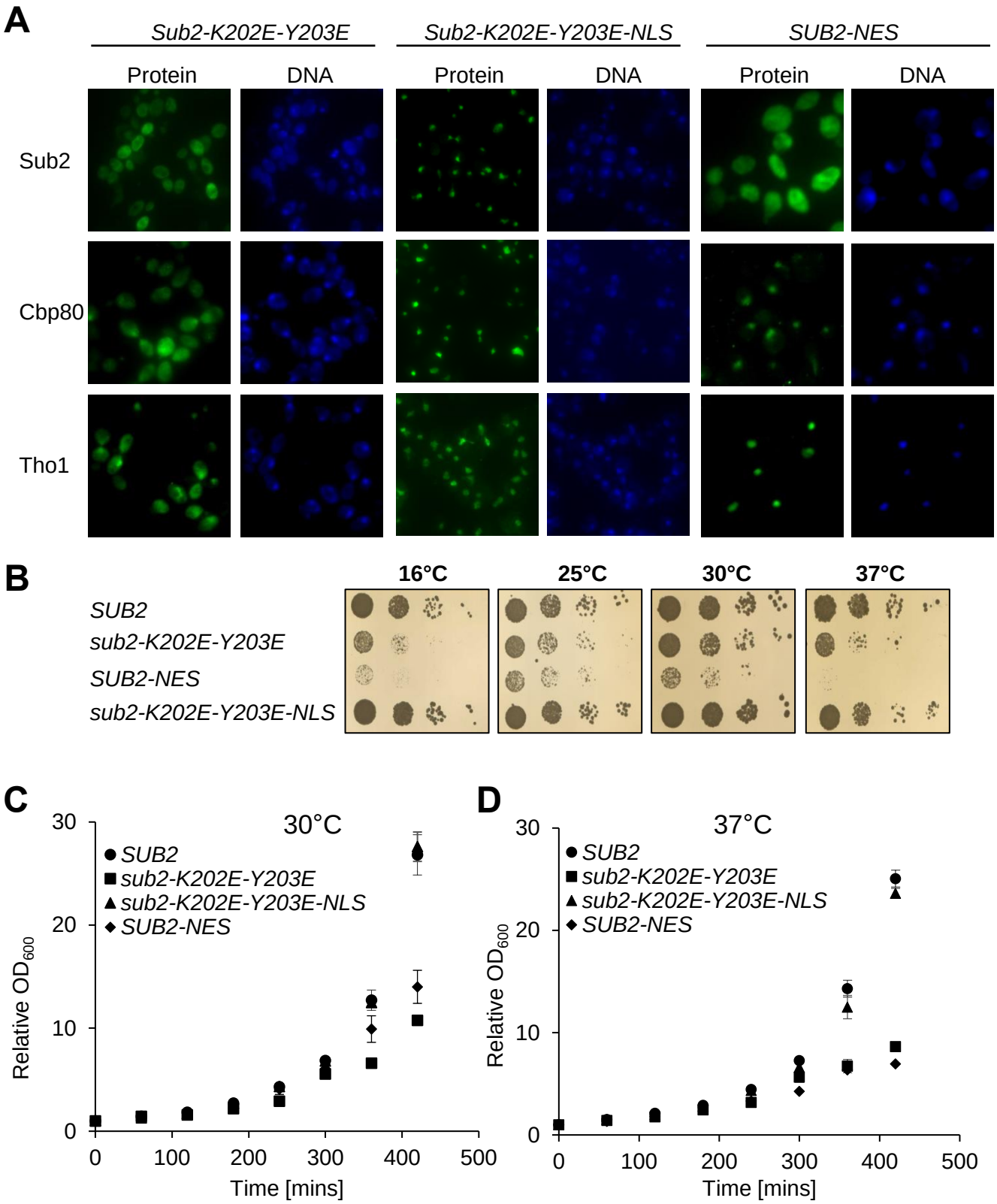

Figure 23: Attaching an NLS to *sub2-K202E-Y203E* rescues its localization and growth defects.
(A) Fusing the HIV Rev NLS to *sub2-K202E-Y203* rescues the cytoplasmic localization of Sub2, Cbp80 and Tho1 to the nucleus. Fusing a PKI NES to Sub2 mislocalizes Sub2, but not Cbp80 and Tho1. DNA visualized with DAPI, and proteins were visualized with secondary antibody conjugated to Alexa Fluor 488 directed against primary antibodies Sub2, Cbp80 and Tho1. **(B-D)** The rescued nuclear localization also rescues the growth defect, and the *SUB2*-NES strain shows a growth defect both on plate **(B)** and in liquid culture **(C-D)**.

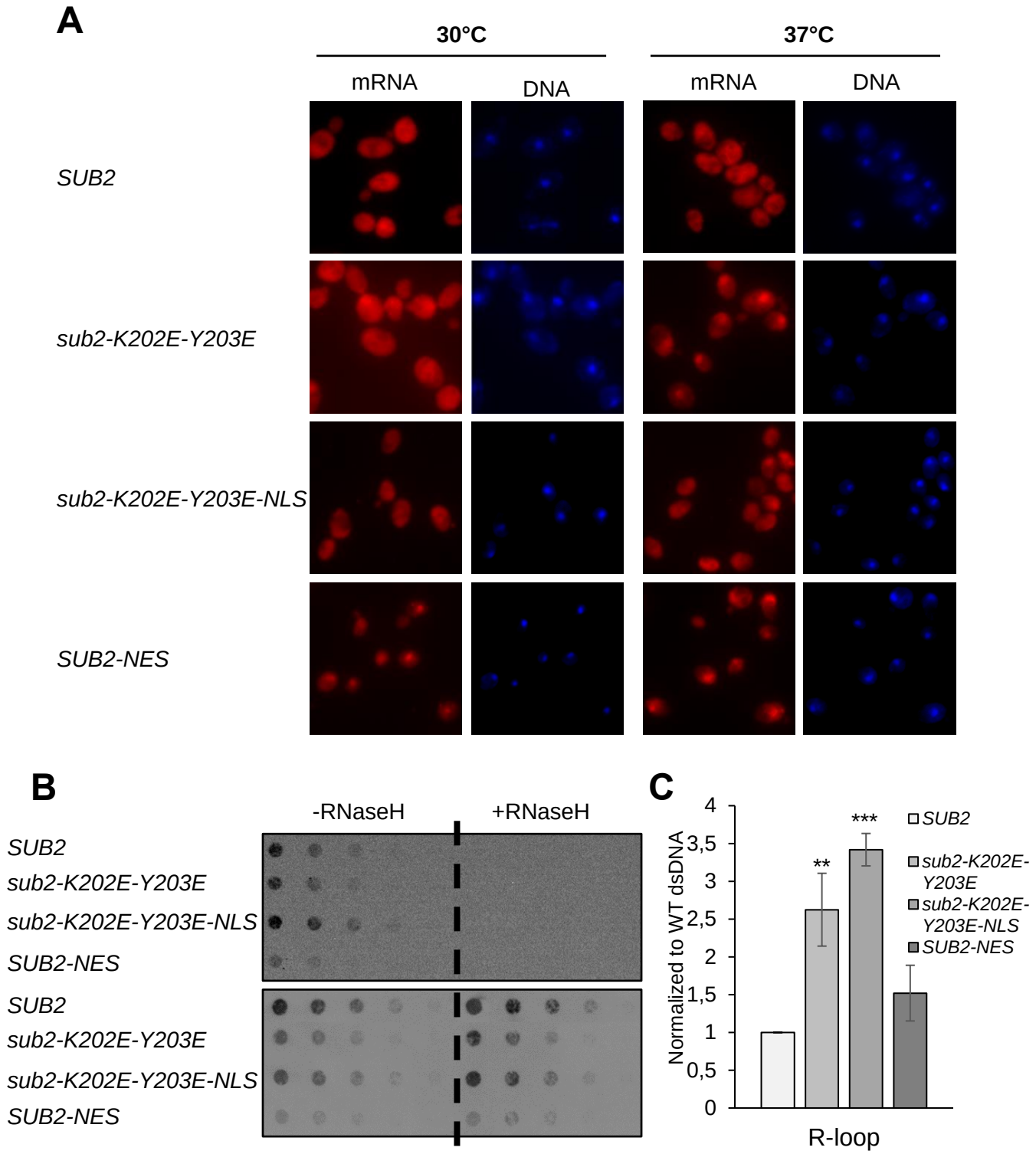

Figure 24: *sub2-K202E-Y203E*-NLS cells have a slight mRNA export defect.
(A) Poly(A)$^+$ RNA was visualized with Cy3-labelled oligo(dT$_{50}$) in *sub2-K202E-Y203E*-NLS and *SUB2-NES* cells in comparison to wild-type *SUB2* and *sub2-K202E-Y203E* cells **(B)** R-loop detection in cells in (A). Nucleic acid samples were RNase treated and then probed with the S9.6 antibody and dsDNA antibody. **(C)** Quantification of S9.6 signal was divided by dsDNA signal intensity, then normalized to the wild-type *SUB2*. Mean ± SD of 3 independent experiments. P-values of student's t-test: **≤ 0.01, *** ≤ 0.001.

4.12 The mislocalization of *sub2-K202E-Y203E* is not mRNA export mediated

Using a temperature-sensitive mutant of Mex67*, mex67-5*, which shows a strong mRNA export defect at 37°C, we asked if the mislocalization of sub2-K202E-Y203E was due to its accompanied export with the mRNA export receptor, Mex67 during mRNA export. We introduced the mutant *sub2-K202E-Y203E* into *mex67-5* cells and shifted the cells to 37°C to induce an mRNA export block. At the permissive temperature of 30°C, sub2-K202E-Y203E was cytoplasmic (Figure 255) as had also been observed in a wild-type *MEX67* background (Figure 15). When cells were shifted to the nonpermissive temperature, sub2-K202E-Y203E remained cytoplasmic, and the export block did not change its localization. At both 30°C and 37°C, wild-type Sub2 remained nuclear.

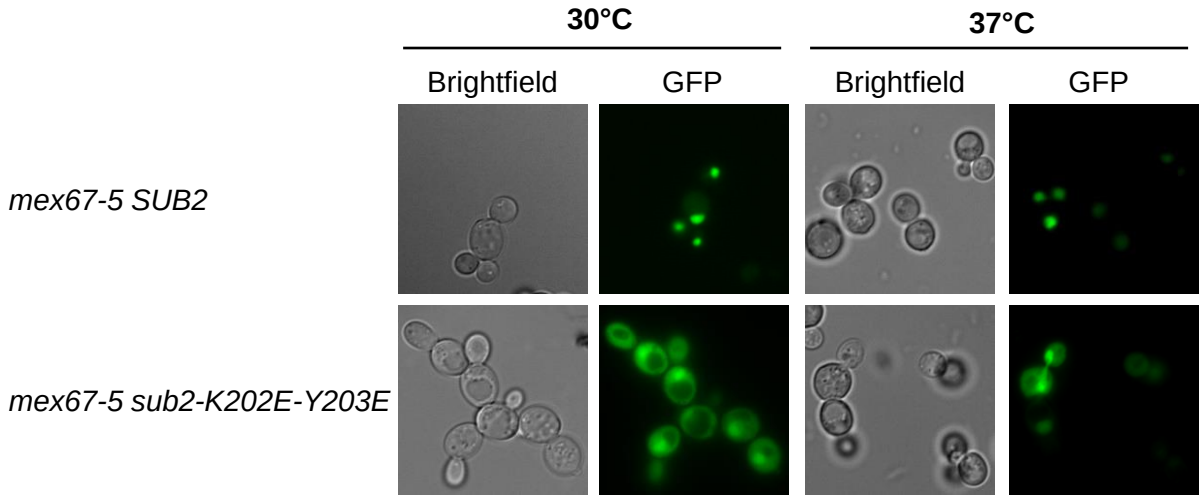

Figure 25: Mex67 does not mediate the export of *sub2-K202E-Y203E*.
The temperature-sensitive mRNA export mutant strain, *mex67-5* was transformed with *SUB2* and *sub2-K202E-Y203E*, grown at 30°C to early log phase and then shifted to 37°C for 1 h. Sub2-GFP was localized by direct fluorescence microscopy of live cells (GFP columns). Brightfield images show overall cell morphology.

4.13 The nuclear localization of Sub2 may be mediated by Mtr10

Protein import is mediated by a family of importins that recognize their cargoes and transport them through the NPC into the nucleus. These receptors include the karyopherin α pathway, which imports NLS-containing proteins, karyopherin β2, which transports a subset of mRNA binding proteins, and the Kap123 pathway which imports ribosomal proteins (Pemberton et al. 1997). Mtr10 mediates the nuclear import of proteins involved in nuclear mRNA export, for example Npl3 (Senger et al. 1998). To elucidate if Mtr10 also mediates the import of Sub2, we deleted *MTR10* in a *SUB2-GFP* strain. Deletion of *MTR10* resulted in a growth defect at 37°C but not at any of the other temperatures (Figure 26A). We observed that Sub2 was nuclear at 30°C (Figure 26B). However, at the non-permissive temperature of 37°C, Sub2 showed a slight accumulation in the cytoplasm, although the signal was mostly nuclear.

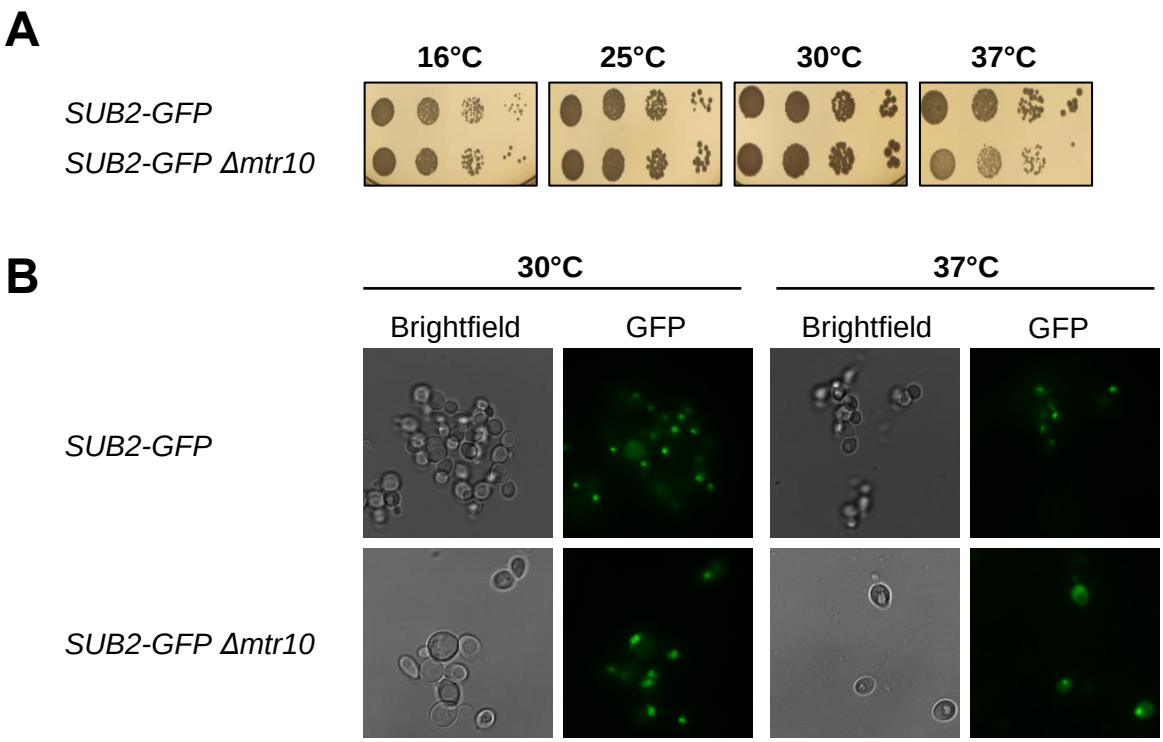

Figure 26: Characterization of *Δmtr10* mutant.
(A) Growth analysis of wild-type and *Δmtr10* strains. The *MTR10* deletion strain displays a mild growth defect at 37°C. **(B)** Sub2-GFP was localized by direct fluorescence microscopy of live cells (GFP columns). Brightfield images show overall cell morphology in wild-type and *Δmtr10* strains.

5 Discussion

Using a directed mutagenic approach, we mutated amino acids of Sub2 that were identified to crosslink to RNA *in vivo*. These mutations were generated to abrogate binding to RNA by the amino acids. These mutations resulted in varying phenotypes. Some mutations affected cell viability, growth, mRNA export, protein localization, impaired interaction with other mRNP components, as well as RNA binding and core helicase activities. The variability of the phenotypes we observed reveals the role of Sub2 in various processes for which different amino acids are essential. This work provides further insight into the molecular mechanisms of Sub2 in mRNP biogenesis.

5.1 Identification of RNA-binding sites

RNA-binding domains (RBDs) mediate RNA binding of RNA-binding proteins (RBPs). However, not all residues in RBDs are required for binding to the RNA target. Some play other roles in substrate processing. For example, some residues in the RBD of Stem-Loop Binding Protein (SLBP) are important for histone pre-mRNA processing (Dominski et al. 2001), due to their interaction with other RBPs (Yang et al. 2002; Cieniková et al. 2015).

RBDs are typically enriched in the amino acids Arg, His, Lys, Phe, Tyr, Glu, and Asp at protein-RNA interfaces and contribute substantial stability to protein-RNA binding (Wilson et al. 2016; Hu et al. 2018). We identified that most amino acids of Sub2 that crosslinked to RNA were Lys, Arg, Tyr and Phe residues (Figure 8), which is consistent with amino acids that readily interact with RNA (Castello et al. 2016). We also identified amino acids in positions of Sub2 that were not previously known to contribute to RNA binding (motifs Ia, Ib, IV and V). A contribution of amino acids outside the RBD to RNA-protein interactions has been observed for other proteins. HnRNP A1, for example, contains two RNA recognition motifs (RRM) and an RGG region that influence RNA binding specificity and strength. However, binding to RNA in a region upstream of its RRM1 domain has been observed (Castello et al. 2016). This region stabilizes the binding to RNA (Leulliot and Varani 2001; Ravindranathan et al. 2010). Thus, residues in RBDs have different functions than RNA binding. Therefore, the identification of amino acid residues outside known RNA-binding motifs of Sub2 reinforces the contribution of other residues to RNA binding.

5.2 Amino acid mutations that influence viability

In the complementation assay, we observed that some mutations did not complement the loss of wild-type *SUB2* (Figure 9). In all the non-viable strains, *sub2-F234E-R235E*, *sub2-R260A-F261A*, *sub2-R368A* and *sub2-Y390A-R393E*, no Sub2 protein could be detected by Western blotting (Figure 10C), indicating that these were null mutations that affected either the transcription and or translation of Sub2. Additionally, these residues are very conserved, and

mutating them could be deleterious to the protein. Hydrophobic residues contribute to the stability of a protein's tertiary structure (Kauzmann 1959; Moelbert et al. 2004) and are often conserved. Mutating them could influence the folding of the protein and thus its stability. For example, the hydrophobic phenylalanine (F) at 234 was exchanged for the hydrophilic residue glutamate (E) which would affect the interaction it makes with other residues in the protein. Whereas F261 was exchanged for another hydrophobic residue, alanine (A), A is smaller in size (MW: 89.09) compared to F (MW: 165.2). This change in size may influence the bending of the peptide chain and the contact it makes with other residues in the protein. This could explain why the mutants *sub2-F234E-R235E* and *sub2-R260A-F261A* were nonviable. Also, in the crystal structure of Sub2-Yra1-RNA complex, the residues F234, R235, R260 and F261 of Sub2 interact with Yra1 (Ren et al. 2017). Therefore, these mutations could have abolished the interaction with Yra1, which also promotes Sub2's interaction with RNA and resulted in a strong RNA-binding defect leading to the nonviability of these cells. Comparatively, the positively charged arginine (R) at residues 368 and 393 were exchanged for an uncharged A and negatively charged E respectively. Although the mutation R368A would not repel RNA, the smaller A (MW: 89.09 compared to the bulkier R, MW: 174.2) would influence the structure of the protein at this position and the interaction it makes with other residues in its vicinity. In a similar manner, exchanging the bulky, neutral tyrosine (Y, MW: 181.1) residue at 393 for a smaller A would also affect protein folding. Therefore, these observations suggests that the characteristics of amino acids, such as hydrophobicity, size and charge matter since these factors affect their spatial arrangement in the protein (Biro 2006) which influences protein folding and how the protein interacts with other macromolecules.

5.3 Effects of mutation on growth

The requirement of Sub2 for growth depends on the strain background (López et al. 1998). In the RS453 strain we used, Sub2 is essential for growth. In the dot spot assay, we observed strong growth defects in *sub2-T62D* and s*ub2-K202E-Y203E* strains. The growth defect resulting from mutating the residue T62 was specific to T62D, but not T62A (Figure 11 and Figure 12). In the human homolog UAP56, this residue is not conserved and instead has a serine (S) at this position (Kistler and Guthrie 2001). S and T have similar sizes (MW=105, 119) and are also uncharged hydrophilic residues (Bruce Alberts et al. 2002). Thus, the residue at this position can be exchanged for a similar residue without considerable effect on protein structure and function. In T62A, the exchange of T for an uncharged A, does not lead to a change in protein folding thus protein function is unaffected. However, when exchanged for the negatively charged and bulkier D (MW=133), these variations influence overall protein folding and the negative charge of D also repels the negatively charged RNA. Consistent with this, we observed that the mutation T62D resulted in reduced *in vivo* binding to the transcripts *DBP2* and *ASC1* (Figure 20C), although, we did not observe a defect in RNA-binding *in vitro*

(Figure 20A-B). It is possible that, *in vivo*, the suboptimal *sub2-T62D* mutant is sequestered from RNA or is not recruited to RNA by other proteins that recruit it to the RNA. However, *in vitro*, no sequestration occurs and the protein in proximity to RNA remains bound. Such sequestration of damaged proteins occurs in cells during stress (Hill et al. 2017). The mutant *sub2-K202E-Y203E* also had a very strong growth defect and impaired binding to RNA both *in vivo* and *in vitro* (Figure 20A-C). Unlike T62 which is not conserved in human, K202 is conserved and suggests that changing this residue could have an impact on protein folding and thus function. These observations are similar to a study in Ded1 where mutational analysis of the SAT (motif III) revealed that the size and charge of an amino acid is important for Ded1's ability to support growth (Banroques et al. 2010). Also, the crystal structure of Sub2 in complex with RNA, shows that the residues K202 and Y203 are close to the RNA molecule (Ren et al. 2017). Thus, K202 could bind RNA directly or contribute to stabilizing the interaction with RNA, and when mutated leads to the impaired RNA-binding and the growth defects we observed. Therefore, these results confirm that the conservation of an amino acid residue is vital to protein function and certain residues with similar properties can be substituted without influencing protein function.

5.4 Functional analysis of *sub2* mutants

Only mRNA that is processed and packaged by proteins into an mRNP can be translocated from the nucleus into the cytoplasm (Strässer et al. 2002; Saguez et al. 2005). Sub2 is a component of TREX complex (Strässer and Hurt 2000, 2001; Zenklusen et al. 2001; Dufu et al. 2010) and is required for export. The mutants *sub2-K53A/D-Y56A/D*, *sub2-K70D* and *sub2-Y144E*, showed no growth defects. In contrast they had mRNA export defects (Figure 13) suggesting that these mutations are of little importance to growth but are required to mediate mRNA export. These findings point to the requirement of Sub2 for mRNA export in contrast to the role it plays as an efficiency factor in splicing and polyadenylation. The mutants *sub2-T62A* and *sub2-K403E* had no growth or export defect, suggesting that these mutations had no consequence on protein function. Importantly, the export defect was not due to low levels of the mutant proteins, as Western blotting analysis of whole cells lysates of strains growth at 30°C and 37°C confirmed that all proteins were expressed at wild-type levels (Figure 14). Moreover, microscopic detection of these mutant proteins, localized them to the nucleus like wild-type *SUB2* (Figure 15). Comparable to the growth defects, the mutants *sub2-T62D* and *sub2-K202E-Y203E* had mRNA export defects. The consistent defects in growth and mRNA export suggests that, although the mutations had no effect on protein expression, they resulted in defective proteins that are incapable of supporting growth and mRNA export. Both mutant proteins were also expressed to wild-type level. However, unlike sub2-T62D which was nuclear, sub2-K202E-Y203E was cytoplasmic.

Further analysis of the mutants *sub2-T62D*, *sub2-K70D* and *sub2-K202E-Y203E* to understand the mRNA export defect we observed, indicated that the detect was due to altered interaction with other mRNPs and thus proteins of the TREX complex. We observed that the mutants *sub2-T62D*, *sub2-K70D* and *sub2-K202E-Y203E* had reduced interaction with the RNA export adaptor Yra1 and the export receptor Mex67 (Figure 22A-B). Both proteins interact with Sub2 in an RNA-dependent manner (Linder and Jankowsky 2011; Zenklusen et al. 2001; Strässer et al. 2002). Therefore, impairing RNA binding as we observed *in vivo* (Figure 20C) would abolish the interaction between these proteins and lead to mRNA export defects. Sub2 associates with Tho2, Hpr1, Mft1, Gbp2, Hrb1, Tex1, Thp2 and Yra1, components of the TREX complex and other associated proteins, Mlp1, Sac3 and Hsp70 (Strässer et al. 2002; Hurt et al. 2004). We observed that the interaction of the mutant Sub2 with these proteins was reduced (Coomassie gel; data not shown). We also observed that sub2-T62D had an increased interaction with Nab2, a regulator of poly(A) tail length and a protein required for mRNA export which is predominantly enriched at the 3' end of transcripts (Tuck and Tollervey 2013; Baejen et al. 2014). The scope of this study did not cover the mechanism leading to the increased interaction of sub2-T62D with Nab2 and the functional effect of this increased interaction. Importantly, the reduced interaction of the mutants with other mRNP components results in the observed mRNA export defect.

5.5 Helicase activities of *sub2* mutants

Having observed that the mutations *sub2-T62D*, *sub2-K70D* and *sub2-K202E-Y203E* resulted in impaired RNA-binding *in vivo*, we assayed if these mutations also affected the helicase activity and R-loop resolution. sub2-T62D retained binding to RNA (Figure 20A-B) and unwound dsRNA close to wild-type level (Figure 21A), suggesting that this mutation did not affect the *in vitro* RNA-binding and helicase activity. sub2-K70D did not also show reduced binding to dsRNA *in vitro*, however, it had a reduced helicase activity compared to wild-type Sub2, suggesting that although binding is retained *in vitro*, it may not be fully functional when it comes to executing *in vitro* helicase activity. sub2-K202E-Y203E showed reduced binding to dsRNA and reduced helicase activity *in vitro*. Suggesting that sub2-K202E-Y203E contributes to RNA binding and helicase activity, and this impairment accounts for the observed functional defects.

Cells have developed strategies to limit R-loops from persisting. These include RNA processing factors (Huertas and Aguilera 2003), topoisomerases (Tuduri et al. 2009), chromatin remodellers (Herrera-Moyano et al. 2014), RNA/DNA helicases (Chang et al. 2017), and RNase H enzymes (Cerritelli and Crouch 2009). Sub2 in concert with THO prevents hyper-recombination associated with R-loops (Gómez-González et al. 2011). Overexpression of Sub2 in a *Δhpr1* strain, suppresses its hyper-recombination phenotype (Fan et al. 2001; Jimeno et al. 2002), and in human cells, depletion of UAP56 leads to a strong genomic

instability phenotype (Domínguez-Sánchez et al. 2011). We observed that all three mutants, *sub2-T62D*, *sub2-K70D* and *K202E-Y203E,* had increased R-loop levels (Figure 21B). *sub2-T62D* had increased R-loops despite wild-type-like helicase activity. In our helicase assay, we only looked at the ability of the mutants to unwind dsRNA but not RNA-DNA hybrids. UAP56 can bind and unwind RNA-DNA hybrids, (Pérez-Calero et al. 2020; Schuller et al. 2020) and a stronger affinity for RNA-DNA has also been shown for Sub2 (unpublished data by Matthias Miosga). Therefore, since *sub2-T62D* had close to wild-type RNA helicase activity which does not explain the increased R-loop, this mutant may be unable to bind RNA-DNA hybrids and subsequently resolve them. To resolve R-loops, Sub2 is recruited to the transcribing gene via the THO complex and components, Tho2 and Hpr1 (Jimeno et al. 2006; Gómez-González et al. 2011; Meinel et al. 2013). (Ren et al. 2017) showed that mutations at the Sub2-N terminal lobe, in the residues A66 and D68 disrupts the interaction between Sub2 and THO. Proximity of T62 to this lobe, implicates it in the interaction with THO and would result in it not being recruited to the RNA when mutated. Consistent with this possibility, we observe that sub2-T62D has reduced interactions with other mRNP components (Figure 22B). Chromatin Immunoprecipitation (ChIP) of the THO complex components Tho2 and Hpr1 could also be performed to determine if the recruitment of sub2-T62D to the transcribing gene is impaired. In the two mutants *sub2-K70D* and *K202E-Y203E*, the loss in helicase activity coincides with the increase in R-loops, suggesting that the defect in RNA helicase activity also affect RNA-DNA hybrid unwinding. Despite all three mutants having variable growth phenotypes, they all show defects in mRNA export and increased R-loops. This is also true for the *Δhpr1* strain, which has increased R-loops and an mRNA export defect. Therefore, the increased R-loops could contribute to the mRNA export defect in these strains, due to the coupling between transcription, mRNA processing and export (Luna et al. 2005; Hocine et al. 2010).

5.6 Mutating K202 affects nuclear localization of Sub2

Mutating the amino acid K202 led to a mislocalization of Sub2 to the cytoplasm (Figure 15), which was not limited to Sub2. The cap-binding complex (CBC) and Tho1 (a TREX interacting protein) also mislocalized to the cytoplasm (Figure 16). The mislocalization was specific to these proteins, as the localization other mRNP components was not affected. The human homolog of Sub2, UAP56, has a Crm1-independent shuttling activity (Thomas et al. 2011), but a shuttling activity of *S. cerevisiae* Sub2 has not been demonstrated. However, it was identified that the amino acids 81-381 of UAP56 (the K202 residue of Sub2 falls in this range) are required for nuclear localization (Thomas et al. 2011). These stretches of residues are not lysine-rich, nor do they fit the definition of classical nuclear localization signal (NLS) motifs. *In silico* searches did not reveal an NLS in Sub2 but fusing the HIV-1 Rev nuclear export signal (NES) to Sub2 was insufficient to make Sub2 cytoplasmic (data not shown), indicating that they may exist a strong import sequence that overcomes the HIV-1 Rev NES. However, the

stronger NES of the protein kinase A inhibitor (PKI) was able to redirect the protein into the cytoplasm (Figure 23A). The mechanism underpinning the cytoplasmic localization of *sub2-K202E-Y203E* remains unclear. But we observed that, this cytoplasmic localization was not mRNA export mediated. When we blocked mRNA export in a temperature-sensitive *mex67* mutant, *mex67-5*, sub2-K202E-Y203E remained cytoplasmic (Figure 25), suggesting that Mex67 does not mediate the shuttling activity of Sub2. Another possibility could be, that, sub2-K202E-Y203E is not imported into the nucleus since the mutation interferes with a putative nuclear import signal. Consistent with this possibility, we observe that attaching an NLS to *sub2-K202E-Y203E* is sufficient to import the protein into the nucleus, which consequently rescues the growth defect associated with this mutant. In a similar manner, a constitutively cytoplasmic Sub2, *SUB2*-NES shows a strong growth defect (Figure 23A, B). These observations reinforce the possibility that the import of Sub2 into the nucleus leads to optimum growth of cells, and blocking import, leads to growth associated defects.

It remains to be understood, the import pathway of Sub2. As a possibility, we probed Mtr10 as a possible import receptor, since it mediates the import of proteins involved in mRNA export such as Npl3 (Senger et al. 1998). We deleted *MTR10* in a *SUB2*-GFP strain and analyzed the localization of Sub2. Similar to previously reported, growth of Δ*mtr10* was impaired at 37°C (Figure 26A) (Ben-Aroya et al. 2008), and Sub2 was nuclear under normal growth conditions at 30°C (Figure 26B). In contrast to a complete cytoplasmic localization of Npl3 at 37°C in a Δ*mtr10* mutant, we observed a nuclear localization of Sub2, with a slight cytoplasmic localization as well (Senger et al. 1998). However, while the Δ*mtr10* strain in the Npl3 study exhibited a growth defect already at 30°C and was nonviable at 37°C, the Δ*mtr10* strain we generated had a growth defect only at 37°C. This difference may explain the incomplete mislocalization of Sub2. The contrasting effect of the role of Mtr10 in Sub2 and Npl3 localization may be due to accumulation of differences in laboratory strains. or alternatively, a different pathway exists to import Sub2. The yeast orthologue of importin β, Kap95 has been shown to interact with Sub2 (Costanzo et al. 2016). But the role of this interaction in the context of the Sub2's import has not been studied. Further analysis into this interaction would provide more insight into the import of Sub2. Studying the localization of Npl3 in our strain would also have to be verified to understand these observed differences.

We also observed the co-mislocalization of Cbp80 and Tho1 in the cytoplasm, which is rescued when an NLS is fused to *sub2-K202E-Y203E* (Figure 23). However, fusing an NES to *SUB2* did not replicate the co-mislocalization of Cbp80 and Tho1. A shuttling activity of Tho1 has not been described, however, Cbp80 shuttles with mRNA although it is predominantly nuclear (Visa et al. 1996; Shen et al. 2000). Cbp80-bound mRNAs undergo a pioneer round of translation (Ishigaki et al. 2001) before the CBC is replaced by the eukaryotic initiation factor 4E (eIF4E) in the cytoplasm in an importin-dependent manner (Sato and Maquat 2009). Sub2

interacts with both Cbp80 and Tho1 (Ito et al. 2001; Libri et al. 2002; Yu et al. 2008; Wilmes et al. 2008). We did not observe an mRNA-dependent export of Sub2; therefore, these proteins could be co-transported in a manner yet to be identified and TAP purification did not show an increased interaction with Sub2 (Figure 22). These proteins may form a trimeric complex that is stabilized by a master regulator that also mediate their import. The mutation of Sub2 may have interrupted the stability of this trimeric complex leading to cytoplasmic localization and the reduced interaction of Sub2 with them in the cytoplasm.

5.7 Conclusion

Although the RNA-binding activity of RNA helicases is known to be largely mediated by its RNA-binding motifs, certain residues outside of these motifs also contribute to binding and the stability of RNA-protein interactions.

In this study, we mutated putative RNA-binding sites of Sub2 that were identified to crosslink to RNA *in vivo* and identified some amino acids that are essential for proper protein folding and function. Detailed analysis of three of these mutants revealed that mutating different residues of Sub2 leads to varied outcomes *in vivo*. Here, we identified a *sub2-T62D* mutant that had growth and mRNA export defects, but no impaired binding to RNA and helicase activity *in vitro*. The location of *sub2-T62D* in the THO-Sub2 crystal structure provides insight into the possibility that this residue mediates interaction of Sub2 with the THO complex. We also identified a *sub2-K70D* mutant, that had no growth defect, but had an mRNA export defect, and mild RNA-binding and reduced helicase activity *in vitro*. We also identified a novel mislocalization mutant *sub2-K202E-Y203E* that mislocalizes Sub2, CBC and Tho1. The location of this mutation in the Sub2-Yra1-RNA crystal structure and its associated phenotypes suggests that this residue participates in mRNA binding. Using this mutant, we could also provide evidence to suggest that the nuclear localization of Sub2 is vital for the growth of cells and does not rely on its ability to bind RNA. However, binding to RNA is required to mediate mRNA export and helicase activities.

Future studies would focus on RNA sequencing to give a global picture on the splicing efficiency and stability of mRNA transcripts in these mutants. A ChIP of these mutants would also be carried out to unravel the mechanism underlying the reduced interaction with other mRNP components on the transcribing gene. Of importance, would be the interaction of sub2-T62D with the THO complex. Another interesting study would be to uncover the mechanism underlying the mislocalization of Sub2 in *sub2-K202E-Y203E*, and if a shuttling activity exists for Sub2. In conclusion, this work provides data to support the role of Sub2 in mRNP formation via its RNA-binding ability and correlates RNA-binding with RNA helicase activity *in vitro*. It also corroborates other studies that mutations to Sub2 affect cell viability and mRNA export.

6 Publication bibliography

Abdel-Monem, M.; Dürwald, H.; Hoffmann-Berling, H. (1976): Enzymic unwinding of DNA. 2. Chain separation by an ATP-dependent DNA unwinding enzyme. In *European journal of biochemistry* 65 (2), pp. 441–449. DOI: 10.1111/j.1432-1033.1976.tb10359.x.

Aguilera, A.; Klein, H. L. (1990): HPR1, a novel yeast gene that prevents intrachromosomal excision recombination, shows carboxy-terminal homology to the Saccharomyces cerevisiae TOP1 gene. In *Molecular and cellular biology* 10 (4), pp. 1439–1451. DOI: 10.1128/mcb.10.4.1439-1451.1990.

Akhtar, Asifa; Gasser, Susan M. (2007): The nuclear envelope and transcriptional control. In *Nature reviews. Genetics* 8 (7), pp. 507–517. DOI: 10.1038/nrg2122.

Alber, Frank; Dokudovskaya, Svetlana; Veenhoff, Liesbeth M.; Zhang, Wenzhu; Kipper, Julia; Devos, Damien et al. (2007): The molecular architecture of the nuclear pore complex. In *Nature* 450 (7170), pp. 695–701. DOI: 10.1038/nature06405.

Alcázar-Román, Abel R.; Tran, Elizabeth J.; Guo, Shuangli; Wente, Susan R. (2006): Inositol hexakisphosphate and Gle1 activate the DEAD-box protein Dbp5 for nuclear mRNA export. In *Nature cell biology* 8 (7), pp. 711–716. DOI: 10.1038/ncb1427.

Amberg, D. C.; Goldstein, A. L.; Cole, C. N. (1992): Isolation and characterization of RAT1: an essential gene of Saccharomyces cerevisiae required for the efficient nucleocytoplasmic trafficking of mRNA. In *Genes & development* 6 (7), pp. 1173–1189. DOI: 10.1101/gad.6.7.1173.

Anderson, J. T.; Wilson, S. M.; Datar, K. V.; Swanson, M. S. (1993): NAB2: a yeast nuclear polyadenylated RNA-binding protein essential for cell viability. In *Molecular and cellular biology* 13 (5), pp. 2730–2741. DOI: 10.1128/mcb.13.5.2730-2741.1993.

Arenas, J. E.; Abelson, J. N. (1997): Prp43: An RNA helicase-like factor involved in spliceosome disassembly. In *Proceedings of the National Academy of Sciences* 94 (22), pp. 11798–11802. DOI: 10.1073/pnas.94.22.11798.

Baejen, Carlo; Torkler, Phillipp; Gressel, Saskia; Essig, Katharina; Söding, Johannes; Cramer, Patrick (2014): Transcriptome maps of mRNP biogenesis factors define pre-mRNA recognition. In *Molecular cell* 55 (5), pp. 745–757. DOI: 10.1016/j.molcel.2014.08.005.

Bannerman, Bridget P.; Kramer, Susanne; Dorrell, Richard G.; Carrington, Mark (2018): Multispecies reconstructions uncover widespread conservation, and lineage-specific elaborations in eukaryotic mRNA metabolism. In *PloS one* 13 (3), e0192633. DOI: 10.1371/journal.pone.0192633.

Banroques, Josette; Doère, Monique; Dreyfus, Marc; Linder, Patrick; Tanner, N. Kyle (2010): Motif III in superfamily 2 "helicases" helps convert the binding energy of ATP into a high-affinity RNA binding site in the yeast DEAD-box protein Ded1. In *Journal of molecular biology* 396 (4), pp. 949–966. DOI: 10.1016/j.jmb.2009.12.025.

Beckmann, Benedikt M.; Horos, Rastislav; Fischer, Bernd; Castello, Alfredo; Eichelbaum, Katrin; Alleaume, Anne-Marie et al. (2015): The RNA-binding proteomes from yeast to man harbour conserved enigmRBPs. In *Nat Commun* 6 (1), p. 10127. DOI: 10.1038/ncomms10127.

Behrens, S. E.; Lührmann, R. (1991): Immunoaffinity purification of a U4/U6.U5 tri-snRNP from human cells. In *Genes & development* 5 (8), pp. 1439–1452. DOI: 10.1101/gad.5.8.1439.

Ben-Aroya, Shay; Coombes, Candice; Kwok, Teresa; O'Donnell, Kathryn A.; Boeke, Jef D.; Hieter, Philip (2008): Toward a comprehensive temperature-sensitive mutant repository of the essential genes of Saccharomyces cerevisiae. In *Molecular cell* 30 (2), pp. 248–258. DOI: 10.1016/j.molcel.2008.02.021.

Bienroth, S.; Keller, W.; Wahle, E. (1993): Assembly of a processive messenger RNA polyadenylation complex. In *The EMBO Journal* 12 (2), pp. 585–594.

Bienroth, S.; Wahle, E.; Suter-Crazzolara, C.; Keller, W. (1991): Purification of the cleavage and polyadenylation factor involved in the 3'-processing of messenger RNA precursors. In *The Journal of biological chemistry* 266 (29), pp. 19768–19776.

Biro, J. C. (2006): Amino acid size, charge, hydropathy indices and matrices for protein structure analysis. In *Theoretical biology & medical modelling* 3, p. 15. DOI: 10.1186/1742-4682-3-15.

Blobel, G. (1985): Gene gating: a hypothesis. In *Proceedings of the National Academy of Sciences* 82 (24), pp. 8527–8529. DOI: 10.1073/pnas.82.24.8527.

Bolger, Timothy A.; Folkmann, Andrew W.; Tran, Elizabeth J.; Wente, Susan R. (2008): The mRNA export factor Gle1 and inositol hexakisphosphate regulate distinct stages of translation. In *Cell* 134 (4), pp. 624–633. DOI: 10.1016/j.cell.2008.06.027.

Bruce Alberts; Alexander Johnson; Julian Lewis; Martin Raff; Keith Roberts; Peter Walter (2002): The Shape and Structure of Proteins. In Bruce Alberts, Alexander Johnson, Julian Lewis, Martin Raff, Keith Roberts, Peter Walter (Eds.): Molecular Biology of the Cell. 4th edition: Garland Science. Available online at https://www.ncbi.nlm.nih.gov/books/NBK26830/.

Cargill, Michael; Venkataraman, Rasika; Lee, Stanley (2021): DEAD-Box RNA Helicases and Genome Stability. In *Genes* 12 (10). DOI: 10.3390/genes12101471.

Carmody, Sean R.; Wente, Susan R. (2009): mRNA nuclear export at a glance. In *Journal of Cell Science* 122 (Pt 12), pp. 1933–1937. DOI: 10.1242/jcs.041236.

Castello, Alfredo; Fischer, Bernd; Frese, Christian K.; Horos, Rastislav; Alleaume, Anne-Marie; Foehr, Sophia et al. (2016): Comprehensive Identification of RNA-Binding Domains in Human Cells. In *Molecular cell* 63 (4), pp. 696–710. DOI: 10.1016/j.molcel.2016.06.029.

Cerritelli, Susana M.; Crouch, Robert J. (2009): Ribonuclease H: the enzymes in eukaryotes. In *The FEBS journal* 276 (6), pp. 1494–1505. DOI: 10.1111/j.1742-4658.2009.06908.x.

Chan, Serena; Choi, Eun-A; Shi, Yongsheng (2011): Pre-mRNA 3'-end processing complex assembly and function. In *Wiley interdisciplinary reviews. RNA* 2 (3), pp. 321–335. DOI: 10.1002/wrna.54.

Chang, Emily Yun-Chia; Novoa, Carolina A.; Aristizabal, Maria J.; Coulombe, Yan; Segovia, Romulo; Chaturvedi, Richa et al. (2017): RECQ-like helicases Sgs1 and BLM regulate R-loop-associated genome instability. In *The Journal of cell biology* 216 (12), pp. 3991–4005. DOI: 10.1083/jcb.201703168.

Chávez, S.; Beilharz, T.; Rondón, A. G.; Erdjument-Bromage, H.; Tempst, P.; Svejstrup, J. Q. et al. (2000): A protein complex containing Tho2, Hpr1, Mft1 and a novel protein, Thp2, connects transcription elongation with mitotic recombination in Saccharomyces cerevisiae. In *The EMBO Journal* 19 (21), pp. 5824–5834. DOI: 10.1093/emboj/19.21.5824.

Cieniková, Zuzana; Jayne, Sandrine; Damberger, Fred Franz; Allain, Frédéric Hai-Trieu; Maris, Christophe (2015): Evidence for cooperative tandem binding of hnRNP C RRMs in mRNA processing. In *RNA (New York, N.Y.)* 21 (11), pp. 1931–1942. DOI: 10.1261/rna.052373.115.

Company, M.; Arenas, J.; Abelson, J. (1991): Requirement of the RNA helicase-like protein PRP22 for release of messenger RNA from spliceosomes. In *Nature* 349 (6309), pp. 487–493. DOI: 10.1038/349487a0.

Corden, Jeffry L. (1990): Tails of RNA polymerase II. In *Trends in biochemical sciences* 15 (10), pp. 383–387. DOI: 10.1016/0968-0004(90)90236-5.

Cordin, Olivier; Banroques, Josette; Tanner, N. Kyle; Linder, Patrick (2006): The DEAD-box protein family of RNA helicases. In *Gene* 367, pp. 17–37. DOI: 10.1016/j.gene.2005.10.019.

Corley, Meredith; Burns, Margaret C.; Yeo, Gene W. (2020): How RNA-Binding Proteins Interact with RNA: Molecules and Mechanisms. In *Molecular cell* 78 (1), pp. 9–29. DOI: 10.1016/j.molcel.2020.03.011.

Costanzo, Michael; VanderSluis, Benjamin; Koch, Elizabeth N.; Baryshnikova, Anastasia; Pons, Carles; Tan, Guihong et al. (2016): A global genetic interaction network maps a wiring diagram of cellular function. In *Science (New York, N.Y.)* 353 (6306). DOI: 10.1126/science.aaf1420.

Culjkovic-Kraljacic, Biljana; Borden, Katherine L. B. (2013): Aiding and abetting cancer: mRNA export and the nuclear pore. In *Trends in Cell Biology* 23 (7), pp. 328–335. DOI: 10.1016/j.tcb.2013.03.004.

Danckwardt, Sven; Hentze, Matthias W.; Kulozik, Andreas E. (2008): 3' end mRNA processing: molecular mechanisms and implications for health and disease. In *The EMBO Journal* 27 (3), pp. 482–498. DOI: 10.1038/sj.emboj.7601932.

Daneholt, B. (2001): Assembly and transport of a premessenger RNP particle. In *Proceedings of the National Academy of Sciences* 98 (13), pp. 7012–7017. DOI: 10.1073/pnas.111145498.

Das, Rita; Zhou, Zhaolan; Reed, Robin (2000): Functional Association of U2 snRNP with the ATP-Independent Spliceosomal Complex E. In *Molecular cell* 5 (5), pp. 779–787. DOI: 10.1016/s1097-2765(00)80318-4.

Denning, Daniel P.; Patel, Samir S.; Uversky, Vladimir; Fink, Anthony L.; Rexach, Michael (2003): Disorder in the nuclear pore complex: the FG repeat regions of nucleoporins are natively unfolded. In *Proceedings of the National Academy of Sciences* 100 (5), pp. 2450–2455. DOI: 10.1073/pnas.0437902100.

Domínguez-Sánchez, María S.; Barroso, Sonia; Gómez-González, Belén; Luna, Rosa; Aguilera, Andrés (2011): Genome instability and transcription elongation impairment in human cells depleted of THO/TREX. In *PLoS genetics* 7 (12), e1002386. DOI: 10.1371/journal.pgen.1002386.

Dominski, Z.; Erkmann, J. A.; Greenland, J. A.; Marzluff, W. F. (2001): Mutations in the RNA binding domain of stem-loop binding protein define separable requirements for RNA binding and for histone pre-mRNA processing. In *Molecular and cellular biology* 21 (6), pp. 2008–2017. DOI: 10.1128/MCB.21.6.2008-2017.2001.

Dufu, Kobina; Livingstone, Michaela J.; Seebacher, Jan; Gygi, Steven P.; Wilson, Stuart A.; Reed, Robin (2010): ATP is required for interactions between UAP56 and two conserved mRNA export proteins, Aly and CIP29, to assemble the TREX complex. In *Genes & development* 24 (18), pp. 2043–2053. DOI: 10.1101/gad.1898610.

Eckner, R.; Ellmeier, W.; Birnstiel, M. L. (1991): Mature mRNA 3' end formation stimulates RNA export from the nucleus. In *The EMBO Journal* 10 (11), pp. 3513–3522.

Elbarbary, Reyad A.; Maquat, Lynne E. (2016): Coupling pre-mRNA splicing and 3' end formation to mRNA export: alternative ways to punch the nuclear export clock. In *Genes & development* 30 (5), pp. 487–488. DOI: 10.1101/gad.278937.116.

Fairbanks, G.; Steck, T. L.; Wallach, D. F. (1971): Electrophoretic analysis of the major polypeptides of the human erythrocyte membrane. In *Biochemistry* 10 (13), pp. 2606–2617. DOI: 10.1021/bi00789a030.

Fan, H. Y.; Merker, R. J.; Klein, H. L. (2001): High-copy-number expression of Sub2p, a member of the RNA helicase superfamily, suppresses hpr1-mediated genomic instability. In *Molecular and cellular biology* 21 (16), pp. 5459–5470. DOI: 10.1128/MCB.21.16.5459-5470.2001.

Fleckner, J.; Zhang, M.; Valcárcel, J.; Green, M. R. (1997): U2AF65 recruits a novel human DEAD box protein required for the U2 snRNP-branchpoint interaction. In *Genes & development* 11 (14), pp. 1864–1872. DOI: 10.1101/gad.11.14.1864.

Folkmann, Andrew W.; Collier, Scott E.; Zhan, Xiaoyan; Aditi; Ohi, Melanie D.; Wente, Susan R. (2013): Gle1 functions during mRNA export in an oligomeric complex that is altered in human disease. In *Cell* 155 (3), pp. 582–593. DOI: 10.1016/j.cell.2013.09.023.

Gan, Wenjian; Guan, Zhishuang; Liu, Jie; Gui, Ting; Shen, Keng; Manley, James L.; Li, Xialu (2011): R-loop-mediated genomic instability is caused by impairment of replication fork progression. In *Genes & development* 25 (19), pp. 2041–2056. DOI: 10.1101/gad.17010011.

García-Rubio, María; Chávez, Sebastián; Huertas, Pablo; Tous, Cristina; Jimeno, Sonia; Luna, Rosa; Aguilera, Andrés (2008): Different physiological relevance of yeast THO/TREX subunits in gene expression and genome integrity. In *Molecular genetics and genomics : MGG* 279 (2), pp. 123–132. DOI: 10.1007/s00438-007-0301-6.

Gesteland, Raymond F.; Cech, Thomas; Atkins, John F. (2006): The RNA world. The nature of modern RNA suggests a prebiotic RNA world / edited by Raymond F. Gesteland, Thomas R. Cech, John F. Atkins. 3rd ed. Cold Spring Harbor, NY: Cold Spring Harbor Laboratory Press (Cold Spring Harbor monograph series, 43).

Giaever, Guri; Chu, Angela M.; Ni, Li; Connelly, Carla; Riles, Linda; Véronneau, Steeve et al. (2002): Functional profiling of the Saccharomyces cerevisiae genome. In *Nature* 418 (6896), pp. 387–391. DOI: 10.1038/nature00935.

Gibson, Daniel G.; Young, Lei; Chuang, Ray-Yuan; Venter, J. Craig; Hutchison, Clyde A.; Smith, Hamilton O. (2009): Enzymatic assembly of DNA molecules up to several hundred kilobases. In *Nature methods* 6 (5), pp. 343–345. DOI: 10.1038/nmeth.1318.

Gil, Anna; Proudfoot, Nicholas J. (1987): Position-dependent sequence elements downstream of AAUAAA are required for efficient rabbit β-globin mRNA 3′ end formation. In *Cell* 49 (3), pp. 399–406. DOI: 10.1016/0092-8674(87)90292-3.

Gillian, Anne Lynn; Svaren, John (2004): The Ddx20/DP103 dead box protein represses transcriptional activation by Egr2/Krox-20. In *The Journal of biological chemistry* 279 (10), pp. 9056–9063. DOI: 10.1074/jbc.M309308200.

Gómez-González, Belén; García-Rubio, María; Bermejo, Rodrigo; Gaillard, Hélène; Shirahige, Katsuhiko; Marín, Antonio et al. (2011): Genome-wide function of THO/TREX in active genes prevents R-loop-dependent replication obstacles. In *The EMBO Journal* 30 (15), pp. 3106–3119. DOI: 10.1038/emboj.2011.206.

González-Aguilera, Cristina; Tous, Cristina; Gómez-González, Belén; Huertas, Pablo; Luna, Rosa; Aguilera, Andrés (2008): The THP1-SAC3-SUS1-CDC31 complex works in transcription elongation-mRNA export preventing RNA-mediated genome instability. In *Molecular biology of the cell* 19 (10), pp. 4310–4318. DOI: 10.1091/mbc.e08-04-0355.

Gorbalenya, Alexander E.; Koonin, Eugene V. (1993): Helicases: amino acid sequence comparisons and structure-function relationships. In *Current opinion in structural biology* 3 (3), pp. 419–429. DOI: 10.1016/S0959-440X(05)80116-2.

Grainger, R. J.; Beggs, J. D. (2013): Pre-mRNA Splicing. In Kelly Hughes, Stanley R. Maloy (Eds.): Brenner's encyclopedia of genetics. 2. ed. London: Academic Press, Elsevier Science, pp. 442–445.

Gross, Thomas; Siepmann, Anja; Sturm, Dorotheé; Windgassen, Merle; Scarcelli, John J.; Seedorf, Matthias et al. (2007): The DEAD-box RNA helicase Dbp5 functions in translation termination. In *Science (New York, N.Y.)* 315 (5812), pp. 646–649. DOI: 10.1126/science.1134641.

Gu, Meigang; Rice, Charles M. (2010): Three conformational snapshots of the hepatitis C virus NS3 helicase reveal a ratchet translocation mechanism. In *Proceedings of the National Academy of Sciences* 107 (2), pp. 521–528. DOI: 10.1073/pnas.0913380107.

Hammell, C. M.; Gross, Stefan; Zenklusen, Daniel; Heath, Catherine V.; Stutz, Francoise; Moore, Claire; Cole, C. N. (2002): Coupling of termination, 3' processing, and mRNA export.

In *Molecular and cellular biology* 22 (18), pp. 6441–6457. DOI: 10.1128/MCB.22.18.6441-6457.2002.

Hautbergue, Guillaume M.; Hung, Ming-Lung; Golovanov, Alexander P.; Lian, Lu-Yun; Wilson, Stuart A. (2008): Mutually exclusive interactions drive handover of mRNA from export adaptors to TAP. In *Proceedings of the National Academy of Sciences* 105 (13), pp. 5154–5159. DOI: 10.1073/pnas.0709167105.

Hector, Ronald E.; Nykamp, Keith R.; Dheur, Sonia; Anderson, James T.; Non, Priscilla J.; Urbinati, Carl R. et al. (2002): Dual requirement for yeast hnRNP Nab2p in mRNA poly(A) tail length control and nuclear export. In *The EMBO Journal* 21 (7), pp. 1800–1810. DOI: 10.1093/emboj/21.7.1800.

Heinrich, Stephanie; Derrer, Carina Patrizia; Lari, Azra; Weis, Karsten; Montpetit, Ben (2017): Temporal and spatial regulation of mRNA export: Single particle RNA-imaging provides new tools and insights. In *BioEssays : news and reviews in molecular, cellular and developmental biology* 39 (2). DOI: 10.1002/bies.201600124.

Herold, A.; Suyama, M.; Rodrigues, J. P.; Braun, I. C.; Kutay, U.; Carmo-Fonseca, M. et al. (2000): TAP (NXF1) belongs to a multigene family of putative RNA export factors with a conserved modular architecture. In *Molecular and cellular biology* 20 (23), pp. 8996–9008. DOI: 10.1128/MCB.20.23.8996-9008.2000.

Herrera-Moyano, Emilia; Mergui, Xénia; García-Rubio, María L.; Barroso, Sonia; Aguilera, Andrés (2014): The yeast and human FACT chromatin-reorganizing complexes solve R-loop-mediated transcription-replication conflicts. In *Genes & development* 28 (7), pp. 735–748. DOI: 10.1101/gad.234070.113.

Hilbert, Manuel; Karow, Anne R.; Klostermeier, Dagmar (2009): The mechanism of ATP-dependent RNA unwinding by DEAD box proteins. In *Biological chemistry* 390 (12), pp. 1237–1250. DOI: 10.1515/BC.2009.135.

Hill, Sandra Malmgren; Hanzén, Sarah; Nyström, Thomas (2017): Restricted access: spatial sequestration of damaged proteins during stress and aging. In *EMBO reports* 18 (3), pp. 377–391. DOI: 10.15252/embr.201643458.

Hocine, Sami; Singer, Robert H.; Grünwald, David (2010): RNA processing and export. In *Cold Spring Harbor perspectives in biology* 2 (12), a000752. DOI: 10.1101/cshperspect.a000752.

Hollerer, Ina; Grund, Kerstin; Hentze, Matthias W.; Kulozik, Andreas E. (2014): mRNA 3'end processing: A tale of the tail reaches the clinic. In *EMBO molecular medicine* 6 (1), pp. 16–26. DOI: 10.1002/emmm.201303300.

HomoloGene - NCBI (2022). Available online at https://www.ncbi.nlm.nih.gov/homologene/48376, updated on 2/11/2022, checked on 2/11/2022.

Houseley, Jonathan; LaCava, John; Tollervey, David (2006): RNA-quality control by the exosome. In *Nature reviews. Molecular cell biology* 7 (7), pp. 529–539. DOI: 10.1038/nrm1964.

Hu, Wen; Qin, Liu; Li, Menglong; Pu, Xuemei; Guo, Yanzhi (2018): A structural dissection of protein–RNA interactions based on different RNA base areas of interfaces. In *RSC Adv.* 8 (19), pp. 10582–10592. DOI: 10.1039/C8RA00598B.

Huang, Y.; Carmichael, G. C. (1996): Role of polyadenylation in nucleocytoplasmic transport of mRNA. In *Molecular and cellular biology* 16 (4), pp. 1534–1542.

Huertas, Pablo; Aguilera, Andrés (2003): Cotranscriptionally formed DNA:RNA hybrids mediate transcription elongation impairment and transcription-associated recombination. In *Molecular cell* 12 (3), pp. 711–721. DOI: 10.1016/j.molcel.2003.08.010.

Hurt, E.; Hannus, S.; Schmelzl, B.; Lau, D.; Tollervey, D.; Simos, G. (1999): A novel in vivo assay reveals inhibition of ribosomal nuclear export in ran-cycle and nucleoporin mutants. In *The Journal of cell biology* 144 (3), pp. 389–401. DOI: 10.1083/jcb.144.3.389.

Hurt, Ed; Luo, Ming-Juan; Röther, Susanne; Reed, Robin; Strässer, Katja (2004): Cotranscriptional recruitment of the serine-arginine-rich (SR)-like proteins Gbp2 and Hrb1 to nascent mRNA via the TREX complex. In *Proceedings of the National Academy of Sciences* 101 (7), pp. 1858–1862. DOI: 10.1073/pnas.0308663100.

Iglesias, Nahid; Stutz, Françoise (2008): Regulation of mRNP dynamics along the export pathway. In *FEBS letters* 582 (14), pp. 1987–1996. DOI: 10.1016/j.febslet.2008.03.038.

Ikeda, H.; Kobayashi, I. (1977): Involvement of DNA-dependent RNA polymerase in a recA-independent pathway of genetic recombination in Escheria coli. In *Proceedings of the National Academy of Sciences* 74 (9), pp. 3932–3936. DOI: 10.1073/pnas.74.9.3932.

Ishigaki, Yasuhito; Li, Xiaojie; Serin, Guillaume; Maquat, Lynne E. (2001): Evidence for a Pioneer Round of mRNA Translation. In *Cell* 106 (5), pp. 607–617. DOI: 10.1016/s0092-8674(01)00475-5.

Ito, T.; Chiba, T.; Ozawa, R.; Yoshida, M.; Hattori, M.; Sakaki, Y. (2001): A comprehensive two-hybrid analysis to explore the yeast protein interactome. In *Proceedings of the National Academy of Sciences* 98 (8), pp. 4569–4574. DOI: 10.1073/pnas.061034498.

Izaurralde, E.; McGuigan, C.; Mattaj, I. W. (1995): Nuclear localization of a cap-binding protein complex. In *Cold Spring Harbor symposia on quantitative biology* 60, pp. 669–675. DOI: 10.1101/sqb.1995.060.01.072.

Izaurralde, Elisa; Lewis, Joe; McGuigan, Caroline; Jankowska, Marzena; Darzynkiewicz, Edward; Mattaj, Iain W. (1994): A nuclear cap binding protein complex involved in pre-mRNA splicing. In *Cell* 78 (4), pp. 657–668. DOI: 10.1016/0092-8674(94)90530-4.

Jacobs Anderson, John S.; Parker, Roy (1996): RNA turnover: The helicase story unwinds. In *Current Biology* 6 (7), pp. 780–782. DOI: 10.1016/s0960-9822(02)00593-6.

Jao, Li-En; Appel, Bruce; Wente, Susan R. (2012): A zebrafish model of lethal congenital contracture syndrome 1 reveals Gle1 function in spinal neural precursor survival and motor axon arborization. In *Development (Cambridge, England)* 139 (7), pp. 1316–1326. DOI: 10.1242/dev.074344.

Jarmoskaite, Inga; Russell, Rick (2011): DEAD-box proteins as RNA helicases and chaperones. In *Wiley interdisciplinary reviews. RNA* 2 (1), pp. 135–152. DOI: 10.1002/wrna.50.

Jensen, Torben Heick; Boulay, Jocelyne; Rosbash, Michael; Libri, Domenico (2001): The DECD box putative ATPase Sub2p is an early mRNA export factor. In *Current Biology* 11 (21), pp. 1711–1715. DOI: 10.1016/s0960-9822(01)00529-2.

Jimeno, S.; Rondón, A. G.; Luna, R.; Aguilera, A. (2002): The yeast THO complex and mRNA export factors link RNA metabolism with transcription and genome instability. In *The EMBO Journal* 21 (13), pp. 3526–3535. DOI: 10.1093/emboj/cdf335.

Jimeno, Sonia; Luna, Rosa; García-Rubio, María; Aguilera, Andrés (2006): Tho1, a novel hnRNP, and Sub2 provide alternative pathways for mRNP biogenesis in yeast THO mutants. In *Molecular and cellular biology* 26 (12), pp. 4387–4398. DOI: 10.1128/MCB.00234-06.

Johnson, Sara A.; Kim, Hyunmin; Erickson, Benjamin; Bentley, David L. (2011): The export factor Yra1 modulates mRNA 3' end processing. In *Nature structural & molecular biology* 18 (10), pp. 1164–1171. DOI: 10.1038/nsmb.2126.

Kaneb, Hannah M.; Folkmann, Andrew W.; Belzil, Véronique V.; Jao, Li-En; Leblond, Claire S.; Girard, Simon L. et al. (2015): Deleterious mutations in the essential mRNA metabolism factor, hGle1, in amyotrophic lateral sclerosis. In *Human molecular genetics* 24 (5), pp. 1363–1373. DOI: 10.1093/hmg/ddu545.

Katahira, Jun (2012): mRNA export and the TREX complex. In *Biochimica et biophysica acta* 1819 (6), pp. 507–513. DOI: 10.1016/j.bbagrm.2011.12.001.

Kataoka, Naoyuki; Yong, Jeongsik; Kim, V.Narry; Velazquez, Francisco; Perkinson, Robert A.; Wang, Fan; Dreyfuss, Gideon (2000): Pre-mRNA Splicing Imprints mRNA in the Nucleus with a Novel RNA-Binding Protein that Persists in the Cytoplasm. In *Molecular cell* 6 (3), pp. 673–682. DOI: 10.1016/S1097-2765(00)00065-4.

Kauzmann, W. (1959): Some Factors in the Interpretation of Protein Denaturation. In : Advances in Protein Chemistry Volume 14, vol. 14: Elsevier (Advances in Protein Chemistry), pp. 1–63.

Keil, Philipp (2021): Function of the RNA-binding activity of the nuclear mRNA-binding protein Npl3 in nuclear mRNA packaging. Universitätsbibliothek Gießen. Available online at https://jlupub.ub.uni-giessen.de/handle/jlupub/289?locale-attribute=en.

Kendirgi, Frederic; Rexer, Deborah J.; Alcázar-Román, Abel R.; Onishko, Halina M.; Wente, Susan R. (2005): Interaction between the shuttling mRNA export factor Gle1 and the nucleoporin hCG1: a conserved mechanism in the export of Hsp70 mRNA. In *Molecular biology of the cell* 16 (9), pp. 4304–4315. DOI: 10.1091/mbc.e04-11-0998.

Kent, Oliver A.; MacMillan, Andrew M. (2002): Early organization of pre-mRNA during spliceosome assembly. In *Nature structural biology* 9 (8), pp. 576–581. DOI: 10.1038/nsb822.

Kerwitz, Yvonne; Kühn, Uwe; Lilie, Hauke; Knoth, Anne; Scheuermann, Till; Friedrich, Henning et al. (2003): Stimulation of poly(A) polymerase through a direct interaction with the nuclear poly(A) binding protein allosterically regulated by RNA. In *The EMBO Journal* 22 (14), pp. 3705–3714. DOI: 10.1093/emboj/cdg347.

Kim, S. H.; Lin, R. J. (1996): Spliceosome activation by PRP2 ATPase prior to the first transesterification reaction of pre-mRNA splicing. In *Molecular and cellular biology* 16 (12), pp. 6810–6819. DOI: 10.1128/MCB.16.12.6810.

Kim, V. N.; Kataoka, N.; Dreyfuss, G. (2001): Role of the nonsense-mediated decay factor hUpf3 in the splicing-dependent exon-exon junction complex. In *Science (New York, N.Y.)* 293 (5536), pp. 1832–1836. DOI: 10.1126/science.1062829.

Kistler, A. L.; Guthrie, C. (2001): Deletion of MUD2, the yeast homolog of U2AF65, can bypass the requirement for sub2, an essential spliceosomal ATPase. In *Genes & development* 15 (1), pp. 42–49. DOI: 10.1101/gad.851301.

Kogoma, T. (1997): Stable DNA replication: interplay between DNA replication, homologous recombination, and transcription. In *Microbiology and molecular biology reviews : MMBR* 61 (2), pp. 212–238. DOI: 10.1128/mmbr.61.2.212-238.1997.

Köhler, Alwin; Hurt, Ed (2007): Exporting RNA from the nucleus to the cytoplasm. In *Nature reviews. Molecular cell biology* 8 (10), pp. 761–773. DOI: 10.1038/nrm2255.

Kressler, D.; La Cruz, J. de; Rojo, M.; Linder, P. (1998): Dbp6p is an essential putative ATP-dependent RNA helicase required for 60S-ribosomal-subunit assembly in Saccharomyces cerevisiae. In *Molecular and cellular biology* 18 (4), pp. 1855–1865. DOI: 10.1128/MCB.18.4.1855.

Kushnirov, Vitaly V. (2000): Rapid and reliable protein extraction from yeast. In *Yeast (Chichester, England)* 16 (9), pp. 857–860. DOI: 10.1002/1097-0061(20000630)16:9<857::AID-YEA561>3.0.CO;2-B.

LAEMMLI, U. K. (1970): Cleavage of structural proteins during the assembly of the head of bacteriophage T4. In *Nature* 227 (5259), pp. 680–685. DOI: 10.1038/227680a0.

Lahue, Elaine; Heckathorn, John; Meyer, Zachary; Smith, Jennie; Wolfe, Christopher (2005): The Saccharomyces cerevisiae Sub2 protein suppresses heterochromatic silencing at

telomeres and subtelomeric genes. In *Yeast (Chichester, England)* 22 (7), pp. 537–551. DOI: 10.1002/yea.1231.

Le Hir, H.; Gatfield, D.; Izaurralde, E.; Moore, M. J. (2001): The exon-exon junction complex provides a binding platform for factors involved in mRNA export and nonsense-mediated mRNA decay. In *The EMBO Journal* 20 (17), pp. 4987–4997. DOI: 10.1093/emboj/20.17.4987.

Lerner, M. R.; Boyle, J. A.; Mount, S. M.; Wolin, S. L.; Steitz, J. A. (1980): Are snRNPs involved in splicing? In *Nature* 283 (5743), pp. 220–224. DOI: 10.1038/283220a0.

Leulliot, N.; Varani, G. (2001): Current topics in RNA-protein recognition: control of specificity and biological function through induced fit and conformational capture. In *Biochemistry* 40 (27), pp. 7947–7956. DOI: 10.1021/bi010680y.

Li, Xialu; Manley, James L. (2005): Inactivation of the SR protein splicing factor ASF/SF2 results in genomic instability. In *Cell* 122 (3), pp. 365–378. DOI: 10.1016/j.cell.2005.06.008.

Libri, D.; Graziani, N.; Saguez, C.; Boulay, J. (2001): Multiple roles for the yeast SUB2/yUAP56 gene in splicing. In *Genes & development* 15 (1), pp. 36–41. DOI: 10.1101/gad.852101.

Libri, Domenico; Dower, Ken; Boulay, Jocelyne; Thomsen, Rune; Rosbash, Michael; Jensen, Torben Heick (2002): Interactions between mRNA export commitment, 3'-end quality control, and nuclear degradation. In *Molecular and cellular biology* 22 (23), pp. 8254–8266. DOI: 10.1128/MCB.22.23.8254-8266.2002.

Linder, Patrick; Jankowsky, Eckhard (2011): From unwinding to clamping - the DEAD box RNA helicase family. In *Nature reviews. Molecular cell biology* 12 (8), pp. 505–516. DOI: 10.1038/nrm3154.

Linder, Patrick; Stutz, Françoise (2001): mRNA export: Travelling with DEAD box proteins. In *Current Biology* 11 (23), R961-R963. DOI: 10.1016/s0960-9822(01)00574-7.

Lohman, Timothy M.; Tomko, Eric J.; Wu, Colin G. (2008): Non-hexameric DNA helicases and translocases: mechanisms and regulation. In *Nature reviews. Molecular cell biology* 9 (5), pp. 391–401. DOI: 10.1038/nrm2394.

Long, R. M.; Elliott, D. J.; Stutz, F.; Rosbash, M.; Singer, R. H. (1995): Spatial consequences of defective processing of specific yeast mRNAs revealed by fluorescent in situ hybridization. In *RNA (New York, N.Y.)* 1 (10), pp. 1071–1078.

López, M. C.; Sánchez, M.; Fermiñán, E.; Domínguez, A. (1998): Disruption of six Saccharomyces cerevisiae genes from chromosome IV and basic phenotypic analysis of deletion mutants. In *Yeast (Chichester, England)* 14 (13), pp. 1199–1208. DOI: 10.1002/(SICI)1097-0061(19980930)14:13<1199::AID-YEA309>3.0.CO;2-V.

Lorković, Zdravko J. (2012): RNA Binding Proteins. Austin, TX: Landes Bioscience (Molecular Biology Intelligence Unit). Available online at http://worldcatlibraries.org/wcpa/oclc/827208014.

Luna, Rosa; Jimeno, Sonia; Marín, Mercedes; Huertas, Pablo; García-Rubio, María; Aguilera, Andrés (2005): Interdependence between transcription and mRNP processing and export, and its impact on genetic stability. In *Molecular cell* 18 (6), pp. 711–722. DOI: 10.1016/j.molcel.2005.05.001.

Lund, Mette K.; Guthrie, Christine (2005): The DEAD-box protein Dbp5p is required to dissociate Mex67p from exported mRNPs at the nuclear rim. In *Molecular cell* 20 (4), pp. 645–651. DOI: 10.1016/j.molcel.2005.10.005.

MacDonald, C. C.; Wilusz, J.; Shenk, T. (1994): The 64-kilodalton subunit of the CstF polyadenylation factor binds to pre-mRNAs downstream of the cleavage site and influences cleavage site location. In *Molecular and cellular biology* 14 (10), pp. 6647–6654. DOI: 10.1128/mcb.14.10.6647-6654.1994.

Madrid, Alexis S.; Weis, Karsten (2006): Nuclear transport is becoming crystal clear. In *Chromosoma* 115 (2), pp. 98–109. DOI: 10.1007/s00412-005-0043-3.

Mangus, David A.; Evans, Matthew C.; Jacobson, Allan (2003): Poly(A)-binding proteins: multifunctional scaffolds for the post-transcriptional control of gene expression. In *Genome biology* 4 (7), p. 223. DOI: 10.1186/gb-2003-4-7-223.

Margossian, S. P.; Butow, R. A. (1996): RNA turnover and the control of mitochondrial gene expression. In *Trends in biochemical sciences* 21 (10), pp. 392–396.

Meinel, Dominik M.; Burkert-Kautzsch, Cornelia; Kieser, Anja; O'Duibhir, Eoghan; Siebert, Matthias; Mayer, Andreas et al. (2013): Recruitment of TREX to the transcription machinery by its direct binding to the phospho-CTD of RNA polymerase II. In *PLoS genetics* 9 (11), e1003914. DOI: 10.1371/journal.pgen.1003914.

Meinel, Dominik M.; Sträßer, Katja (2015): Co-transcriptional mRNP formation is coordinated within a molecular mRNP packaging station in S. cerevisiae. In *BioEssays : news and reviews in molecular, cellular and developmental biology* 37 (6), pp. 666–677. DOI: 10.1002/bies.201400220.

Minvielle-Sebastia, L.; Preker, P. J.; Wiederkehr, T.; Strahm, Y.; Keller, W. (1997): The major yeast poly(A)-binding protein is associated with cleavage factor IA and functions in premessenger RNA 3'-end formation. In *Proceedings of the National Academy of Sciences* 94 (15), pp. 7897–7902. DOI: 10.1073/pnas.94.15.7897.

Mischo, Hannah E.; Gómez-González, Belén; Grzechnik, Pawel; Rondón, Ana G.; Wei, Wu; Steinmetz, Lars et al. (2011): Yeast Sen1 helicase protects the genome from transcription-associated instability. In *Molecular cell* 41 (1), pp. 21–32. DOI: 10.1016/j.molcel.2010.12.007.

Moelbert, Susanne; Emberly, Eldon; Tang, Chao (2004): Correlation between sequence hydrophobicity and surface-exposure pattern of database proteins. In *Protein science : a publication of the Protein Society* 13 (3), pp. 752–762. DOI: 10.1110/ps.03431704.

Mohammadi, Shahin; Saberidokht, Baharak; Subramaniam, Shankar; Grama, Ananth (2015): Scope and limitations of yeast as a model organism for studying human tissue-specific pathways. In *BMC Syst Biol* 9 (1), p. 96. DOI: 10.1186/s12918-015-0253-0.

Moore, Michael J.; Schwartzfarb, Elissa M.; Silver, Pamela A.; Yu, Michael C. (2006): Differential recruitment of the splicing machinery during transcription predicts genome-wide patterns of mRNA splicing. In *Molecular cell* 24 (6), pp. 903–915. DOI: 10.1016/j.molcel.2006.12.006.

Moteki, Shin; Price, David (2002): Functional Coupling of Capping and Transcription of mRNA. In *Molecular cell* 10 (3), pp. 599–609. DOI: 10.1016/s1097-2765(02)00660-3.

Müller-McNicoll, Michaela; Neugebauer, Karla M. (2013): How cells get the message: dynamic assembly and function of mRNA-protein complexes. In *Nat Rev Genet* 14 (4), pp. 275–287. DOI: 10.1038/nrg3434.

Murphy, R.; Wente, S. R. (1996): An RNA-export mediator with an essential nuclear export signal. In *Nature* 383 (6598), pp. 357–360. DOI: 10.1038/383357a0.

Nachury, M. V.; Weis, K. (1999): The direction of transport through the nuclear pore can be inverted. In *Proceedings of the National Academy of Sciences* 96 (17), pp. 9622–9627. DOI: 10.1073/pnas.96.17.9622.

Nair, S.; Dey, R.; Sanford, J. P.; Doyle, D. (1992): Molecular cloning and analysis of an eIF-4A-related rat liver nuclear protein. In *The Journal of biological chemistry* 267 (18), pp. 12928–12935. DOI: 10.1016/S0021-9258(18)42363-0.

Neumüller, Ralph A.; Gross, Thomas; Samsonova, Anastasia A.; Vinayagam, Arunachalam; Buckner, Michael; Founk, Karen et al. (2013): Conserved regulators of nucleolar size revealed by global phenotypic analyses. In *Science signaling* 6 (289), ra70. DOI: 10.1126/scisignal.2004145.

Newman, A. J.; Norman, C. (1992): U5 snRNA interacts with exon sequences at 5′ and 3′ splice sites. In *Cell* 68 (4), pp. 743–754. DOI: 10.1016/0092-8674(92)90149-7.

Nickoloff, J. A.; Reynolds, R. J. (1990): Transcription stimulates homologous recombination in mammalian cells. In *Molecular and cellular biology* 10 (9), pp. 4837–4845. DOI: 10.1128/mcb.10.9.4837-4845.1990.

Noble, Suzanne M. (1995): The BRR genes encode novel factors involved in RNA processing. Available online at https://escholarship.org/content/qt5p66q0cm/qt5p66q0cm.pdf.

Nonet, M. L.; Young, R. A. (1989): Intragenic and extragenic suppressors of mutations in the heptapeptide repeat domain of Saccharomyces cerevisiae RNA polymerase II. In *Genetics* 123 (4), pp. 715–724. DOI: 10.1093/genetics/123.4.715.

Nousiainen, Heidi O.; Kestilä, Marjo; Pakkasjärvi, Niklas; Honkala, Heli; Kuure, Satu; Tallila, Jonna et al. (2008): Mutations in mRNA export mediator GLE1 result in a fetal motoneuron disease. In *Nature genetics* 40 (2), pp. 155–157. DOI: 10.1038/ng.2007.65.

Ordabayev, Y. A.; Nguyen, B.; Niedziela-Majka, A.; Lohman, T. M. (2018): Regulation of UvrD Helicase Activity by MutL. In *J. Mol. Biol.* 430 (21), pp. 4260–4274. DOI: 10.1016/j.jmb.2018.08.022.

Padgett, R. A.; Grabowski, P. J.; Konarska, M. M.; Seiler, S.; Sharp, P. A. (1986): Splicing of messenger RNA precursors. In *Annual review of biochemistry* 55, pp. 1119–1150. DOI: 10.1146/annurev.bi.55.070186.005351.

Pause, Arnim; Sonenberg, Nahum (1993): Helicases and RNA unwinding in translation. In *Current opinion in structural biology* 3 (6), pp. 953–959. DOI: 10.1016/0959-440X(93)90161-D.

Pemberton, L. F.; Rosenblum, J. S.; Blobel, G. (1997): A distinct and parallel pathway for the nuclear import of an mRNA-binding protein. In *The Journal of cell biology* 139 (7), pp. 1645–1653. DOI: 10.1083/jcb.139.7.1645.

Peña, Alvaro; Gewartowski, Kamil; Mroczek, Seweryn; Cuéllar, Jorge; Szykowska, Aleksandra; Prokop, Andrzej et al. (2012): Architecture and nucleic acids recognition mechanism of the THO complex, an mRNP assembly factor. In *The EMBO Journal* 31 (6), pp. 1605–1616. DOI: 10.1038/emboj.2012.10.

Pérez-Calero, Carmen; Bayona-Feliu, Aleix; Xue, Xiaoyu; Barroso, Sonia I.; Muñoz, Sergio; González-Basallote, Víctor M. et al. (2020): UAP56/DDX39B is a major cotranscriptional RNA-DNA helicase that unwinds harmful R loops genome-wide. In *Genes & development* 34 (13-14), pp. 898–912. DOI: 10.1101/gad.336024.119.

Perriman, Rhonda; Ares, Manuel (2000): ATP can be dispensable for prespliceosome formation in yeast. In *Genes & development* 14 (1), pp. 97–107.

Perriman, Rhonda; Barta, Imre; Voeltz, Gia K.; Abelson, John; Ares, Manuel (2003): ATP requirement for Prp5p function is determined by Cus2p and the structure of U2 small nuclear RNA. In *Proceedings of the National Academy of Sciences* 100 (24), pp. 13857–13862. DOI: 10.1073/pnas.2036312100.

Proudfoot, N. J.; Brownlee, G. G. (1976): 3' non-coding region sequences in eukaryotic messenger RNA. In *Nature* 263 (5574), pp. 211–214. DOI: 10.1038/263211a0.

Proudfoot, Nick (2000): Connecting transcription to messenger RNA processing. In *Trends in biochemical sciences* 25 (6), pp. 290–293. DOI: 10.1016/S0968-0004(00)01591-7.

Proudfoot, Nick J. (2011): Ending the message: poly(A) signals then and now. In *Genes & development* 25 (17), pp. 1770–1782. DOI: 10.1101/gad.17268411.

Puig, O.; Caspary, F.; Rigaut, G.; Rutz, B.; Bouveret, E.; Bragado-Nilsson, E. et al. (2001): The tandem affinity purification (TAP) method: a general procedure of protein complex purification. In *Methods* 24 (3), pp. 218–229. DOI: 10.1006/meth.2001.1183.

Putnam, Andrea; Jankowsky, Eckhard (2012): Analysis of duplex unwinding by RNA helicases using stopped-flow fluorescence spectroscopy. In *Methods in enzymology* 511, pp. 1–27. DOI: 10.1016/B978-0-12-396546-2.00001-2.

Putnam, Andrea A.; Jankowsky, Eckhard (2013): DEAD-box Helicases as Integrators of RNA, Nucleotide and Protein Binding. In *Biochimica et biophysica acta* 1829 (8), pp. 884–893. DOI: 10.1016/j.bbagrm.2013.02.002.

Pyle, Anna Marie (2008): Translocation and unwinding mechanisms of RNA and DNA helicases. In *Annual review of biophysics* 37, pp. 317–336. DOI: 10.1146/annurev.biophys.37.032807.125908.

Raghunathan, Pratima L.; Guthrie, Christine (1998): RNA unwinding in U4/U6 snRNPs requires ATP hydrolysis and the DEIH-box splicing factor Brr2. In *Current Biology* 8 (15), pp. 847–855. DOI: 10.1016/s0960-9822(07)00345-4.

Ramanathan, Anand; Robb, G. Brett; Chan, Siu-Hong (2016): mRNA capping: biological functions and applications. In *Nucleic acids research* 44 (16), pp. 7511–7526. DOI: 10.1093/nar/gkw551.

Ravindranathan, Sapna; Oberstrass, Florian C.; Allain, Frédéric H-T (2010): Increase in backbone mobility of the VTS1p-SAM domain on binding to SRE-RNA. In *Journal of molecular biology* 396 (3), pp. 732–746. DOI: 10.1016/j.jmb.2009.12.004.

Re, Angela; Joshi, Tejal; Kulberkyte, Eleonora; Morris, Quaid; Workman, Christopher T. (2014): RNA-protein interactions: an overview. In *Methods in molecular biology (Clifton, N.J.)* 1097, pp. 491–521. DOI: 10.1007/978-1-62703-709-9_23.

Reed, Robin; Hurt, Ed (2002): A Conserved mRNA Export Machinery Coupled to pre-mRNA Splicing. In *Cell* 108 (4), pp. 523–531. DOI: 10.1016/S0092-8674(02)00627-X.

Ren, Yi; Schmiege, Philip; Blobel, Günter (2017): Structural and biochemical analyses of the DEAD-box ATPase Sub2 in association with THO or Yra1. In *eLife* 6. DOI: 10.7554/eLife.20070.

Rigaut, G.; Shevchenko, A.; Rutz, B.; Wilm, M.; Mann, M.; Séraphin, B. (1999): A generic protein purification method for protein complex characterization and proteome exploration. In *Nat Biotechnol* 17 (10), pp. 1030–1032. DOI: 10.1038/13732.

Ripmaster, T. L.; Vaughn, G. P.; Woolford, J. L. (1992): A putative ATP-dependent RNA helicase involved in Saccharomyces cerevisiae ribosome assembly. In *Proceedings of the National Academy of Sciences* 89 (23), pp. 11131–11135. DOI: 10.1073/pnas.89.23.11131.

Rocak, Sanda; Linder, Patrick (2004): DEAD-box proteins: the driving forces behind RNA metabolism. In *Nature reviews. Molecular cell biology* 5 (3), pp. 232–241. DOI: 10.1038/nrm1335.

Rodríguez-Navarro, Susana; Hurt, Ed (2011): Linking gene regulation to mRNA production and export. In *Current opinion in cell biology* 23 (3), pp. 302–309. DOI: 10.1016/j.ceb.2010.12.002.

Rogers, G. W.; Richter, N. J.; Merrick, W. C. (1999): Biochemical and kinetic characterization of the RNA helicase activity of eukaryotic initiation factor 4A. In *The Journal of biological chemistry* 274 (18), pp. 12236–12244. DOI: 10.1074/jbc.274.18.12236.

Rougemaille, Mathieu; Gudipati, Rajani Kanth; Olesen, Jens Raabjerg; Thomsen, Rune; Seraphin, Bertrand; Libri, Domenico; Jensen, Torben Heick (2007): Dissecting mechanisms of nuclear mRNA surveillance in THO/sub2 complex mutants. In *The EMBO Journal* 26 (9), pp. 2317–2326. DOI: 10.1038/sj.emboj.7601669.

Rymond, Brian C., Michael Rosbash. (1993): Yeast pre-mRNA splicing. 21, 143-143: COLD SPRING HARBOR MONOGRAPH SERIES.

Sachs, Alan B.; Davis, Ronald W. (1989): The poly(A) binding protein is required for poly(A) shortening and 60S ribosomal subunit-dependent translation initiation. In *Cell* 58 (5), pp. 857–867. DOI: 10.1016/0092-8674(89)90938-0.

Saguez, Cyril; Gonzales, Fernando A.; Schmid, Manfred; Bøggild, Andreas; Latrick, Chrysa M.; Malagon, Francisco et al. (2013): Mutational analysis of the yeast RNA helicase Sub2p reveals conserved domains required for growth, mRNA export, and genomic stability. In *RNA (New York, N.Y.)* 19 (10), pp. 1363–1371. DOI: 10.1261/rna.040048.113.

Saguez, Cyril; Olesen, Jens Raabjerg; Jensen, Torben Heick (2005): Formation of export-competent mRNP: escaping nuclear destruction. In *Current opinion in cell biology* 17 (3), pp. 287–293. DOI: 10.1016/j.ceb.2005.04.009.

Saguez, Cyril; Schmid, Manfred; Olesen, Jens Raabjerg; Ghazy, Mohamed Abd El-Hady; Qu, Xiangping; Poulsen, Mathias Bach et al. (2008): Nuclear mRNA surveillance in THO/sub2 mutants is triggered by inefficient polyadenylation. In *Molecular cell* 31 (1), pp. 91–103. DOI: 10.1016/j.molcel.2008.04.030.

Saikrishnan, Kayarat; Powell, Benjamin; Cook, Nicola J.; Webb, Martin R.; Wigley, Dale B. (2009): Mechanistic basis of 5'-3' translocation in SF1B helicases. In *Cell* 137 (5), pp. 849–859. DOI: 10.1016/j.cell.2009.03.036.

Sambrook, Joseph; Russell, David W. (2001): Molecular cloning. A laboratory manual / Joseph Sambrook, David W. Russell. Vol. 3. 3rd ed. Cold Spring Harbor, N.Y.: Cold Spring Harbor Laboratory Press.

Sato, Hanae; Maquat, Lynne E. (2009): Remodeling of the pioneer translation initiation complex involves translation and the karyopherin importin beta. In *Genes & development* 23 (21), pp. 2537–2550. DOI: 10.1101/gad.1817109.

Schmitt, C.; Kobbe, C. von; Bachi, A.; Panté, N.; Rodrigues, J. P.; Boscheron, C. et al. (1999): Dbp5, a DEAD-box protein required for mRNA export, is recruited to the cytoplasmic fibrils of nuclear pore complex via a conserved interaction with CAN/Nup159p. In *The EMBO Journal* 18 (15), pp. 4332–4347. DOI: 10.1093/emboj/18.15.4332.

Schuller, Sandra K.; Schuller, Jan M.; Prabu, J. Rajan; Baumgärtner, Marc; Bonneau, Fabien; Basquin, Jérôme; Conti, Elena (2020): Structural insights into the nucleic acid remodeling mechanisms of the yeast THO-Sub2 complex. In *eLife* 9. DOI: 10.7554/eLife.61467.

Schwer, B.; Guthrie, C. (1991): PRP16 is an RNA-dependent ATPase that interacts transiently with the spliceosome. In *Nature* 349 (6309), pp. 494–499. DOI: 10.1038/349494a0.

Segref, A.; Sharma, K.; Doye, V.; Hellwig, A.; Huber, J.; Lührmann, R.; Hurt, E. (1997): Mex67p, a novel factor for nuclear mRNA export, binds to both poly(A)+ RNA and nuclear pores. In *The EMBO Journal* 16 (11), pp. 3256–3271. DOI: 10.1093/emboj/16.11.3256.

Senger, B.; Simos, G.; Bischoff, F. R.; Podtelejnikov, A.; Mann, M.; Hurt, E. (1998): Mtr10p functions as a nuclear import receptor for the mRNA-binding protein Npl3p. In *The EMBO Journal* 17 (8), pp. 2196–2207. DOI: 10.1093/emboj/17.8.2196.

Shatkin, A. J.; Manley, J. L. (2000): The ends of the affair: capping and polyadenylation. In *Nature structural biology* 7 (10), pp. 838–842. DOI: 10.1038/79583.

Shen, E. C.; Stage-Zimmermann, T.; Chui, P.; Silver, P. A. (2000): 7The yeast mRNA-binding protein Npl3p interacts with the cap-binding complex. In *The Journal of biological chemistry* 275 (31), pp. 23718–23724. DOI: 10.1074/jbc.M002312200.

Sikorski, R. S.; Hieter, P. (1989): A system of shuttle vectors and yeast host strains designed for efficient manipulation of DNA in Saccharomyces cerevisiae. In *Genetics* 122 (1), pp. 19–27. DOI: 10.1093/genetics/122.1.19.

Singleton, Martin R.; Dillingham, Mark S.; Wigley, Dale B. (2007): Structure and mechanism of helicases and nucleic acid translocases. In *Annual review of biochemistry* 76, pp. 23–50. DOI: 10.1146/annurev.biochem.76.052305.115300.

Skourti-Stathaki, Konstantina; Proudfoot, Nicholas J.; Gromak, Natalia (2011): Human senataxin resolves RNA/DNA hybrids formed at transcriptional pause sites to promote Xrn2-dependent termination. In *Molecular cell* 42 (6), pp. 794–805. DOI: 10.1016/j.molcel.2011.04.026.

Snay-Hodge, C. A.; Colot, H. V.; Goldstein, A. L.; Cole, C. N. (1998): Dbp5p/Rat8p is a yeast nuclear pore-associated DEAD-box protein essential for RNA export. In *The EMBO Journal* 17 (9), pp. 2663–2676. DOI: 10.1093/emboj/17.9.2663.

Staley, Jonathan P.; Guthrie, Christine (1998): Mechanical Devices of the Spliceosome: Motors, Clocks, Springs, and Things. In *Cell* 92 (3), pp. 315–326. DOI: 10.1016/s0092-8674(00)80925-3.

Staley, Jonathan P.; Guthrie, Christine (1999): An RNA Switch at the 5′ Splice Site Requires ATP and the DEAD Box Protein Prp28p. In *Molecular cell* 3 (1), pp. 55–64. DOI: 10.1016/s1097-2765(00)80174-4.

Stirling, Peter C.; Bloom, Michelle S.; Solanki-Patil, Tejomayee; Smith, Stephanie; Sipahimalani, Payal; Li, Zhijian et al. (2011): The complete spectrum of yeast chromosome instability genes identifies candidate CIN cancer genes and functional roles for ASTRA complex components. In *PLoS genetics* 7 (4), e1002057. DOI: 10.1371/journal.pgen.1002057.

Stirling, Peter C.; Chan, Yujia A.; Minaker, Sean W.; Aristizabal, Maria J.; Barrett, Irene; Sipahimalani, Payal et al. (2012): R-loop-mediated genome instability in mRNA cleavage and polyadenylation mutants. In *Genes & development* 26 (2), pp. 163–175. DOI: 10.1101/gad.179721.111.

Story, R. M.; Li, H.; Abelson, J. N. (2001): Crystal structure of a DEAD box protein from the hyperthermophile Methanococcus jannaschii. In *Proceedings of the National Academy of Sciences* 98 (4), pp. 1465–1470. DOI: 10.1073/pnas.98.4.1465.

Strahm, Y.; Fahrenkrog, B.; Zenklusen, D.; Rychner, E.; Kantor, J.; Rosbach, M.; Stutz, F. (1999): The RNA export factor Gle1p is located on the cytoplasmic fibrils of the NPC and physically interacts with the FG-nucleoporin Rip1p, the DEAD-box protein Rat8p/Dbp5p and a new protein Ymr 255p. In *The EMBO Journal* 18 (20), pp. 5761–5777. DOI: 10.1093/emboj/18.20.5761.

Strässer, K.; Hurt, E. (2000): Yra1p, a conserved nuclear RNA-binding protein, interacts directly with Mex67p and is required for mRNA export. In *The EMBO Journal* 19 (3), pp. 410–420. DOI: 10.1093/emboj/19.3.410.

Strässer, K.; Hurt, E. (2001): Splicing factor Sub2p is required for nuclear mRNA export through its interaction with Yra1p. In *Nature* 413 (6856), pp. 648–652. DOI: 10.1038/35098113.

Strässer, Katja; Masuda, Seiji; Mason, Paul; Pfannstiel, Jens; Oppizzi, Marisa; Rodriguez-Navarro, Susana et al. (2002): TREX is a conserved complex coupling transcription with messenger RNA export. In *Nature* 417 (6886), pp. 304–308. DOI: 10.1038/nature746.

Sun, Qianwen; Csorba, Tibor; Skourti-Stathaki, Konstantina; Proudfoot, Nicholas J.; Dean, Caroline (2013): R-loop stabilization represses antisense transcription at the Arabidopsis FLC locus. In *Science (New York, N.Y.)* 340 (6132), pp. 619–621. DOI: 10.1126/science.1234848.

Tanford, Charles (1968): Protein Denaturation. In Christian B. Anfinsen (Ed.): Advances in protein chemistry, vol. 23. New York, London: Academic Press (Advances in Protein Chemistry, v. 23), pp. 121–282.

Taniguchi, Ichiro; Ohno, Mutsuhito (2008): ATP-dependent recruitment of export factor Aly/REF onto intronless mRNAs by RNA helicase UAP56. In *Molecular and cellular biology* 28 (2), pp. 601–608. DOI: 10.1128/MCB.01341-07.

Tarun, S. Z.; Sachs, A. B. (1995): A common function for mRNA 5' and 3' ends in translation initiation in yeast. In *Genes & development* 9 (23), pp. 2997–3007. DOI: 10.1101/gad.9.23.2997.

Taylor, R. G.; Walker, D. C.; McInnes, R. R. (1993): E. coli host strains significantly affect the quality of small scale plasmid DNA preparations used for sequencing. In *Nucleic acids research* 21 (7), pp. 1677–1678.

Thomas, Barbara J.; Rothstein, Rodney (1989): Elevated recombination rates in transcriptionally active DNA. In *Cell* 56 (4), pp. 619–630. DOI: 10.1016/0092-8674(89)90584-9.

Thomas, Marco; Lischka, Peter; Müller, Regina; Stamminger, Thomas (2011): The cellular DExD/H-box RNA-helicases UAP56 and URH49 exhibit a CRM1-independent nucleocytoplasmic shuttling activity. In *PloS one* 6 (7), e22671. DOI: 10.1371/journal.pone.0022671.

Topisirovic, Ivan; Svitkin, Yuri V.; Sonenberg, Nahum; Shatkin, Aaron J. (2011): Cap and cap-binding proteins in the control of gene expression. In *Wiley interdisciplinary reviews. RNA* 2 (2), pp. 277–298. DOI: 10.1002/wrna.52.

Towbin, H.; Staehelin, T.; Gordon, J. (1979): Electrophoretic transfer of proteins from polyacrylamide gels to nitrocellulose sheets: procedure and some applications. In *Proceedings of the National Academy of Sciences* 76 (9), pp. 4350–4354. DOI: 10.1073/pnas.76.9.4350.

Tran, Elizabeth J.; Wente, Susan R. (2006): Dynamic nuclear pore complexes: life on the edge. In *Cell* 125 (6), pp. 1041–1053. DOI: 10.1016/j.cell.2006.05.027.

Tran, Elizabeth J.; Zhou, Yingna; Corbett, Anita H.; Wente, Susan R. (2007): The DEAD-box protein Dbp5 controls mRNA export by triggering specific RNA:protein remodeling events. In *Molecular cell* 28 (5), pp. 850–859. DOI: 10.1016/j.molcel.2007.09.019.

Tsai, Rong-Tzong; Fu, Ru-Huei; Yeh, Fu-Lung; Tseng, Chi-Kang; Lin, Yu-Chieh; Huang, Yu-Hsin; Cheng, Soo-Chen (2005): Spliceosome disassembly catalyzed by Prp43 and its associated components Ntr1 and Ntr2. In *Genes & development* 19 (24), pp. 2991–3003. DOI: 10.1101/gad.1377405.

Tseng, S. S.; Weaver, P. L.; Liu, Y.; Hitomi, M.; Tartakoff, A. M.; Chang, T. H. (1998): Dbp5p, a cytosolic RNA helicase, is required for poly(A)+ RNA export. In *The EMBO Journal* 17 (9), pp. 2651–2662. DOI: 10.1093/emboj/17.9.2651.

Tuck, Alex Charles; Tollervey, David (2013): A transcriptome-wide atlas of RNP composition reveals diverse classes of mRNAs and lncRNAs. In *Cell* 154 (5), pp. 996–1009. DOI: 10.1016/j.cell.2013.07.047.

Tuduri, Sandie; Crabbé, Laure; Conti, Chiara; Tourrière, Hélène; Holtgreve-Grez, Heidi; Jauch, Anna et al. (2009): Topoisomerase I suppresses genomic instability by preventing interference between replication and transcription. In *Nature cell biology* 11 (11), pp. 1315–1324. DOI: 10.1038/ncb1984.

Tutucci, Evelina; Stutz, Françoise (2011): Keeping mRNPs in check during assembly and nuclear export. In *Nature reviews. Molecular cell biology* 12 (6), pp. 377–384. DOI: 10.1038/nrm3119.

Venema, J.; Tollervey, D. (1995): Processing of pre-ribosomal RNA in Saccharomyces cerevisiae. In *Yeast (Chichester, England)* 11 (16), pp. 1629–1650. DOI: 10.1002/yea.320111607.

Viphakone, Nicolas; Voisinet-Hakil, Florence; Minvielle-Sebastia, Lionel (2008): Molecular dissection of mRNA poly(A) tail length control in yeast. In *Nucleic acids research* 36 (7), pp. 2418–2433. DOI: 10.1093/nar/gkn080.

Visa, N.; Izaurralde, E.; Ferreira, J.; Daneholt, B.; Mattaj, I. W. (1996): A nuclear cap-binding complex binds Balbiani ring pre-mRNA cotranscriptionally and accompanies the ribonucleoprotein particle during nuclear export. In *The Journal of cell biology* 133 (1), pp. 5–14. DOI: 10.1083/jcb.133.1.5.

Wahba, Lamia; Amon, Jeremy D.; Koshland, Douglas; Vuica-Ross, Milena (2011): RNase H and multiple RNA biogenesis factors cooperate to prevent RNA:DNA hybrids from generating genome instability. In *Molecular cell* 44 (6), pp. 978–988. DOI: 10.1016/j.molcel.2011.10.017.

Wahle, Elmar (1991): A novel poly(A)-binding protein acts as a specificity factor in the second phase of messenger RNA polyadenylation. In *Cell* 66 (4), pp. 759–768. DOI: 10.1016/0092-8674(91)90119-J.

Wang, Qiang; Zhang, Li; Lynn, Bert; Rymond, Brian C. (2008): A BBP-Mud2p heterodimer mediates branchpoint recognition and influences splicing substrate abundance in budding yeast. In *Nucleic acids research* 36 (8), pp. 2787–2798. DOI: 10.1093/nar/gkn144.

Weirich, Christine S.; Erzberger, Jan P.; Berger, James M.; Weis, Karsten (2004): The N-terminal domain of Nup159 forms a beta-propeller that functions in mRNA export by tethering the helicase Dbp5 to the nuclear pore. In *Molecular cell* 16 (5), pp. 749–760. DOI: 10.1016/j.molcel.2004.10.032.

Weirich, Christine S.; Erzberger, Jan P.; Flick, Jeffrey S.; Berger, James M.; Thorner, Jeremy; Weis, Karsten (2006): Activation of the DExD/H-box protein Dbp5 by the nuclear-pore protein Gle1 and its coactivator InsP6 is required for mRNA export. In *Nature cell biology* 8 (7), pp. 668–676. DOI: 10.1038/ncb1424.

Wente, Susan R.; Rout, Michael P. (2010): The nuclear pore complex and nuclear transport. In *Cold Spring Harbor perspectives in biology* 2 (10), a000562. DOI: 10.1101/cshperspect.a000562.

Wigington, Callie P.; Williams, Kathryn R.; Meers, Michael P.; Bassell, Gary J.; Corbett, Anita H. (2014): Poly(A) RNA-binding proteins and polyadenosine RNA: new members and novel functions. In *Wiley interdisciplinary reviews. RNA* 5 (5), pp. 601–622. DOI: 10.1002/wrna.1233.

Will, Cindy L.; Lührmann, Reinhard (2011): Spliceosome structure and function. In *Cold Spring Harbor perspectives in biology* 3 (7). DOI: 10.1101/cshperspect.a003707.

Wilmes, Gwendolyn M.; Bergkessel, Megan; Bandyopadhyay, Sourav; Shales, Michael; Braberg, Hannes; Cagney, Gerard et al. (2008): A genetic interaction map of RNA-processing factors reveals links between Sem1/Dss1-containing complexes and mRNA export and splicing. In *Molecular cell* 32 (5), pp. 735–746. DOI: 10.1016/j.molcel.2008.11.012.

Wilson, Katie A.; Holland, Devany J.; Wetmore, Stacey D. (2016): Topology of RNA-protein nucleobase-amino acid π-π interactions and comparison to analogous DNA-protein π-π contacts. In *RNA (New York, N.Y.)* 22 (5), pp. 696–708. DOI: 10.1261/rna.054924.115.

Wolf, Elmar; Kastner, Berthold; Deckert, Jochen; Merz, Christian; Stark, Holger; Lührmann, Reinhard (2009): Exon, intron and splice site locations in the spliceosomal B complex. In *The EMBO Journal* 28 (15), pp. 2283–2292. DOI: 10.1038/emboj.2009.171.

Wong, C.; Sridhara, S.; Bardwell, J. C.; Jakob, U. (2000): Heating greatly speeds Coomassie blue staining and destaining. In *BioTechniques* 28 (3), 426-8, 430, 432. DOI: 10.2144/00283bm07.

Wood, William B. (1966): Host specificity of DNA produced by Escherichia coli: Bacterial mutations affecting the restriction and modification of DNA. In *Journal of molecular biology* 16 (1), 118-IN3. DOI: 10.1016/s0022-2836(66)80267-x.

Wu, J. A.; Manley, J. L. (1991): Base pairing between U2 and U6 snRNAs is necessary for splicing of a mammalian pre-mRNA. In *Nature* 352 (6338), pp. 818–821. DOI: 10.1038/352818a0.

Yan, Xiaomei; Mouillet, Jean-François; Ou, Qinglin; Sadovsky, Yoel (2003): A novel domain within the DEAD-box protein DP103 is essential for transcriptional repression and helicase activity. In *Molecular and cellular biology* 23 (1), pp. 414–423. DOI: 10.1128/MCB.23.1.414-423.2003.

Yang, Quansheng; Del Campo, Mark; Lambowitz, Alan M.; Jankowsky, Eckhard (2007): DEAD-box proteins unwind duplexes by local strand separation. In *Molecular cell* 28 (2), pp. 253–263. DOI: 10.1016/j.molcel.2007.08.016.

Yang, Quansheng; Jankowsky, Eckhard (2006): The DEAD-box protein Ded1 unwinds RNA duplexes by a mode distinct from translocating helicases. In *Nature structural & molecular biology* 13 (11), pp. 981–986. DOI: 10.1038/nsmb1165.

Yang, Yinshan; Declerck, Nathalie; Manival, Xavier; Aymerich, Stéphane; Kochoyan, Michel (2002): Solution structure of the LicT-RNA antitermination complex: CAT clamping RAT. In *The EMBO Journal* 21 (8), pp. 1987–1997. DOI: 10.1093/emboj/21.8.1987.

Yoo, Hyun Hee; Chung, In Kwon (2011): Requirement of DDX39 DEAD box RNA helicase for genome integrity and telomere protection. In *Aging cell* 10 (4), pp. 557–571. DOI: 10.1111/j.1474-9726.2011.00696.x.

Young, R. A. (1991): RNA polymerase II. In *Annual review of biochemistry* 60, pp. 689–715. DOI: 10.1146/annurev.bi.60.070191.003353.

Yu, Haiyuan; Braun, Pascal; Yildirim, Muhammed A.; Lemmens, Irma; Venkatesan, Kavitha; Sahalie, Julie et al. (2008): High-quality binary protein interaction map of the yeast interactome network. In *Science (New York, N.Y.)* 322 (5898), pp. 104–110. DOI: 10.1126/science.1158684.

Yu, Kefei; Chedin, Frederic; Hsieh, Chih-Lin; Wilson, Thomas E.; Lieber, Michael R. (2003): R-loops at immunoglobulin class switch regions in the chromosomes of stimulated B cells. In *Nature immunology* 4 (5), pp. 442–451. DOI: 10.1038/ni919.

Zeitler, Bryan; Weis, Karsten (2004): The FG-repeat asymmetry of the nuclear pore complex is dispensable for bulk nucleocytoplasmic transport in vivo. In *The Journal of cell biology* 167 (4), pp. 583–590. DOI: 10.1083/jcb.200407156.

Zenklusen, D.; Vinciguerra, P.; Strahm, Y.; Stutz, F. (2001): The yeast hnRNP-Like proteins Yra1p and Yra2p participate in mRNA export through interaction with Mex67p. In *Molecular and cellular biology* 21 (13), pp. 4219–4232. DOI: 10.1128/MCB.21.13.4219-4232.2001.

Zhang, M.; Green, M. R. (2001): Identification and characterization of yUAP/Sub2p, a yeast homolog of the essential human pre-mRNA splicing factor hUAP56. In *Genes & development* 15 (1), pp. 30–35. DOI: 10.1101/gad.851701.

Zhou, Z.; Luo, M. J.; Straesser, K.; Katahira, J.; Hurt, E.; Reed, R. (2000): The protein Aly links pre-messenger-RNA splicing to nuclear export in metazoans. In *Nature* 407 (6802), pp. 401–405. DOI: 10.1038/35030160.

7 Table of figures

8 List of Tables

9 Abbreviations

Table 17: Abbreviations

Abbreviation	Description
5-FOA	5-Fluoroorotic acid
°C	degree Celsius
A	Alanine
AA	Amino acid
APA	Alternative polyadenylation
ATP	Adenosine triphosphate
Bp	Base pair
BP	Branch point
BBP	Branch point binding protein
CBC	cap-binding complex
CF	Cleavage factor
CPF	Cleavage and polyadenylation factor
CPSF	Cleavage and polyadenylation signal factor
CStF	Cleavage stimulating factor
CTD	carboxy-terminal domain of RNAPII
CC	Commitment complex
D	Aspartic acid
Da	Dalton
DEAD	Aspartate Glutamate Alanine Aspartate
DECD	Aspartate Glutamate Cysteine Aspartate
dNTP	Dinucleotide triphosphate
DNA	Deoxyribonucleic acid
Ds	Double stranded
E	Glutamic acid
ECL	enhanced chemiluminescence (detection solution)
E. coli	*Escherichia coli*
et al.	et alii (Latin for “and others”)
EtOH	Ethanol
F	Phenylalanine
FG-	phenylalanine glycine-
FISH	Fluorescence *in situ* hybridization
Fwd	Forward PCR primer
G	Glycine
H	Hour (s)
hnRNP	heterogeneous nuclear ribonucleoprotein
HRP	Horse radish peroxidase
IP	Immunoprecipitation
J	Joules
K	Lysine
kDa	Kilodalton
LB	Luria Bertani medium (for *E. coli*)
m^7G	m^7 methyl guanosine
M	Molar
min	Minutes
ml	Milliliter
mRNA	messenger ribonucleic acid
mRNP	messenger ribonucleoprotein particle
MW	Molecular weight
NPC	nuclear pore complex
nt	Nucleotide
Nup	Nucleoporin

OD	optical density
PABP	poly(A)-binding protein
PAP	Poly adenylation polymerase
PAR-CLIP	Photoactivatable ribonucleoside-enhanced crosslinking and immunoprecipitation
PCR	polymerase chain reaction
poly(A)	Poly-adenylation
R	Arginine
RBP	RNA binding protein
Rev	Reverse PCR primer
RIP	RNA immunoprecipitation
RNA	Ribonucleic acid
RNAPII	RNA polymerase II
RNP	Ribonucleoprotein
Rpm	rotations per minute
RT	Room temperature
(RT)-qPCR	(Reverse transcription)- quantitative polymerase chain reaction
sec	Seconds
S. cerevisiae	*Saccharomyces cerevisiae*
ss	Single stranded
snRNP	small nuclear RNP
SR	serine-arginine
T	Threonine
TAP	tandem affinity purification
TEV	Tobacco etch virus
ts	Temperature sensitive
TREX	transcription and export
WB	Western blot
Y	Tyrosine
YPD	Yeast extract, peptone, dextrose

Acknowledgements

This far by grace. My utmost gratitude to the Almighty God for bringing me this far and for seeing me through this journey successfully.

I would also like to express my appreciation to my supervisor Prof. Dr. Katja Sträßer for giving me the opportunity to conduct my PhD under her supervision. For the opportunity to grow in my pursuit of knowledge, for her guidance, correction and always pushing me beyond my limit.

Also, to Prof. Dr. Elena Evguenieva-Hackenberg for being the second examiner of my thesis. I would also like to thank Prof. Dr. Lienhard Schmitz, both of whom are members of my Thesis Advisory committee, and Prof. Dr. Reinhard Dammann and Prof. Dr. Tilman Borggrefe for being members of my thesis evaluation committee.

Appreciation also goes to the RTG2355 for funding my PhD project as well and the IMPRS-Bad Nauheim. Both of which provided training and direction during my graduate program.

I would also express gratitude to the entire team. To Peter Friedhoff, Cornelia Kilchert and Wolfgang Wende for their immense support in diverse ways during my time in the lab and which contributed to the success of my PhD. Special thanks to Heike for being always warm and for her listening ears. To my colleagues in the lab, you made my time in the lab memorable and worth it. Through all the ups and downs, you guys were around. Thank you also for the engaging and fun discussions we had.

To my family, you have been my backbone through it all. You have inspired me to be more than I could be. To my dad, Solomon Amoah-Ota, I dedicate this to you. You are not here to witness this, but I hope I have made you proud. To my mum, Rose-Mary Amoah for being the woman we needed. I dedicate this also to you. To my siblings, Priscilla, Lawrence, and Gifty. Thank you for keeping me in prayers all the time. To Jesse, we made it. Thank you for being there for me during the good and the difficult times. To Albert, thank you for always giving me an escape from myself and for the fun times.

To the Frankfurters (Florence and Thompson), the Giesseners (Ratnal, Stephen and Dominic) and Abigail thank you for the bond we formed and the memories we created. You made the experience worth it and the load lighter.

Thank you all for your support in diverse ways!

Eidesstattliche Erklärung

Ich erkläre: Ich habe die vorgelegte Dissertation selbstständig und ohne unerlaubte fremde Hilfe und nur mit den Hilfen angefertigt, die ich in der Dissertation angegeben habe. Alle Textstellen, die wörtlich oder sinngemäß aus veröffentlichten Schriften entnommen sind, und alle Angaben, die auf mündlichen Auskünften beruhen, sind als solche kenntlich gemacht. Ich stimme einer evtl. Überprüfung meiner Dissertation durch eine Antiplagiat-Software zu. Bei den von mir durchgeführten und in der Dissertation erwähnten Untersuchungen habe ich die Grundsätze guter wissenschaftlicher Praxis, wie sie in der “Satzung der Justus-Liebig-Universität Gießen zur Sicherung guter wissenschaftlicher Praxis” niedergelegt sind, eingehalten.

I declare that I have completed this dissertation single-handedly without the unauthorized help of a second party and only with the assistance acknowledged therein. I have appropriately acknowledged and cited all text passages that are derived verbatim from or are based on the content of published work of others, and all information relating to verbal communications. I consent to the use of an anti-plagiarism software to check the results of my thesis. I have abided by the principles of good scientific conduct laid down in the charter of the Justus Liebig University Giessen “Satzung der Justus-Liebig-Universität Gießen zur Sicherung guter wissenschaftlicher Praxis” in carrying out the investigations described in the dissertation”.

Giessen, den 2022

Francisca Nana Amoah